


UNIVERSITA' DEGLI STUDI DI SASSARI

Scuola di Dottorato di ricerca in Scienze Biomolecolari e Biotecnologiche
Indirizzo in Microbiologia Molecolare e Clinica
XXIV ciclo

Coordinatore:
Prof. Bruno Masala

Functional transcriptome of *Mycobacterium avium* subsp. *paratuberculosis* in human macrophage infection and immunological relevance of its specific antigens in type I Diabetes mellitus

Tutor:
Prof. Leonardo Antonio Sechi

Tesi di Dottorato di:
Dott. Andrea Cossu

Anno Accademico 2010/2011

TABLE OF CONTENTS

RIASSUNTO

Recenti studi hanno suggerito un ruolo per il *Mycobacterium avium* subsp. *paratuberculosis* (*Map*) nello sviluppo di alcune patologie a carattere autoimmunitario dell'uomo. Di conseguenza, poichè l'interesse clinico del batterio si amplia ora anche verso l'ospite umano, è necessaria una conoscenza approfondita della espressione genica del batterio durante l'infezione nell'uomo oltre che alla individuazione di fattori immunogenici e/o virulenti per lo sviluppo di adeguati strumenti diagnostici o terapeutici. Al fine di caratterizzare il trascrittoma del *Map* durante l'infezione di macrofagi umani, è stato portato avanti da un lato un lavoro di analisi dell'intero trascrittoma del batterio mediante la tecnologia del DNA-microarray in condizioni intrafagosomali simulate grazie ad uno stress multiplo di carattere acido-nitrico, dall'altro con l'infezione della linea macrofagica umana THP-1. I risultati mostrano come il *Map* sposti il suo trascrittoma verso un metabolismo di tipo adattivo per un ambiente anossico e di sofferenza nutrizionale insieme ad un'interessante spoliazione passiva dal peptidoglicano quando si trova all'interno del macrofago. In aggiunta, è stata ricercata in sieri di pazienti affetti da diabete mellito di tipo 1 (T1DM) e di tipo 2 (T2DM) la presenza di anticorpi rivolti contro due nuove proteine ricombinanti specifiche del *Map* (MptD e MAP3738c). I risultati hanno mostrato una risposta positiva ad entrambe le proteine nei pazienti T1DM mentre non è stata individuata alcuna differenza tra i sieri di pazienti T2DM e sieri di soggetti sani, suggerendo perciò una possibile associazione tra il T1DM e l'infezione batterica.

ABSTRACT

Recent studies have identified in *Mycobacterium avium* subsp. *paratuberculosis* (*Map*) a potential zoonotic agent in the development of some autoimmune diseases in humans. Therefore, it is necessary a thorough understanding of *Map*'s gene expression during infection of human host as well as the identification of its immunogenic and/or virulence factors for the development of appropriate diagnostic or therapeutic tools. In order to characterize *Map*'s transcriptome during the infection of human macrophages, the whole gene expression of *Map* was analyzed with DNA-microarray technology in simulated intraphagosomal conditions created with an acid-nitrosative culture preparation and after intracellular infection of the human macrophage cell line THP-1. Results showed that *Map* shifts its transcriptome to an adaptive metabolism for an anoxic environment and nutrient starvation, up-regulating several response factors to oxidative stress or intracellular conditions and allowing a passive surface peptidoglycan spoliation within the macrophage. Additionally, the presence of antibodies against two specific proteins of *Map* (MptD and MAP3738c) was investigated in sera of patients affected by type 1 Diabetes mellitus (T1DM) and type 2 Diabetes mellitus (T2DM). Results showed a positive response to both proteins in T1DM patients whereas no difference with controls was found for T2DM patients suggesting a potential association between T1DM and the bacterial infection.

1. INTRODUCTION

1.1 The *Mycobacterium avium* subsp. *paratuberculosis (Map)*

Mycobacterium avium subspecies *paratuberculosis* (*Map*) is the causative agent of Johne's disease (JD) or Paratuberculosis, a chronic enteritis that mainly affects ruminants, causing a general debilitation of the infected organism (Harris et al., 2001). The disease is characterized by having several phases that include, besides the initial phase of infection, a subclinical asymptomatic stage dominated by a Th1 type immune response, which usually is not able to eliminate the infection due to bacterial mechanisms of evasion (Sohal et al., 2008), then gradually replaced by a Th2 humoral immune response (Coussens et al., 2001). Since the humoral response is not able to fight against intracellular infection, the symptoms in the clinical phase becomes evident with the appearance of granulomatous lesions *in loco*, intestinal disorders and weight loss, culminating in the death of the infected animals (Beard et al., 1999).

The Paratuberculosis seems to have many common features with the pathogenesis and the symptoms of Crohn's disease (CD) (Chiodini et al., 1989), a chronic inflammatory bowel disease that causes inflammation of the human gastrointestinal tract. As a matter of fact, although the bacterium has been recognized as a pathogen for poultry, ruminants and primates (Gerlach, 2002) extensive evidence such as the isolation of *Map* in the intestinal tissue of Crohn's disease patients (Bull et al., 2003; Sechi et al., 2005) and the humoral response of patients suffering from autoimmune diseases to specific antigens of the bacterium (Cossu et al., 2011) have suggested the possible potential of the bacterium as a zoonotic agent.

Map can survive for long periods under different environmental conditions

(Whittington et al., 2004) and is able to resist to several heat treatments conventionally used in the agricultural supply chain for transformation of various foodstuffs (Donaghy et al., 2004), moreover the bacterium is characterized by having a slow growth rate *in vitro* (Sechi et al., 2005) as well as a persistent infection with a slow course (de Lisle et al., 1998), that make it difficult to detect the infection with early diagnosis and microbiological cultural methods, respectively.

1.2 *Map*'s mechanisms of infection

Most of the mechanisms underlying the development of disease caused by *Map* have been proposed following those based on diseases triggered by *Mycobacterium tuberculosis* and *Mycobacterium avium* ssp. *avium* (Kuehnel et al., 2001). Mycobacteria infect mainly macrophage cells (Hestvik et al., 2005), for this reason they were forced to develop defense mechanisms to face the hostile environment they encounter within the phagosomal compartment. Consequently, the mycobacterial pathogens have developed a particular resistance to the common weapons of defense and destruction relied by phagocityc cells such as liberation of reactive nitrogen intermediates and oxygen radicals in addition to the acidification of the phagosome along with the release of antimicrobial peptides (Alonso et al., 2007). The main mechanism of defense implemented by the mycobacterium is the inhibition of acidification within the macrophage through the defective phagosome-lysosome fusion, so that mycobacteria may proliferate within it (Bannantine et al., 2002). However, the precise molecular mechanism by which the mycobacteria is able to avoid the occurrence of mature phagolysosome in order to achieve an efficient degradation of the bacterium is still unknown.

For this reason, many studies concerning the transcriptional regulation of macrophage lines during infection by *Map* have already been carried out (Murphy et al., 2006, Verschoor et al., 2010) using DNA-microarray technology that has become by now a useful tool for the study of mycobacterial gene expression under different environmental conditions (Boshoff et al., 2004), indirectly revealing the biochemical mechanisms underlying the development and regulation of the disease but still leaving a gap in the direct knowledge of gene expression during *Map* infection and its *modus operandi*, although some experiments have been already carried out to identify the transcriptome of the bacterium during infection of bovine cell lines, revealing some aspects of its intracellular persistence (Zhu et al., 2008; Janagama et al., 2010). Additionally, the importance of *Map* in terms of zoonotic relevance is recently gaining considerable attention from scientists in various autoimmune diseases in which the bacterium could be involved (Sechi et al., 2008; Cossu et al., 2011). In light of this, the characterization of *Map* transcriptome during infection of human macrophage cell lines would be of great help in bridging a gap still present in the state of the art for this organism.

1.3 *Map* and autoimmune diseases

Paratuberculosis is present in more than 50% of Sardinian herds, therefore Sardinia inhabitants may be exposed to potential contamination by *Map*, and it has been reported that occupational exposure is linked to increased humoral response against *Map* (Chiodini et al., 1996). Moreover, genetic segregation of the Sardinian population (Passarino et al., 2001) together with NOD2/CARD15 (Sechi et al., 2006a) as well as SLC11A1 (Paccagnini et al., 2009) allele polymorphisms (both involved in pathogen detection and

clearance) may create the ideal setting for *Map* infection in susceptible individuals.

Some authors speculated on the mimicry between bacterial and host heat shock proteins that share common epitopes, during infection (Dow, 2008), and it was assumed that host response triggered by microbial antigens would activate an immune response against self-epitopes. In particular, infections caused by pathogens that share antigens with high homology to proteins of the host, may activate T cells specific immune response to self antigens, causing autoimmune disease. The mechanism is due to the properties of antigen recognition by a T cell receptor (TcR) that is degenerate and thus flexible. In this way, antigens belonging to infectious organisms that have cross-reactivity with self-epitopes can also activate T cells that have a low affinity for self-molecules and escaped negative selection (Getts et al., 2010).

In line with this view, experimental analysis of the correlation between humoral response against *Map* and T1DM by using immunological assays with specific proteins has been already proposed (Sechi et al., 2008). Within this scenario, the purification of mycobacterial antigens highly likely unique in sequence and preferentially located on the cell surface of the bacterium, may open up new horizons for the development of immunodiagnostic preparations or vaccines against *Map*.

2. AIM OF THE STUDY

In order to characterize the *Map*'s transcriptome during the infection of human macrophages this work was carried out by analyzing the whole *Map* transcriptome with DNA-microarray technology in simulated conditions of multiple intraphagosomal stresses, through the preparation of an acid-nitrosative multi-stress, as well as for the first time in intracellular infection of the human macrophage cell line THP-1. The comparison of the two transcriptional repertoires will help identify genes that are induced or repressed in *Map* under these conditions in order to deeply understand the metabolic, regulatory and virulence patterns of the bacterium with the aim to identify possible key factors that may lead to the development of new diagnostic or therapeutic tools.

In addition, besides the above mentioned fundamental research line based on a functional genomics approach, another goal of the study was also to test the reactivity of sardinian type I, type II diabetic sera and healthy controls against MAP3733c (MptD an expected membrane protein) and MAP3738c (a factor involved in the biosynthesis of cell surface components) in ELISA (Enzyme-Linked-Immunosorbent-Assay) experiments, in order to thoroughly investigate the linkage between *Map* and the autoimmune disease T1DM.

3. MATERIALS AND METHODS

3.1 Bacterial cultures and growth media

Mycobacterium avium subsp. *paratuberculosis 1515* (ATCC 43015) was cultured in Middlebrook 7H9 medium (Sigma), 0.2% glycerol (Sigma), 0.05% Tween 80 (Sigma) supplemented with 10% v/v albumine dextrose catalase (ADC, Sigma) and 2 mg/L of Mycobactin J (MicJ) (Allied Monitors, Fayette, MO, USA) in 25 cm^2 vented tissue culture flasks at 37°C.

Escherichia coli (*E. coli*) strains *M15 (pREP4)* (Qiagen, Hilden, Germany) and *BL21(DE3) codon plus* (Stratagene, La Jolla, CA, USA), were grown at 37°C in LB broth (Microbiol, Cagliari, Italy) or LB agar (Agar 1.5% (Invitrogen, Carlsbad, CA, USA) added to LB) with supplementation of desired antibiotics as kanamycin (Sigma) 30 µg/ml or ampicillin (Sigma) 100 µg/ml.

3.2 Acid-Nitrosative multi-stress

Map's transcriptome in acid-nitrosative stress conditions was examined in 7H9-ADC medium. Early log-phase mycobacteria were exposed to the stress for 3 hours at 37°C. The acid-nitrosative stress was performed with a final concentration of 5 mM of sodium nitrite ($NaNO_2$) (Sigma) in a buffered pH 5.3 broth with addiction of MicJ.

After stress, cells were harvested and resuspended in RNA later solution (Ambion) to preserve bacterial RNA. Bacterial pellets were then incubated overnight at 4°C and stored at -80°C until RNA extraction. Acid-nitrosative stress condition and relative control were conducted in triplicate and the entire process was repeated in a second experiment.

3.3 Cell cultures

THP-1 cells, a human monocyte cell line (ATTC TIB-202), were grown in T75 vented flasks (DB, Falcon) in RPMI-1640 medium (Invitrogen) supplemented with 10% heat-inactivated fetal bovine serum (Sigma) and antibiotic-antimycotic solution (1X) (Sigma) at 37°C under an atmosphere of 5% CO_2. Cells were differentiated into macrophages with the addiction of phorbol 12-myristate 13-acetate (PMA) (Sigma) (50 ng/ml) when they reached a concentration of $5x10^5$ cells/ml, and incubated for 24h to allow differentiation. The next day adherence was confirmed by microscopy and monolayer was ready to be infected.

3.4 Cellular infection with *Map*

Infections were performed in T75 vented flasks containing monolayers with a confluence of approximately $1x10^5$ cells/cm^2. Monolayers were washed 3 times with sterile PBS to remove antibiotics and 25 ml of fresh medium were added to the monolayer before infection. Inocula for infection were prepared by centrifugation (5000 x *g*, 15 min) of 10 ml of *Map* culture with a density of $8x10^8$ bacteria/ml. Bacterial pellet was resuspended in 10 ml of pre-warmed RPMI medium at 37°C and cells were declumped by 10 passages through a 21 gauge needle. Monolayers were infected by *Map* with a multiplicity of infection (MOI) of 10:1 for 24 h at 37°C at 5% CO2. The next day, extracellular bacteria were killed by amikacin (Sigma) treatment (200 µg/ml) for 2h at 37°C. Supernatant was removed and monolayer was washed with 3 x PBS rounds. Infected cells were selectively lysed by addiction of 10 ml of lysis buffer per monolayer (4M guanidine thiocyanate, 0.5% Na N-lauryl sarcosine, 25 mM sodium citrate, and 0.1M β-mercaptoethanol) without killing intracellular bacteria as previously

described (Rohde et al., 2007; Butcher et al., 1998). Flasks were shaked at 100 rpm for 15 min at room temperature (RT) and recovered lysate was thoroughly vortexed for 2 min before being passed five times through a 21 gauge needle to shear infected cells and reduce viscosity. One hundred milliliters of lysate belonging to ten T75 flasks were centrifuged at 5000 x *g* for 30 min at 14°C and pellet was resuspended in 1 ml of fresh lysis buffer. A final centrifugation at 10000 x *g* for 2 min was performed to harvest bacterial cells and pellet was then stored at -80°C until RNA extraction.

3.5 RNA extraction

RNA was extracted by using the RiboPure-Bacteria Kit (Ambion) following the manufacturer's instructions with some modifications. Briefly, approximately $1x10^9$ mycobacterial cells were resuspended in 350 µl of RNAWIZ solution (Ambion) and transferred to a 0.5 ml skirted screw-capped microcentrifuge tube containing 300 µl of ice-cold Zirconia Beads. Tubes were immediately processed in the RiboLyser FP120-HY-230 RNA Lysing machine (Hybaid) for three cycles (30 s at speed 6.5) with cooling on ice for 1 min between pulses. Remaining steps were performed according to the manufacturer's instructions. RNA yield and purity was evaluated with the Nanodrop spectrophotometer (NanoDrop1000, Thermo Scientific) while RNA quality was examined by denaturing gel electrophoresis. All RNA samples were treated with Dnase I (Ambion) to remove trace amounts of genomic DNA.

3.6 mRNA enrichment and linear amplification of mycobacterial RNA

The 16S and 23S ribosomal RNAs were removed from total RNA (tot-RNA) by using the MICROBExpress Bacterial mRNA Purification Kit (Ambion). Ten

micrograms of input tot-RNA were used to get an average of 1-2 µg of output enriched mRNA. rRNAs removal was confirmed by denaturing gel electrophoresis. Enriched mycobacterial mRNA was then amplified by using the MessageAmp II Bacterial Kit (Ambion) with amino-allyl-UTP in order to incorporate modified uracyl nucleotides into amplified RNA (aRNA) during the IVT reaction to allow subsequently fluorescence dyes coupling.

3.7 Labelling of aRNA

Fourty micrograms of aRNA were labelled with Alexa Fluor dyes 647 or 555 (Invitrogen) respectively for control samples and for experimental sample, following the manufacturer's protocol. Purification of coupled aRNA was performed by RNeasy purification system (Qiagen) and incorporation of dye was evaluated using Nanodrop. Before hybridization, coupled aRNA was fragmented using RNA fragmentation reagents (Ambion) following manufacturer's protocol.

3.8 Microarray hybridizations

Microarray slides were purchased from Biodiscovery LLC (Ann Arbor, MI, USA). *Mycobacterium avium* subsp. *paratuberculosis* K10 expression microarray contains one probe per gene for a total of 4337 probes covering 99.7% of all genes with 4 probe replicates per array in a 3 arrays format per slides for a total of 3x20K per slide. Each hybridization has been prepared following the Recommended Sample Preparation and Hybridization Protocols for Use with MYcroarrays (Biodiscovery LLC) with some modifications. Briefly, an hybridization solution of 220 µl (66 µl of 20X SSPE (3M NaCl, 20mM EDTA, 118.2mM NaH_2PO_4, 81.8mM Na_2HPO_4), formamide (10%), BSA (0.01 mg/ml), Tween-20 (0.01 %), DTT (1 mM), manufacturer

control oligos 1 %, 10 µg of each target coupled-aRNA, RNAse free water until final volume) was prepared and pre-warmed at 56°C before hybridization. All hybridizations were carried out in a water bath at 55°C for 18h in OneArray Sealed Hybridization Chambers (PhalanxBio Inc., Palo Alto, CA, USA) applicated to array slides following manufacturer's protocol. After incubation, microarrays were washed at RT with two rounds of SSPE 1X with DTT (0.1 mM) for 2 min, a 30 s final wash of SSPE 0.25 X with DTT (0.1 mM) and dried with spray air before been immediately scanned. All scans were carried out with an Axon 4200A scanner (Molecular Devices) at 5 µm resolution with full dynamic range of signal intensities at 1–65,000 in two-color mode (635 nm and 532 nm filters).

3.9 Microarrays data analysis

Scanned images were obtained using the GenePix 6.0 software (Molecular devices). The signal intensity of each gene in both colors was calculated by the mean of median intensity of each replicate spot for each gene in array giving a mean for each gene extrapolated from 4 single spot signals. Median intensity values were corrected by background subtraction and negative corrected intensities were set to 10. Data were further normalized using the ratio-based setting for GenePix and gpr files belonging to hybridization signals analyzed by GenePix software were then loaded into the Multi Experiment viewer (MeV) from TM4 software suite for subsequent expression analysis. All values were log2 transformed for further analysis and a minimum 2-fold change in the ratio intensities with a p-value <0.05 was considered significant for a differential gene expression. Transcriptional profile files have been submitted to the GEO database at NCBI (accession number GSE32243). *In silico* analysis to define each

metabolic pattern was achieved using the Kyoto Encyclopedia of Genes and Genomes (KEGG) (Kanehisa et al., 2000) for the identification of the metabolic pathway for each entry, Microbial Genome Database (MBGD) (Uchiyama, 2007) for comparative analysis and InterPRO database (Hunter et al., 2009) for the gene metabolic functions.

3.10 RT-Real-Time qPCR analysis

Reverse transcription was carried out at 42°C, using 1 µg of RNA, 0.025 µg/µl random primers and the GoScript™ Reverse Transcriptase (Promega), in a final volume of 20 µl, following the manufacturer's instructions. PCR primers were designed with the Primer3 web software and verified for non-specific annealing with primer-blast. Control reactions, lacking reverse transcriptase, were performed for every RNA sample. Real time PCR reactions were accomplished using the iQ™5 Real-Time PCR Detection System (Bio-Rad), in a total volume of 25 µl, using 5 µl of diluted cDNA, 200 nM each of gene-specific primers and the GoTaq® qPCR Master Mix (Promega). After 2 min at 95°C, the PCR program consisted in 40 cycles at 95°C for 15 s and 60°C for 1 min. Fluorescence was measured at the end of the annealing/extension step. Reactions were run in triplicate for each gene and the specificity of the PCR products was verified by gel electrophoresis and melting curve analysis. Results were normalized to the gene 16s rRNA as endogenous control and expression value calculated using the $2^{-\Delta\Delta CT}$ method. For each condition, RNA from three independent cultures was utilized and the mean and standard deviation determined. Primer sequences used in this study and Real-Time qPCR analysis of selected genes are provided in Appendices section (App. 5).

3.11 Diabetic patients' sera

Sera from 43 Sardinian T1DM patients, 56 T2DM subjects, and 48 healthy controls were collected to perform ELISA tests as already described (Sechi et al., 2008). All patient donors gave specific informed consent for the study.

3.12 MAP3733c (MptD) and MAP3738c cloning and protein purification

Nucleotide sequences were originally retrieved from the GenBank *MAP3733c* sequence (GeneID: 2717486) and the *MAP3738c* sequence (GeneID: 2721098) of *Map* strain *K-10* whole genome (NC_002944) GenBank: AE016958 (Li et al., 2005). Genes were amplified using the genomic DNA of *Map* as template purified by phenol-chloroform extraction method (Paccagnini et al., 2009).

Forward primer BamHI-MAP3733c-Fw (5′-GCGCGGATCCATGACGGCCACTAGCTCGACGACCCAGTCCAGTCGCCGC-3'), containing the BamHI restriction site (underlined sequence), and reverse primer PstI-MAP3733c-Rv (5'-GCCGCTGCAGTTATCAAGCTAGGCCGGCCCTCTG-3'), containing the PstI restriction site (underlined sequence), were used to amplify the complete *MAP3733c Map* gene using the proofreading Phusion™ High-Fidelity DNA Polymerase (New England Biolabs, Ipswich, MA, USA) with the following PCR mix: 5x Phusion HF Buffer (10 µl), dNTPs (200 µM), Primer Forward MAP3733c-BamHI (0.4 µM), Primer Reverse MAP3733c-PstI (0.4 µM), Phusion DNA Polymerase (2U), genomic *Map* DNA (150 ng), H_2O until a volume of 50 µl; thermal cycling conditions were as follows: an initial denaturation step at 98°C for 30 s followed by 35 cycles consisting in 98°C for 10 s, 61°C for 20 s and 72°C for 30 s. Eventually, a final extension of 72°C

for 5 min has completed the amplification.

Amplification product was cloned into the expression vector pQE-30 (Qiagen) after double digestion with BamHI and PstI (New England Biolabs) restriction enzymes. Ligation was performed with T4 DNA ligase (Invitrogen) for 2 h at 37°C and construct was electroporated into *E. coli M15 (pREP4)*. Kanamycin/ampicillin resistant clones were confirmed by colony PCR and plasmid restriction analysis to assess *MAP3733c* fragment presence. Briefly, a PCR mix solution (10x Taq buffer (3 µl), MgCl2 (1.5 mM), dNTPs (200 µM), forward primer BamHI-MAP3733c-Fw (0.3 µM), reverse primer PstI-MAP3733c-Rv (0.3 µM), DNAmize Taq Enzyme (1U) (Finnzymes, Woburn, MA, USA) in a final volume of 30 µl) was used to amplify the fragment with the following thermocycler parameters: initial denaturation at 95°C for 3 min and 35 cycles formed by 95°C for 40 s, 65°C for 40 s and 72°C for 1 min, ending with a 72°C final extension for 10 min.

Selected clones were grown until an exponential phase of OD_{600}=0.4 and 100 ml of culture were induced for expression at 27°C for 8 h by the addition of 0.5 mM isopropyl-α-D-thiogalactopyranoside (IPTG) (Sigma). Cells were harvested by centrifugation at 4000 x *g* for 20 min at 4°C and pellet was resuspended in 16 ml of denaturing Ni-NTA lysis buffer (Invitrogen) (6 M Guanidine Hydrochloride, 20 mM NaH_2PO_4, pH 7.8, 500 mM NaCl) supplemented with Triton X-100 (0.25 %). Sample was homogenized by sonication (Bandelin, UW2070) and lysate was then clarified at 4.000 x *g* for 30 min at 4°C. Protein purification was performed by immobilized metal affinity chromatography (IMAC) following the protocol of Ni-NTA resin purification system (Invitrogen) under hybrid conditions with some modifications. Briefly, the lysate was incubated in a column with the resin for 16 h at 4°C with gentle agitation. The next day, the

supernatant was removed and the resin was washed 2 times with 6 volumes of Denaturing Binding Buffer (8 M urea, 20 mM NaH_2PO_4 pH 7.8, 500 mM NaCl), 2 times with 5 volumes of Denaturing Wash Buffer (8 m Urea, 20 mM NaH_2PO_4, pH 6.0, 500 mM NaCl) and 5 times with 7 volumes of Native wash buffer (50 mM NaH_2PO_4, pH 8.0, 500 mM NaCl, 20 mM imidazole). Finally, the recombinant protein was eluted with 10 ml of Native Elution Buffer (50 mM NaH_2PO_4, pH 8.0, 500 mM NaCl, 250 mM imidazole) splitting the eluate in fractions of 1 ml each. Elution fractions were analyzed by sodium dodecyl sulfate (SDS)-polyacrylamide gel electrophoresis (PAGE) to assess protein yield, purity and size by BSA standard (Invitrogen) comparison on gel. Fraction containing purified recombinant protein was concentrated and dialyzed against PBS supplemented with Phenylmethanesulfonyl fluoride (PMSF) 1 mM (Fluka, Biochemika) in Amicon centrifugal filter devices (Millipore, Billerica, MA, USA).

Forward primer NdeI-MAP3738c-Fw (5'-GCGCCATATGAGCGTGACACCTGGCGCCGATC-3'), containing the NdeI restriction site (underlined sequence), and reverse primer XhoI-MAP3738c-Rv (5'-GCGCCTCGAGCCGTGGGTGCAGCACACCGATGA-3'), containing the XhoI restriction site (underlined sequence), were used to amplify *MAP3738c* gene as mentioned above for *MAP3733c* gene. The *MAP3738c* PCR product was cloned into the expression vector pET-28a+(Novagen) and ligated construct was then electroporated into *E. coli BL21(DE3)cp* cells as host for expression. Positive clones were selected by kanamycin resistance and confirmed by colony-PCR and restriction analysis.

Protein expression was induced at OD_{600}=0.5 for 3 h at 37°C by the addition of 1 mM IPTG to 400 ml of cell culture. Cells were harvested by centrifugation, resuspended in 30 ml of Profinia® native lysis buffer

(Biorad, Hercules, CA, USA) (300 mM KCl, 50 mM KH_2PO_4, 5mM imidazole, pH 8.0) and lysozime (1 mg/ml) to be subsequently sonicated as above. Lysate was then clarified and MAP3738c fusion protein was purified by Profinia® protein purification system (Biorad) according to the manufacturer's protocol for native conditions using solutions provided with the commercial kit. Gel electrophoresis, concentration and dialyzation to assess yield and size were performed as above.

3.13 ELISA, bioinformatics and statistical analysis

ELISA experiments to evaluate the humoral responses in T1DM and T2DM sera against the two recombinant antigens MptD and MAP3738c were performed as already described (Sechi et al., 2008).

In silico protein analysis was performed with Sequence Analysis software (Informagen, Inc.) to assess proteins' sizes and physical-chemical properties. ELISA's statistical analysis was carried out with a two-tailed Student's t-test using www.graphpad.com online tool to evaluate the difference between the OD405 average value of diabetic patients and healthy controls. A level of P-value <0.05 has been considered statistically significant among averages. All data were also compared using a Chi-square with Yate's correction assuming a cut-off value derived from the average of healthy control plus two standard deviations (SD) as well as with a Receiver Operating Characteristic (ROC) analysis curve to convalidate the experimental accuracy.

4. RESULTS

4.1 Differential transcriptome of *Map* in acid-nitrosative multi-stress

The whole transcriptome of *Map* that has been highlighted as differentially expressed during the acid-nitrosative stress (Fig. 1) was defined by an up-regulation of 510 genes (App. 1) and a down-regulation of 478 genes (App. 2) for a total of 988 genes differentially expressed. Transcriptional profile may be divided into different types of metabolic patterns according to their functional class. Splitting the entire profile into five macro-metabolic subcategories (Intermediate metabolism, Energy metabolism, Cell wall & membrane, Information metabolism, Cell processes), the transcriptional data can be delineated as follows:

4.1.1 Intermediate metabolism

The subgroup of amino acid metabolism is characterized by a significant up-regulation of the anabolic profile of several amino acids, such as the synthesis of branched-chain amino acids with catalytic subunits of *acetolactate synthase 2* (MAP4208; MAP3000c; MAP0649), and specifically the synthesis of leucine with *2-isopropylmalate synthase* (*leuA*) (MAP0312), as well as an up-regulation of genes involved in the synthesis of aromatic amino acids with *shikimate kinase* (*aroK*) (MAP1092) and *chorismate synthase* (MAP3942) active in the shikimate pathway (Griffin et al., 1995) or specifically with entries for the synthesis of tryptophan such as *anthranilate synthase component I* (*trpE*) (MAP1303) and *tryptophan synthase subunit* (*trpB*) (MAP1306) along with *prephenate dehydrogenase* (*tyrA*) (MAP0277c) for the synthesis of tyrosine. Additional genes for the synthesis of amino acids are up-regulated, such as *alanine dehydrogenase* (*ald*)

(MAP2888) which is involved in the synthesis of alanine from pyruvate, aside from the up-regulation of the synthesis of lysine with more than one entry such as *dihydrodipicolinate synthase* (*dapA*) (MAP1059) and *dihydrodipicolinate reductase* (*dapB*) (MAP2878c) together with *succinyl-diaminopimelate desuccinylase* (*dapE*) (MAP2574c). Worthy of mention is the up-regulation of the metabolism of the methionine's synthesis with *homoserine O-acetyltransferase* (*metA*) (MAP3458) in the first step of synthesis of methionine from homoserine and *methionine synthase* (MAP3055c), which is responsible for the last step of this process (Alaminos et al., 2001). Finally, in the same pattern there is an up-regulation of the synthesis of glutamine with *glutamine synthetase* (*glnA3*) (MAP1599) and a couple of entries related to the synthesis of arginine with *ornithine carbamoyltransferase* (*argF*) (MAP1365) and *argininosuccinate lyase* (*argH*) (MAP1368).

The down-regulation of amino acid metabolism in acid-nitrosative stress is instead featured by the repression of several amino acid anabolisms such as the synthesis of proline with the suppression of the gene *gamma-glutamyl phosphate reductase* (*proA*) (MAP2247c) that is responsible for the second step of the synthesis of proline from glutamate, together with the decrease in synthesis of histidine with *phosphoribosyl isomerase A* (*hisA*) (MAP1297) and *histidinol-phosphate aminotransferase* (*hisC*) (MAP0252c) in the fourth and seventh step of histidine biosynthesis, respectively. Furthermore, there is also a down-regulation of *L-asparaginase* (*ansA*) (MAP1249c) that participates in the synthesis of aspartate through asparagine hydrolysis. The only amino acid catabolism that is down-regulated under acid-nitrosative stress is represented by the repression of the degradation of cysteine with *cysteine dioxygenase type I protein* (MAP1014) and *cysteine*

desulfurase (MAP3058c) required for the production of both sulfate and elemental sulfur.

Another subcategory of intermediary metabolism is given by the metabolism of carbohydrates for which, during acid-nitrosative stress, there is an up-regulation in the catabolism of glycogen with *glycogen debranching enzyme* (*glgX*) (MAP3262c) and *glycogen / alpha-glucan phosphorylase* (*glgP*) (MAP2432c) identified as an enzyme used in starvation periods, sporulation and stress adaptation or during growth adaptation to new environments (Schinzel et al., 1999), together with two *glycoside hydrolase 15* (MAP2215; MAP1384c) which cleave the non-reducing terminal of dextrose-based polysaccharide complexes leading to D-glucose release. On the contrary, in the down-regulated profile, genes responsible for the synthesis of glycogen are repressed such as *glycogen branching enzyme* (*glgB*) (MAP2434) and *glucose-1-phosphate adenylyltransferase* (*glgC*) (MAP2564c) as well as the synthesis of polyhydroxyalkanoic acids (PHAs) with the suppression of *poly-beta-hydroxybutyrate polymerase acid synthase* (MAP1389).

Regarding lipid metabolism, data show a notable shift towards up-regulation of genes involved in the biosynthesis of lipids rather than in the fatty acids degradation. As a matter of fact, genes for lipid biosynthesis are markedly up-regulated such as *beta-ketoacyl synthase* (*kas*) (MAP2603c) for the elongation of the growing acyl chains and *3-oxoacyl-carrier reductase* (MAP3507) together with *3-ketoacyl-(acyl-carrier-protein) reductase* (*fabG4*) (MAP3692c) both employed in the type II fatty acid biosynthesis (Campbell et al., 2001) as well as a *MaoC dehydratase* (MAP3479c). Further up-regulated genes for lipid anabolism are *Malonyl CoA-acyl carrier protein transacylase* (*fabD2*) (MAP4122) and *acyl-[acylcarrier-protein] desaturase*

(*desA2*) (MAP2698c) that participates in the insertion of a double bond in the fatty chain during the synthesis. Finally, the last up-regulated genes involved in the biosynthesis of lipids are *biotin carboxylase-like protein* (MAP1701c), that cooperates in the carboxylation of acetyl-CoA (Jitrapakdee et al., 2003), and *diacylglycerol O-acyltransferase* (MAP1156) in the last step of triglycerides synthesis.

In line with this, in the down-regulated pattern there is a marked increase in the repression of genes involved in lipid degradation, since many genes for lipid catabolism are down-regulated. Among these, repressed entries are *AMP-dependent synthetase and ligase* (MAP2400; MAP2747; MAP3659) required for the transfer of CoA to the fatty acid and entries that participate in fatty acid beta-oxidation such as *acyl-CoA dehydrogenase* (*fadE1*, MAP3539c; *fadE2*, MAP3570c; *fadE15*, MAP1195c; *fadE12*, MAP0910c; MAP2655; *fadE3*, MAP3651c; *fadE25*, MAP0150c; MAP2352; MAP0682; MAP2656; MAP2351; MAP1758c; MAP3238) in the first step of beta-oxidation together with entries for *enoyl-CoA hydratase* (*echA7*, MAP0909c; *echA21*, MAP0249c; *echA6*, MAP0840; *echA12*, MAP1197) required for the hydration of the fatty acid chain. Interestingly, the *patatin protein* (MAP1011), which is involved in the cleavage of fatty acids from membrane lipids, together with the *lipolytic enzyme G-D-S-L family protein* (MAP1022c) is down-regulated.

In addition to lipid metabolism, the subclass of the metabolism of terpenes and terpenoids, in contrast to the general lipid metabolism, is dominated by an increased number of genes for degradation of terpenes and terpenoids during acid-nitrosative stress since entries such as *acyl-CoA dehydrogenase protein* (*fadE3*, MAP2405c; *fadE14*, MAP1553c; *fadE26*, MAP2585), responsible for the degradation of derivatives from geraniol and *cytochrome*

P450 (MAP0009; MAP3553; MAP2015; MAP0522), required for the degradation of limonene and pinene derivatives, are up-regulated. Differently, genes involved in the synthesis of terpenoids are repressed since entries such as *2-C-methyl-D-erythritol 4-phosphate cytidylyltransferase* (*ispD*) (MAP0476) in the synthesis of isoprenoids through the non-mevalonate pathway (Kishida et al., 2003) and *isopentenyl pyrophosphate isomerase* (MAP3079c) are down-regulated.

Within the pattern of nucleotide metabolism it is interesting to note an up-regulation of the pyrimidine biosynthetic (*pyr)* operon repressor *pyrimidine regulatory protein* (*pyrR*) (MAP1114), for this reason *Map* must make up for the loss of synthesis of pyrimidines through a bypass with *FAD-dependent thymidylate synthase* (*thyX*) (MAP2865c) required for the synthesis of dTMP and *deoxycytidine triphosphate deaminase* (*dcd*) (MAP3820) which is involved in the production of dUMP, the immediate precursor of thymidine nucleotides. An up-regulation can be observed also for *ribonucleotide reductase stimulatory protein* (*nrdI*) (MAP3101c) employed in the synthesis of deoxyribose and eventually in degrading damaged nucleotides with *hydrolase, NUDIX protein* (MAP3088c) (Bessman et al., 1996).

Otherwise, a reduction of the expression for genes involved in the recycling of purines was observed as can be seen by the down-regulation of *hypoxanthine-guanine phosphoribosyltransferase* (*hpt*) (MAP0439) and *guanylate kinase* (*gmk*) (MAP1123) in the salvage of GMP in addition to an entry required for adenine deamination as a source of nitrogen such as a*denine deaminase protein* (MAP4314). In contrast to the up-regulation pattern, where a repression of *pyr* operon was triggered, coherently the *pyr* system appears down-regulated with *CTP synthetase* (*pyrG*) (MAP1406) in the synthesis of CTP and *orotidine 5'-phosphate decarboxylase* (*pyrF*)

(MAP1120) involved in the synthesis of pyrimidines via the classical *pyr* pathway.

As for the last subclass of intermediary metabolism, represented by the metabolism of vitamins and cofactors, an up-regulation of enzymes required for the synthesis of vitamin B12 was observed with entries such as *cobalamin biosynthesis protein* (*cbiX*) (MAP2037), which participates in the anaerobic insertion of cobalt into the corrin ring, *cobyrinic acid a,c-diamide synthase* (MAP3314c), *cobalamin synthesis protein* (*cobW*) (MAP3772c) and *nicotine-nucleotide-dimethylbenzimidazole phosphoribosyltransferase* (*cobT*) (MAP1948) required for the assembling of the cofactor's nucleotide loop in anaerobic metabolism. The synthesis of molybdopterin appears to be up-regulated with *molybdenum cofactor biosynthesis* (*mog*) (MAP0803) and *UBA/THIF-type NAD/FAD binding protein* (*moeB*) (MAP3306c) as well as the synthesis of folate with entries such as *aminodeoxychorismate lyase protein* (MAP1079), *GTP cyclohydrolase I* (*folE*) (MAP0449) in the first step of tetrahydofolate synthesis and *dihydropteroate synthase* (*folP*) (MAP0450) from the second step to the seventh step of the synthesis. The synthesis of menaquinone is up-regulated with three entries such as *isochorismate synthase* (*entC*) (MAP3316) which is responsible for the first step, *O-succinylbenzoic acid-CoA ligase* (*menE*) (MAP4038c) required for the fourth and *O-succinylbenzoate synthase* (*menC*) (MAP4050), in addition there is also an up-regulation of heme synthesis with *uroporphyrinogen decarboxylase* (*hemE*) (MAP2799c) in the fifth step and *glutamate-1-semialdehyde aminotransferase* (*hemL*) (MAP4020).

Unlike from the up-regulation pattern, genes involved in the synthesis of FMN or FAD are repressed with *bifunctional riboflavin kinase / FMN adenylyltransferase* (*ribF*) (MAP2893c), in addition to the down-regulation

of *lipoyl synthase* (*lipA*) (MAP1959) in the synthesis of lipoate and *ribokinase:carbohydrate kinase (*MAP0876c) in the synthesis of thiamine. Eventually, there is also a down-regulation of the synthesis of ubiquinone with the repression of *3-octaprenyl-4-hydroxybenzoate carboxy-lyase* (*ubiX*) (MAP1635c) together with a suppression of the biotin synthesis with *biotin synthase* (*bioB*) (MAP1283) required for the last step of synthesis followed by the repression of *pantothenate kinase* (*coaA*) (MAP2700; MAP0458) in the synthesis of coenzyme A and several entries for *pyridoxamine 5′-phosphate oxidase-related FMN-binding protein* (MAP3177; MAP3028; MAP2630c; MAP0828) related to the synthesis of vitamin B6.

4.1.2 Energy metabolism

The energy metabolism of *Map* during the acid-nitrosative stress includes the up-regulation of genes involved in glycolysis such as *phosphopyruvate hydratase* (*eno*) (MAP0990; MAP3133c) responsible for the enolization and the production of pyruvate, which participates in acetyl-CoA synthesis entering the pyruvate dehydrogenase complex that is up-regulated with three entries such as *dihydrolipoamide acetyltransferase dlaT* (*sucB*) (MAP1956), *pyruvate dehydrogenase E1 component, beta subunit* (*pdhB*) (MAP2308c) and *flavoprotein disulfide reductase* (*lpdA*) (MAP3424c). However, in this stress experiment, it seems that acetate originates also from the degradation of citrate to oxaloacetate and acetyl-CoA with *citrate lyase beta subunit* (*citE*, MAP2310c; MAP1688) which is up-regulated. The acetate could then enter the Krebs cycle, some entries of which are also up-regulated such as *citrate synthase type II* (*gltA2*) (MAP0829) in the first step, *isocitrate dehydrogenase NADP-dependent* (*icd2*) (MAP3456c) and *succinate dehydrogenase cytochrome b subunit* (*sdhC*) (MAP3441). The

reducing power is then channeled to the electron transport chain, some components of which are up-regulated such as *NAD(P)H quinone oxidoreductase, PIG3 family* (MAP0263c), but with a different final electron acceptor than molecular oxygen with the up-regulation of *nitrite reductase (NAD(P)H) small subunit* (*nirD*) (MAP3703) that reduces nitrite to ammonia and *periplasmic nitrate reductase* (MAP4100c) for nitrate as a final acceptor (Bacon et al., 2004). Alternative to Krebs cycle, but in parallel, *Map* up-regulates components of the glyoxylate pathway with two entries such as *isocitrate lyase* (*aceAb*) (MAP1643) and *isocitrate lyase protein* (MAP0296c). Conversely, in the down-regulation pattern *Map* represses oxidative phosphorylation by attenuating the expression of entries such as *F0F1 ATP synthase subunit* (*atpC*) (MAP2450c), *NADH dehydrogenase subunit* (*nuoG*) (MAP3207), *ubiquinol-cytochrome c reductase cytochrome b subunit* (*qcrB*) (MAP1935) and *fumarate reductase / succinate dehydrogenase flavoprotein domain protein* (MAP0691c) that together describe a repression of aerobic respiration with molecular oxygen as final electron acceptor during this stress.

4.1.3 Cell wall & membrane

The metabolism of transport in acid-nitrosative stress is represented by an up-regulation of genes involved in the uptake of cobalt such as *cobalt / nickel transport system permease protein* (MAP3732c) and *sulfonate / nitrate / taurine transport system permease protein* (MAP0146; MAP1809c; MAP1109) required for the transport of nitrate together with the transport of chloride with the up-regulation of *chloride channel protein* (MAP3690). During the stress there is an increase in the iron storage with the up-regulation of *siderophore interacting FAD binding protein* (MAP1864c)

although with two factors for iron uptake such as *iron complex transport system substrate-binding protein* (*fecB*, MAP3092; MAP3727). Finally, a factor required for the uptake of carbohydrates such as *mannitol dehydrogenase domain protein* (MAP0879c) which belongs to the phosphotransferase system (PTS) (Fischer et al., 1991) is up-regulated.

Among the down-regulated entries are genes for cation transport, coherently consistent with the uptake of anions in the up-regulated outline, with the repression of two entries for *cation diffusion facilitator family transporter* (MAP3865c; MAP2784), *SAPB family trasnporter* (*mgtC*) (MAP1524) for magnesium, *modD* (MAP1569) for molybdenum and *SPFH domain-containing protein / band 7 family protein* (MAP3183) along with the down-regulation of phosphate uptake by forced *pho* system (Kim et al., 1993) since *phoH family protein* (*phoH2*) (MAP2697c) is repressed. Moreover genes involved in the transport of lipids such as *DegV family protein* (MAP2240c) and *transmembrane transport protein* (*mmpL10*) (MAP2232) are down-regulated. Unlike the up-regulated profile, in the down-regulated pattern there is an increased expression of genes related to the synthesis of mycobactin with two entries such as *mycobactin salicylate-AMP ligase* (*mbtA*) (MAP2178) and *mycobactin polyketide synthetase* (*mbtC*) (MAP2175c) thus emphasizing the repressive feature on iron uptake rather than the induced iron storage in the up-regulated outline.

It is interesting to notice that during acid-nitrosative stress, within the cell wall and membrane metabolism, genes involved in cell wall construction are up-regulated such as *UDP-N-acetylglucosamine 1-carboxyvinyltransferase* (*murA*) (MAP2447c), *UDP-N-acetylmuramoylalanyl-D-glutamate-2,6-diaminopimelate ligase* (*murE*) (MAP1902c), and *esterase protein* (*fbpC2*) (MAP3531c) along with *S-layer domain protein* (MAP0951)

for the assembly of the surface polycrystalline layer of glycoproteins above the lypoglican envelope (Sara et al., 2000), *D-alanyl-D-alanine carboxypeptidase* (MAP0904) and *ErfK / YbiS / YcfS / YnhG family protein* (MAP3634). It is important to note an up-regulation of the lipopolysaccharide (LPS) synthesis with entries such as *UDP-galactopyranose mutase* (*glf*) (MAP0211), *NAD-dependent epimerase / dehydratase* (*rmlB2*) (MAP0430) and *DTDP-4-dehydrorhamnose reductase* (*rmlD*) (MAP3380c) in the synthesis of rhamnose-derived units of the O-antigen. Moreover, among up-regulated genes are *glycosyl transferase group 1* (MAP1666c), *exopolysaccharide biosynthesis tyrosine-protein kinase* (MAP0952) and *D,d-heptose 1,7-bisphosphate phosphatase protein* (MAP3251) required for the construction of the the inner core's precursor (Kneidinger et al., 2002). Finally, the biosynthesis of membrane phospholipids seems up-regulated in acid-nitrosative stress with entries such as *PA-phosphatase related protein* (MAP1265) involved in the synthesis of diacylglycerol useful to produce phosphatidylcholine and phosphatidylethanolamine, together with *phosphatidylethanolamine N-methyltransferase* (MAP3086c) responsible for the synthesis of phosphatidyl-N-methylethanolamine, *PBP family phospholipid-binding protein* (MAP1885c), *phospholipid / glycerol acyltransferase* (MAP3059c), *diacylglycerol kinase catalytic region* (MAP3285c), which is involved in the synthesis of phosphatidic acid (PA) (Smith et al., 1994) and *phosphatidylserine decarboxylase* (*psd*) (MAP3930c).

On the contrary, in the down-regulation pattern of cell wall and membrane metabolism, it is worth noting that during the acid-nitrosative stress there is a repression of genes involved in the degradation of the cell wall such as *carbohydrate-binding protein* (MAP0847), *lytic transglycosylase* (4324c)

required for the degradation of murein in the cell wall recycling process during division and separation (van Asselt et al., 1999), *membrane-bound lytic murein transglycosylase B-like protein* (MAP2552) and finally a couple of *transglycosylase domain protein* (MAP0805c; MAP0974) together with *mannan endo-1,4-beta-mannosidase* (MAP1971). In addition to these, a repression of cell division was inferred, since c*ell division FtsK / SpoIIIE* (MAP4321c) for cytokinetic ring assembly (Begg et al., 1995), *cell division initiation protein DivIVA* (*wag31*) (MAP1889c) and *ATPase involved in chromosome partitioning-like protein* (MAP3043c) were down-regulated along with a *protein of unknown function DUF881* (MAP0014) involved in the division process.

Finally, there is a down-regulation of the synthesis of mycolic acids consistent with the repression of *2-trans-enoyl-acyl carrier protein reductase* (*inhA*) (MAP1210), c*yclopropane-fatty-acyl-phospholipid synthase* (*mmaA4*) (MAP4116c), *3-oxoacyl-(acyl carrier protein) synthase II* (*kasB*) (MAP1999) and *methyltransferase type 12 / Cyclopropane-fatty-acyl-phospholipid synthase* (MAP3738c) in the synthesis of cyclopropane fatty acids.

4.1.4 Information metabolism

The subcategory of the information metabolism during acid-nitrosative stress is characterized by the up-regulation of *two-component transcriptional regulator* (*phoP*) (MAP0591) recognized as a positive regulator for the phosphate regulon as well as a virulence factor in *M. tuberculosis* (Perez et al., 2001). Several transcription factors are up-regulated during the stress such as *protein of unknown function YGGT* (MAP1890c) thought to be activated in response to hyperosmotic stress (Ito

et al., 2009), *transcriptional regulator CRP / FNR family* (MAP0082) which responds to various stress stimuli such as oxidative stress and nitrosative stress (Körner et al., 2003); interestingly, among up-regulated entries are also *RNA polymerase sigma factor sigE* (MAP2557c) induced by oxidative stress or during infection of macrophages (Graham et al., 1999), *transcriptional regulator oxyS* (MAP3522) as regulator of oxidative stress response that mimics *oxyR* (Domenech et al., 2001). It is important to note the up-regulation of transcription factors for activating the uptake and catabolism of carbohydrates such as *transcriptional regulator araC family* (MAP1652c; MAP0223c) along with *ferric uptake regulator Fur family protein* (*furB*) (MAP2139) a key protein in the control of intracellular iron concentration.

Within the down-regulated transcriptional profile, it is worth noting the suppression of *anti-sigma regulatory factor, serine / threonine protein kinase* (*rsbU*) (MAP2361) which makes possible, through the activation of *rsbV*, the release of *sigB* factor sequestered by *rsbW* (Delumeau et al., 2004), moreover among repressed entries is *RNA polymerase sigma factor sigH* (MAP3324c) that is one of the activators of *sigB*. It is interesting to notice that also *RNA polymerase sigma factor sigA* (MAP2820), an important sigma factor recognised as differently expressed in other studies (Manganelli et al., 1999; Sechi et al., 2007; Lam et al., 2008) is repressed, along with several *transcriptional regulator, merR family* (MAP1541; MAP1543; *hspR*, MAP3843), that can be traced to a general stress of starvation maybe due to a partial stationary phase condition, and many *transcriptional regulator, tetR family* (MAP1477c; MAP3052c; MAP2394; MAP0969; MAP3891; MAP2023c; MAP1721c; MAP3689; MAP0179c; MAP2262; MAP4290; MAP2003c) involved in the suppression of the susceptibility to hydrophobic

antibiotics such as tetracycline (Kisker et al., 1995). During the stress there is also a down-regulation of *transcriptional regulator, arsR family protein* (MAP0661c) required for the suppression of resistance to arsenic compounds together with the repressor of the cell wall synthesis *cell wall envelope-related protein transcriptional attenuator* (MAP3565). Finally, it is worth noting the repression of *transcription factor regulator WhiB* (*whiB4*) (MAP0393), which is useful for differentiation and cell division.

The second subgroup of the information metabolism is the translation where it is possible to notice a marked up-regulation of translation apparatus with several ribosomal proteins (*rpmG*, MAP3769c; *rpsC*, MAP4167; *rpmE*, MAP2463c; *rplA*, MAP4113; MAP3771; *rpsJ*, MAP4160; *rpsH*, MAP4181; *rplB*, MAP4164) and elongation factors such as *translation elongation factor Tu* (*tuf*) (MAP4143). Regarding the up-regulation of factors involved in the synthesis of tRNAs a specific up-regulation of *tryptophanyl-tRNA synthetase* (*trpS*) (MAP3453c), *methionyl-tRNA synthetase* (*metS*) (MAP0972c), *aspartyl / glutamyl-tRNA amidotransferase subunit* (*gatA*) (MAP3045c) and *aspartyl / glutamyl-tRNA amidotransferase subunit* (*gatC*) (MAP3046c) was detected whereas *phenylalanyl-tRNA synthetase subunit* (*pheS*) (MAP1359) was repressed.

The last subgroup of the information metabolism is the signal transduction within which, during acid-nitrosative stress, transduction through kinases is up-regulated with *sensor signal transduction histidine kinase* (MAP1101), a couple of *serine / threonine protein kinase* (*pknG*, MAP3893c; *pknL*, MAP1914) together with a *two-component system, OmpR family, sensor histidine kinase* (*prrB*) (MAP0833c) which is involved in the adaptation to a new environment or to intracellular growth (Graham et al., 1999). Together with this, an increase of signal transduction through inositol was registered

with the up-regulation of *inositol monophosphatase* (*impA*) (MAP1298).

On the other hand, it is important to note a repression of phosphatase-mediated signal transduction since entries such as *protein tyrosine phosphatase* (*ptpA*) (MAP1985), already known in intracellular persistence (Bach et al., 2008), are down-regulated as well as are the transduction by G proteins with *40-residue YVTN family beta-propeller repeat protein* (MAP1007) and by cAMP with *adenylate cyclase protein* (MAP2672) along with the suppression of cation-mediated signaling with *K+-transporting ATPase chain subunit* (*KdpC*, MAP0997c; *KdpE*, MAP0995c) in the response to nutritional stimuli or changes in osmolarity (Treuner-Lange et al., 1997).

4.1.5 Cell processes

During acid-nitrosative stress, the *Map*'s metabolism of detoxification reveals an up-regulation of detoxification enzymes such as *copper / zinc superoxide dismutase* (*sodC*) (MAP3921), which is responsible for the degradation of superoxides, together with *catalase / peroxidase HPI* (*katG*) (MAP1668c) and *alpha / beta hydrolase fold protein* (*bpoC*) (MAP3537c) for peroxides elimination, as well as *arsenate reductase* (*arsC*) (MAP0982c) and *arsenical pump membrane protein* (*arsb2*) (MAP0484c) for detoxification from arsenic acid or heavy metals (Rosen, 1990). It is important to note the up-regulation of the resistance to multiple antibiotics with several entries such as *aminoglycoside phosphotransferase* (MAP2082; MAP3197; MAP0267c) required for the inactivation of aminoglycosidic antibiotics by phosphorylation, *antibiotic transport system permease protein* (MAP3532c) and *prolyl 4-hydroxylase, alpha subunit* (MAP1976) in the hydroxylation-mediated inactivation.

Within the down-regulated pattern, thiol-specific antioxidant genes are

repressed since *thiol peroxidase* (*tpx*) (MAP1653), *alkyl hydroperoxide reductase / Thiol specific antioxidant / Mal allergen* (MAP0401) and *bacterioferritin comigratory protein, alkyl hydroperoxide reductase / thiol specific antioxidant* (*bcp*) (MAP2329) are down-regulated as well as some general antioxidants such as *thioredoxin* (*trxC*) (MAP4340) and *alpha / beta hydrolase fold protein* (*ephE*) (MAP0404c) involved in the detoxification from oxidatively damaged lipids.

Regarding the subgroup of antigenicity and virulence, it is worth noting the up-regulation of *PE-PGRS family protein* (MAP4144) and several PPE proteins (MAP0123; MAP1516; MAP1519; MAP2595; MAP3185; MAP1003c) thought to be responsible for the antigenic diversity. Furthermore, several virulence factors required for cell invasion or escape are up-regulated such as *hemolysin / protein of unknown function DUF21: transporter* (MAP1551c) and three *mammalian cell entry associated membrane protein* (*mce)* (MAP1857; MAP0767c; MAP3609) together with a couple of *cutinase* (MAP4237c; MAP3495c) perhaps involved in the destruction of the host cell membrane lipids (Schue' et al., 2010).

Otherwise, the down-regulated data of this sub-metabolism show the repression of several immunogenic factors such as *immunogenic protein MPT6* (MAP2950c), *ESAT-6 like protein* (*esxD*) (MAP0160) and *secretion protein* (*snm4*) (MAP1510), as well as an *unknown function DUF1396 protein* (*lprG*) (MAP1138c), all virulence factors but not necessarily immunogenic, suggesting a change in the antigenic profile of the bacterium, not due to a repression of the antigenic diversity, but to an alternative antigenic profile.

The response to acid-nitrosative stress is characterized by the up-regulation of many stress chaperonins such as c*haperone protein DnaJ* (MAP1695c),

heat shock protein Hsp20 (MAP1698c), *co-chaperone GroES/Cpn10* (MAP4264), *chaperonin GroEL* (MAP4265) for the protein folding along with resistance factors such as *acid resistance membrane protein* (MAP1317c) for resistance to acids and three entries of *acyltransferase 3* (MAP3276c; MAP3514; MAP1271c) required for peptidoglycan O-acylation in order to increase its resistance (Bera et al., 2006). There is also an up-regulation in the response to DNA damage with the activation of a not-SOS dependent repair system with *endonuclease IV* (*end*) (MAP4132), *excinuclease ABC subunit* (*uvrA*) (MAP1341), *exodeoxyribonuclease III xthA* (MAP3916c) for the removal of damaged nucleotides (Mol et al., 1995), *uracil-DNA glycosylase: Phage SPO1 DNA polymerase-related protein* (MAP3256c) and *formamidopyrimidine-DNA glycosylase* (MAP0889) specific for oxidized purines (Sugahara et al., 2000).

Lastly, the *Map*'s transcriptome under acid-nitrosative stress shows the repression of few general chaperonins, probably due to stationary phase starvation, such as *chaperonin GroEL2* (MAP3936) and *universal stress protein uspA* (MAP1741c) identified in "stress endurance" response not due to acute stress (Sousa et al., 2001), as well as the down-regulation of *activator of Hsp90 ATPase 1 protein family* (MAP1640c) and *DO serine protease htrA* (MAP2555c), a heat shock protein together with the *osmoprotectant transport system permease protein* (*proW*) (MAP0274) for osmotic shock.

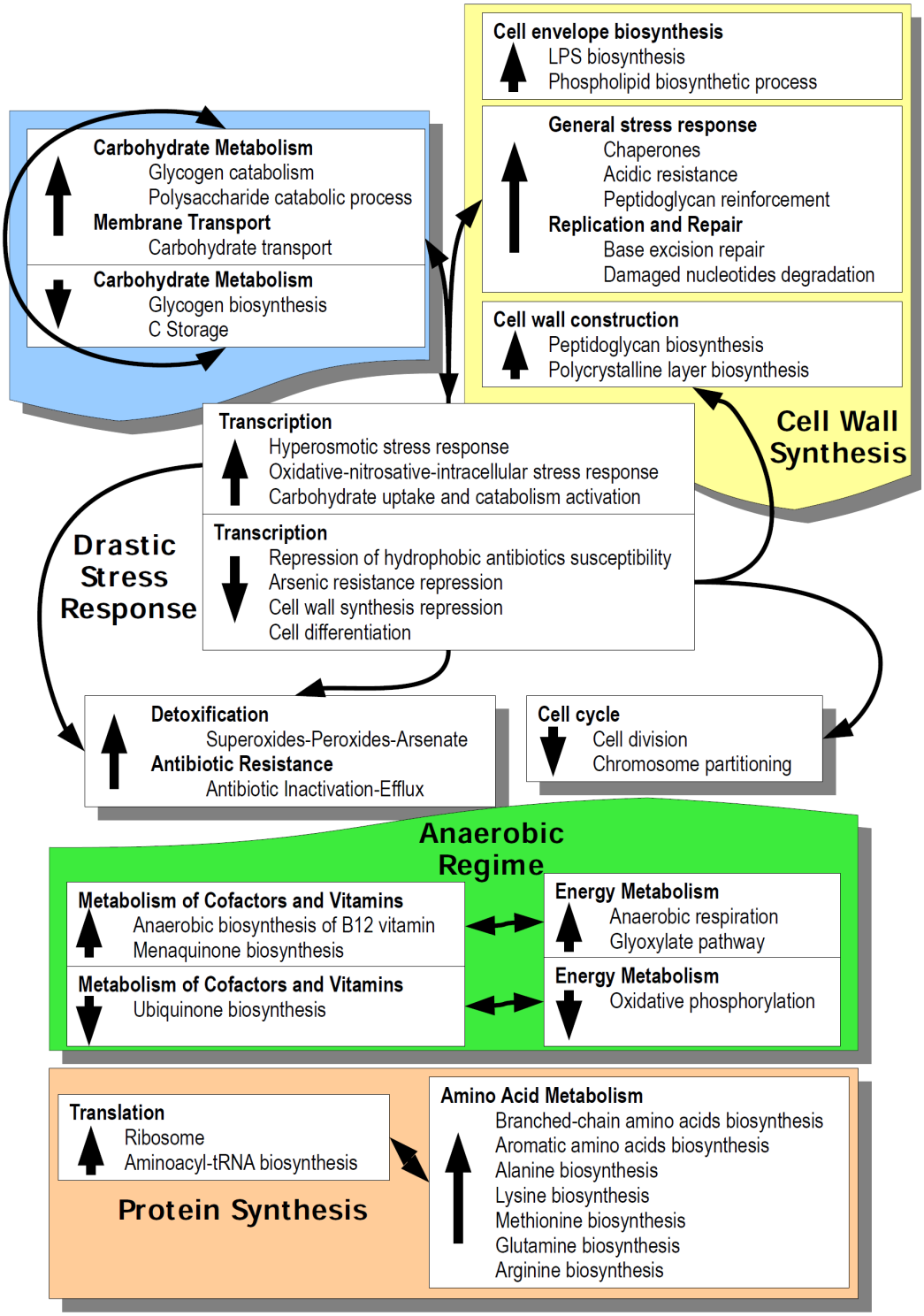

Figure 1. Schematic diagram of the metabolic hightlights from the *Map* transcriptional profile in the acid-nitrosative multistress. Differentially expressed genes during multi-stress were grouped based on the Kyoto Encyclopedia of Genes and Genomes (KEGG) classification and sorted by function. Colored frames indicate functional inter-related macro-groups. Unidirectional arrows indicate possible transcriptional relationship in terms of consequentiality as well as bidirectional arrows indicate bijective correlations between different transcriptional sections.

4.2 Differential transcriptome of *Map* during the infection of THP-1 human macrophages

In vitro infection of the macrophage cell line THP-1 with *Map* (shown representatively in Fig. 2) has led to a differential transcriptional pattern of the bacterium (Fig. 3) with the expression of a total of 455 genes, 171 of which are up-regulated (App. 3) and 284 are down-regulated (App. 4), hence it is possible to notice that there is a greater number of down-regulated genes than up-regulated genes.

4.2.1 Intermediate metabolism

Concerning the intermediate metabolism, the subcategory of amino acid metabolism shows a marked difference during infection between the up-regulated framework, dominated by a relevant increase in the degradation of amino acids, and the down-regulated pattern, from which it can be noted that there is a suppression of the amino acid synthesis during the macrophage infection. In particular it is interesting to notice that in the up-regulated framework there is an increased expression of genes in the degradation of asparagine with *L-asparaginase* (*ansA*) (MAP1249c) that catalyzes the hydrolysis of asparagine to aspartate and ammonium, together with the degradation of glutamate with *NAD-glutamate dehydrogenase* (MAP2294c) required for its deamination and two entries that play a significant role in the catabolism of phenylalanine such as *3-(3-hydroxyphenyl)propionate hydroxylase* (*mphA*) (MAP0694) that catalyzes the oxygenation of the phenylic ring and *fumarylacetoacetate hydrolase protein* (MAP0881) in the last step in the degradation path of phenylalanine (Bateman et al., 2001). Finally, it is important to note that the catabolism of cysteine is up-regulated with *cysteine desulfurase / selenocysteine lyase*

(MAP1190), which is involved in the removal of sulfur to yield alanine, an important gene in the synthesis of S-based cofactors (Mihara et al., 2002).

Differently, in the down-regulation pattern there is a clear shift towards the amino acid anabolism. Therefore, the synthesis of histidine is down-regulated with three entries such as *phosphoribosyl-ATP pyrophosphatase* (*hisI*) (MAP1847c) in the second step of the synthesis path, *histidinol-phosphate aminotransferase* (MAP4211) in the seventh step, which requires vitamin B6 as a cofactor and *histidinol dehydrogenase* (*hisD*) (MAP1293) in the last step concerning the oxidation of histidinol to histidine. Among down-regulated entries are also those required for the synthesis of methionine with four repressed genes such as *O-acetylhomoserine aminocarboxypropyltransferase* (*metC*) (MAP3457), *homocysteine methyltransferase* (MAP2279), *B12 synthase-dependent methionine* (*metH*) (1859c) involved in the last step of *de novo* synthesis that requires vitamin B12 as cofactor, and lastly *cystathione beta-lyase* (MAP2055) in the synthesis of methionine from cysteine using vitamin B6 as cofactor. The synthesis of threonine seems down-regulated with *threonine synthase* (*thrC*) (MAP2467c) together with the synthesis of glutamine for which *glutamine synthetase* (*glnA2*) (MAP1966c), responsible for the condensation of glutamate and ammonia to yield glutamine, was repressed along with the down-regulation of the synthesis of lysine with *dihydrodipicolinate reductase protein* (MAP2013c; MAP3619) in the second step of lysine synthesis.

The second subgroup of the intermediate metabolism, the metabolism of carbohydrates, shows during THP-1 infection an up-regulation of *beta-glucosidase* (*lpqI*) (MAP3688) which participates in the hydrolysis of beta-linkages in polysaccharides and the consequently release of free glucose.

The down-regulated profile shows rather the opposite process to the degradation of polysaccharides, although with formation of alpha-linkages, with *glucose-1-phosphate adenylyltransferase* (*glgC*) (MAP2564c) involved in the synthesis of glycogen.

The lipid metabolism is characterized by a slight up-regulation of the synthesis of lipids with two entries such as *3-ketoacyl-(acyl-carrier-protein) reductase* (*fabG2*) (MAP2408c) required for the synthesis of fatty acids and *MaoC domain protein dehydratase* (MAP3479c).

On the other hand during the THP-1 infection, *Map*'s degradation of lipids is heavily down-regulated with the repression of *AMP-dependent synthetase and ligase* (*fadD13*) (MAP2874c) responsible for the entrance of fatty acids in the beta-oxidation pathway, *acyl-CoA dehydrogenase-related protein* (MAP3238) and *acyl-CoA dehydrogenase domain protein* (*fadE6*) (MAP3716c) which catalyzes the first cycle of the beta-oxidation, as well as three entries for *enoyl-CoA hydratase* (*echA9*, MAP1018c; *echA19*, MAP0549c; *echA16*, MAP2904) that participate in hydration of the chain and *acetyl-CoA acyltransferase* (*fadA6*) (MAP3337) which catalyzes the last step of degradation. Lastly, a gene involved in the degradation of sterols, *steroid delta-5-3-ketosteroid isomerase* (MAP1773c), is down-regulated.

The metabolism of terpenes and terpenoids during the THP-1 infection is in line with the general metabolism of lipids, since there is a down-regulation of the degradation of terpenes, terpenoids and their derivatives, with the repression of *3-oxoacid CoA-transferase, subunit A* (MAP0515c) and *acyl-CoA dehydrogenase protein* (*fadE9*) (MAP4214c) involved in the degradation of geraniol derivatives as well as two *cytochrome P450* (MAP0344c; MAP1614c) required for degradating limonene derivatives and *limonene-1,2-epoxide hydrolase* (MAP2852) responsible for the hydrolysis of epoxides

which are formed upon activation of limonene derivatives (Arand et al., 2003).

The nucleotide metabolism is characterized by the up-regulation of genes involved in the elimination of potentially toxic nucleotide derivatives from the nucleotide pool with entries such as *ADP-ribose pyrophosphatase* (MAP1407) for degradating ADP-ribose to AMP and ribose and *adenosine kinase* (*cbhK*) (MAP1942c) that catalyzes the salvage synthesis of 5'-AMP from adenosine and ATP (Long et al., 2003). In parallel, there is an up-regulation of *deoxyuridine 5'-triphosphate nucleotidohydrolase* (*dut*) (MAP2814c) for the removal of UTP to synthesize UMP and *cytidylate kinase* (*cmk*) (MAP1414) in the phosphorylation of CMP to CDP.

Within the nucleotide metabolism, among the down-regulated entries are genes involved in the synthesis of purines with *amidophosphoribosyltransferase* (*purF*) (MAP0638) and *phosphoribosylglycinamide formyltransferase 2* (*purT*) (MAP3871) which catalyzes the third step of synthesis path. It is interesting to notice that there is also a down-regulation in the synthesis of pyrimidines with *orotate phosphoribosyltransferase* (*umpA*) (MAP3857) and specifically for uracil with *CMP / dCMP deaminase zinc-binding protein* (MAP0662c).

As far as the metabolism of cofactors and vitamins is concerned, among up-regulated genes are those specific for the synthesis of folate such as *aminodeoxychorismate lyase protein* (MAP1079) and *dihydrofolate reductase* (dfrA) (MAP2868c) along with genes responsible for the synthesis of porphyrins such as *uroporphyrinogen decarboxylase* (*hemE*) (MAP2799c) and *ferrochelatase* (*hemZ*) (MAP1211) for heme production. In addition, there is an increase in the synthesis of B12 cofactor through anaerobic process by up-regulation of *nicotine-nucleotide-*

dimethylbenzimidazole phosphoribosyltransferase (*cobT*) (MAP1948) together with the up-regulation of the synthesis of biotin with *8-amino-7-oxononanoate synthase* (*bioF*) (MAP1275) in the first committed step required for its production and the biosynthesis of menaquinone that is up-regulated with *naphthoate synthase* (*menB*) (MAP4044c).

In opposite to the up-regulation profile, in the down-regulation pattern is traceable a repression of genes involved in the synthesis of B12 cofactor under aerobic conditions with *cobaltochelatase subunit* (*cobN*) (MAP1805c) required for the aerobic synthesis of its corrin ring, along with the down-regulation of the synthesis of coenzyme A with *pantothenate kinase* (*coaA*) (MAP2700) and *dephospho-CoA kinase / protein folding accessory domain-containing protein* (MAP1326) which catalyzes the last step in CoA synthesis.

4.2.2 Energy metabolism

During THP-1 infection *Map* up-regulates *aconitic hydratase 1* (*acn*) (MAP1201c) that is used both in Tricarboxylic acid (TCA) cycle and in glyoxylate pathway. In addition there is also an up-regulation of the the pentose phosphate pathway with *glucose-6-phosphate 1-dehydrogenase* (MAP1687) required for the first step of the path.

On the other hand, among down-regulated genes are two entries for TCA cycle with *citrate synthase* (*gltA1*) (MAP0295c) involved in the first step of the path and *malate dehydrogenase* (*mdh*) (MAP2541c), as well as five entries for oxidative phosphorylation and ATP synthesis using molecular oxygen as final electron acceptor such as *NADH dehydrogenase subunit* (*nuoG*) (MAP3207), *NADH dehydrogenase* (*ndh*) (MAP1561c), *NAD(P)H quinone oxidoreductase, PIG3 family* (MAP0245c) and finally *ATP synthase I*

(MAP2458c) together with *F0F1 ATP synthase subunit* (*atpE*) (MAP2456c).

4.2.3 Cell wall & membrane

As far as the metabolism of transport is concerned, it is important to note an increase in protein translocation with the up-regulation of three entries such as *preprotein translocase subunit* (*secG*) (MAP1167) and a couple of *peptide / nickel transport system permease protein* (MAP1087; MAP1088). There is also an up-regulation of factors concerning the transport of chloride such as *chloride channel protein* (MAP3690) and the "low-affinity" uptake of phosphate with *phosphate transporter* (*pitA*) (MAP4041c) (Gebhard et al., 2009) as well as *sulfonate / nitrate / taurine transport system permease protein* (MAP1109) involved in the nitrate transport. Finally, it is worth noting how the *binding-protein-dependent transport system inner membrane component* (*sugB*) (MAP2546c), which is responsible for sugar transport and uptake, is up-regulated together with *isochorismatase hydrolase protein* (*entB*) (MAP2259) required for capturing iron from host cell's iron chelator compounds (Payne, 1994).

On the other hand, in the down-regulated expression profile there is a repression of the "forced" system of phosphate uptake with four entries such as *phoH like family protein* (MAP2160c), *phosphate transport system permease protein* (*pstA1_2*) (MAP0874), *phosphate transport system permease protein* (*pstA1_1*) (MAP0653) and *phosphate transporter ATP-binding protein* (*phoT*) (MAP0654), thus showing the repression both in the activation of the *pho* system and in the induction of the *pst* system. It is interesting to notice that the down-regulated pattern is also dominated by the repression of the uptake of cationic metals such as nickel with *high affinity nickel transporter protein* (*nicT*) (MAP2924) and molybdenum with

modD (MAP1569) and *molybdate transport system ATP-binding protein* (*modC*) (MAP1568). It is also worth noting how the transport of lipids is suppressed with *mmpL11* (MAP3637c) and *mmpl domain-containing protein* (MAP2233) along with the down-regulation of the mycobactin synthesis with *mbtH domain protein* (*mbtH*) (MAP1419).

The cell wall and membrane metabolism of *Map* during the THP-1 infection is characterized by the up-regulation of genes involved in the synthesis of membrane lipid structures such as LPS with the up-regulation of *D,d-heptose-1,7-bisphosphate phosphatase protein* (MAP3251) involved in the production of the precursor of the LPS inner core as well as entries required for the synthesis of phospholipids such as *phospholipid / glycerol acyltransferase* (MAP1160c), *1-acyl-sn-glycerol-3-phosphate acyltransferase* (MAP1920c), *phospholipid / glycerol acyltransferase, hemolysin* (MAP3059c), *CDP-diacylglycerol--glycerol-3-phosphate 3-phosphatidyltransferase* (*pgsA2*) (MAP1535), which participates in the synthesis of cardiolipin (Jackson et al., 2000) and *CDP-diacylglycerol--glycerol-3-phosphate 3-phosphatidyltransferase* (*pgsA3*) (MAP2857c). Finally, there is also an up-regulation in the production of mycolic acids with *esterase protein* (*fbpC2*) (MAP3531c) that is necessary for the biogenesis of the chord factor.

On the contrary, the down-regulated expression pattern is mainly featured by the suppression of the synthesis of peptidoglycan with genes such as *GDPmannose 4,6-dehydratase* (*gmdA*) (MAP1231) required for the first step in the synthesis of GDP-fucose from rhamnose (Kneidinger et al., 2001), *bifunctional phosphoglucose / phosphomannose isomerase* (MAP3368c), which is involved in the biosynthesis of the capsular polysaccharide, *undecaprenyldiphospho-muramoylpentapeptide beta-N-*

acetylglucosaminyltransferase (*murG*) (MAP1897c), responsible for the last step in the intra-linkage of the glycan structure, *phospho-N-acetylmuramoyl-pentapeptide-transferase* (*murX*) (MAP1900c), which participates in the formation of the first lipid intermediate of peptidoglycan and finally *UDP-N-acetylmuramoylalanyl-D-glutamate--2,6-diaminopimelate ligase* (*murE*) (MAP1902c). It is interesting to note the down-regulation of *maf-like protein* (MAP3401) responsible for the inhibition of the partitioning septum, thus suggesting a possible increase in cell division during infection.

4.2.4 Information metabolism

The differential expression pattern of the up-regulated profile related to the regulation of transcription is characterized by the up-regulation of genes concerning the regulation of sugar metabolism such as *transcriptional regulator, araC family* (MAP3758c; MAP1652c) and *transcriptional regulator, gntR family* (MAP3599c) that regulate the biosynthesis of sugars. The last up-regulated entry is *transcriptional regulator, merR family* (MAP3267c) which is important for the response to oxidative stress and antibiotics.

Among the down-regulated genes are two sigma factors such as *ECF subfamily RNA polymerase sigma-24 factor SigI* (MAP0170) which is activated in response to general stress and *RNA polymerase sigma factor SigJ* (MAP3446c) required for the regulation of expression in stationary phase cultures (Hu et al., 2001). The susceptibility to lipophilic antibiotics is repressed since four genes coding for *transcriptional regulator, tetR family* (MAP3052c; MAP0155; MAP2262; MAP0335) are down-regulated along with the repression of the glyoxylate path with *transcriptional regulator, iclR family* (MAP1446c).

The translational apparatus appeared to be down-regulated with three ribosomal proteins (*rplN*, MAP4177; *rpsM*, MAP4230; *rpmI*, MAP1353) repressed together with the processing of rRNA and tRNA with the down-regulation of *ribonuclease BN* (MAP3452c; MAP1682c) and *tRNA delta(2)-isopentenylpyrophosphate transferase* (*miaA*) (MAP2841c).

Regarding signal transduction, the last subgroup of information metabolism, worth of note is the up-regulation of phosphatases with *phosphodiesterase, MJ0936 family* (MAP3534c), in addition to *K+-transporting ATPase B chain* (MAP0998c) involved in the cation-mediated response and *two-component response transcriptional regulator* (*tcrA*) (MAP1102c).

Genes that were identified as down-regulated are *inositol monophosphatase* (MAP3187) required for signaling through inositol and *serine / threonine protein kinase* (*pknA*, MAP0018c; MAP3844) which is responsible for signaling through kinases. Moreover among down-regulated genes are *mechanosensitive ion channel / cyclic nucleotide-binding domain-containing protein* (MAP2248c) in osmotic stress response (Pivetti et al., 2003), *cheB methylesterase* (MAP3232; MAP3235c) in chemotaxis (Djordjevic et al., 1998) and *diguanylate cyclase / phosphodiesterase with PAS / PAC sensor (s)* (MAP1346c; MAP2512) acting as oxygen sensors (Taylor et al., 1999).

4.2.5 Cell processes

With respect to the detoxification metabolism during macrophage infection, *Map* up-regulates *copper / zinc superoxide dismutase* (*sodC*) (MAP3921) in order to dismutate superoxides, and increases its antibiotic resistance by up-regulating genes such as *aminoglycoside phosphotransferase* (MAP3197), which catalyzes the phosphorylation of aminoglycosides, *prolyl 4-*

hydroxylase, alpha subunit (MAP1976), required for the hydroxylation of antibiotics and *antibiotic transport system permease protein* (MAP3532c) for their efflux.

On the other hand, in this metabolism it is worth of note that among down-regulated genes are those involved in the repression of the arsenate detoxification system with two *permease* (*arsA*, MAP2805; *arsC*, MAP0982c), and *alpha / beta hydrolase fold protein* (*ephF*) (MAP3550) responsible for the detoxification from oxidatively damaged lipids.

Virulence and antigenicity of *Map* during infection of THP-1 are dominated by the up-regulation of *mpt64* (MAP3290c), *hemolysin A* (*tlyA*) (MAP1401), *peptidase M22* (MAP4261), and one *PE-PGRS protein* (MAP4144).

On the contrary, *iron-regulated heparin binding hemagglutinin* (*hbha*) (MAP3968) for host cell adhesion, as well as *MCE-family protein mce1C* (MAP4086) for the invasion of mammalian host cells, are down-regulated thus limiting the invasive feature of *Map* during intramacrophage infection.

Lastly, there is a down-regulation of components belonging to antigenic variability such as four *PPE family protein* (MAP0966c; MAP2927; MAP1515; MAP3737) that are repressed.

Finally, it is worth noting that in the stress metabolism there is an up-regulation of *acid-resistance membrane protein* (MAP1317c) specific for resistance to acidic environment, *universal stress protein, uspA* (MAP1754c) and two entries for the repair of damaged DNA such as *recombination protein* (*recR*) (MAP0316c) and *endonuclease IV* (*end*) (MAP4132).

On the other hand, within this metabolism two entries such as *heat shock protein Hsp20* (MAP3268) and *chaperone protein* (*dnaJ*) (MAP1695c) are repressed along with *domain-containing protein PitT* (MAP2680c; MAP2027c) required for *Map*'s survival under nutritional stress.

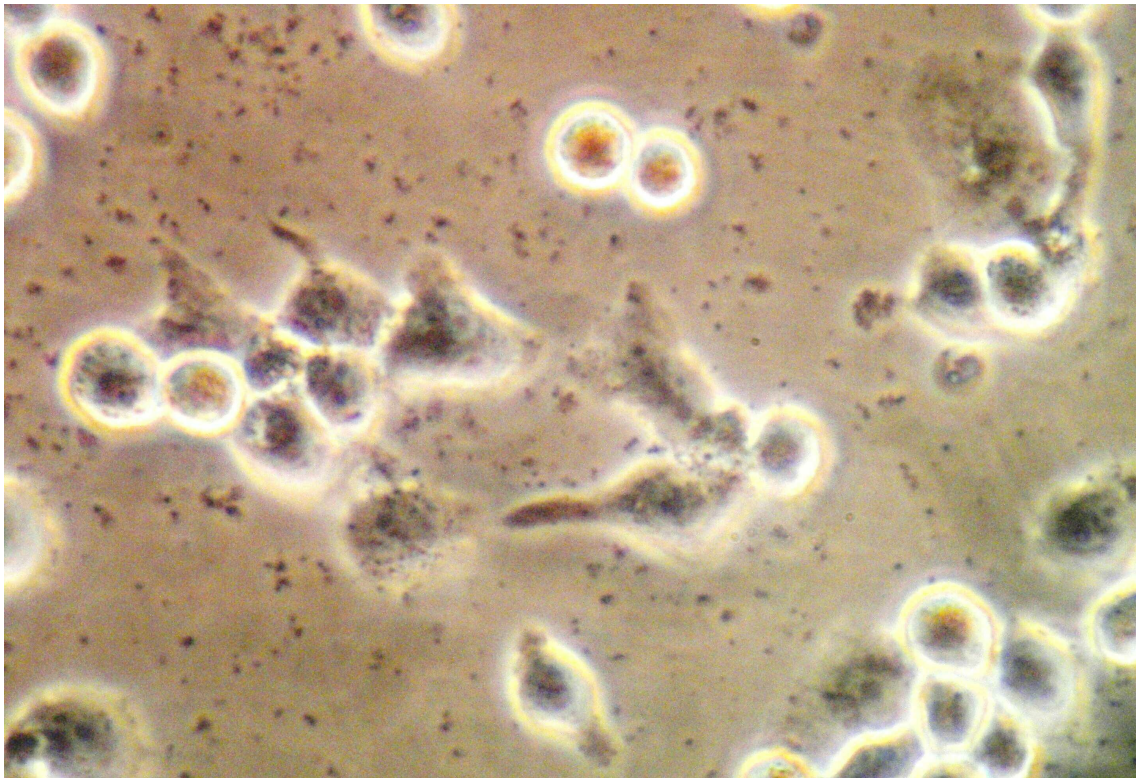

Figure 2. THP-1 cells infected with *M. paratuberculosis*. Infections were performed in T75 vented flasks containing monolayers with a confluence of approximately $1x10^5$ cells/cm2. Inocula for infection were prepared by resuspending bacteria in pre-warmed RPMI medium at 37°C and cells were declumped through a 21 gauge needle. Cells were infected for 24 h at 37°C at 5% CO_2.

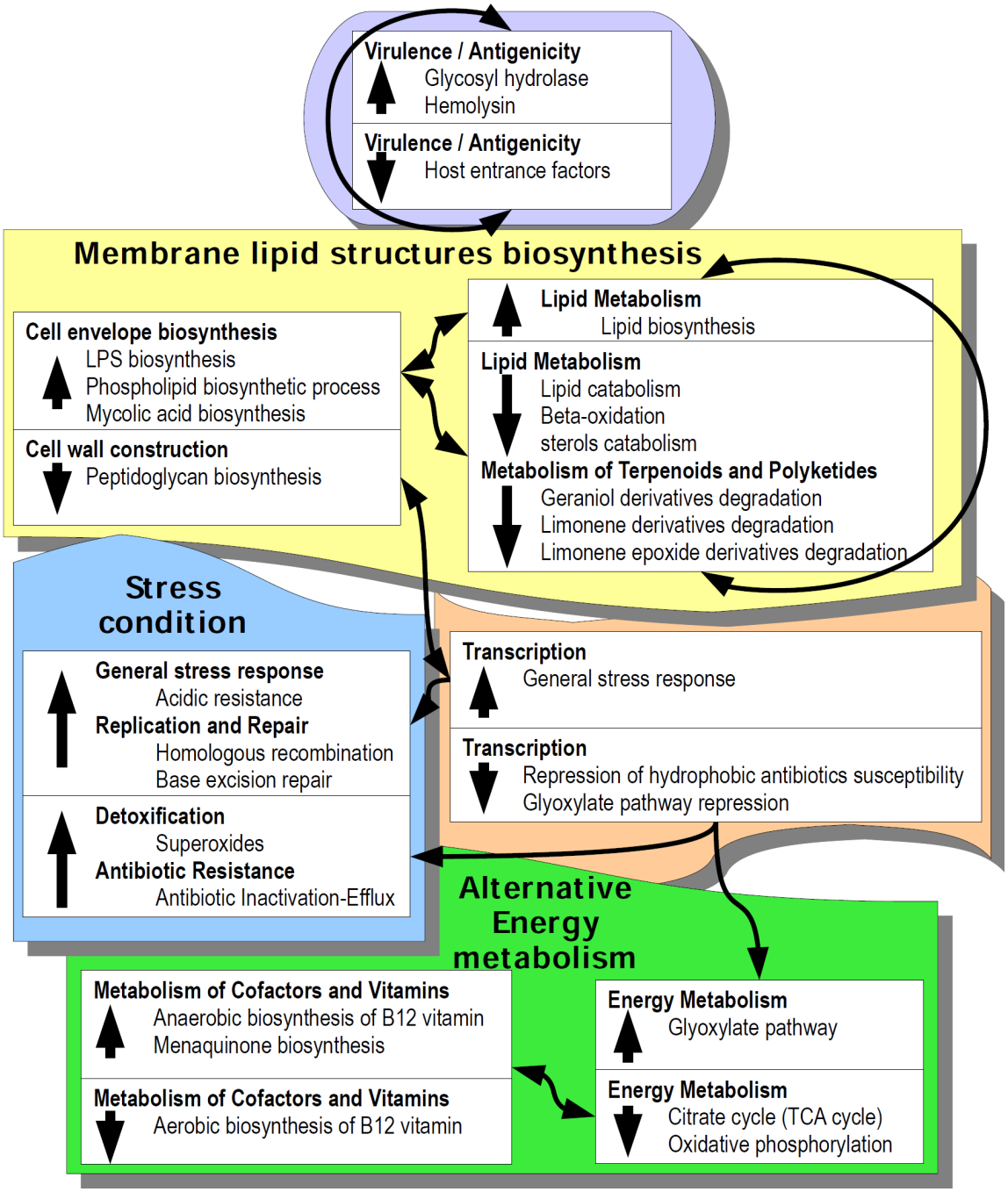

Figure 3. Schematic diagram of the metabolic hightlights from the *Map* transcriptional profile during THP-1 infection. Differentially expressed genes during cellular infection were grouped based on the Kyoto Encyclopedia of Genes and Genomes (KEGG) classification and sorted by function. Colored frames indicate functional inter-related macro-groups. Unidirectional arrows indicate possible transcriptional relationship in terms of consequentiality as well as bidirectional arrows indicate bijective correlations between different transcriptional sections.

4.3 Comparison of acid-nitrosative multi-stress and THP-1 infection *Map*'s transcriptomes

Map's transcriptome resulting from the acid-nitrosative stress is more complex and rich (n = 988) than the detectable transcriptome during infection of the macrophage line THP-1 (n = 455). Between the two transcriptomes it is possible to find analogies of up-regulation or down-regulation for several entries since 50 and 24 genes are commonly up-regulated and down-regulated, respectively (Fig. 4). Homologies can be found in the intermediate metabolism, where there is a repression of the synthesis of glycogen both in the acid-nitrosative stress (*glgB*, *glgC*) and in the cellular infection (*glgC*), thus highlighting a limitation in extracellular sources of carbohydrates. In the lipid metabolism both transcriptional profiles underline an up-regulation trend towards the lipid synthesis (MAP3479c) together with a repression of lipid degradation (MAP3238), in broad agreement with other studies where lipid synthesis was already observed as up-regulated in experiments of multiple-stress in *M. tuberculosis (*Deb et al., 2009) since they may serve as nutrient storage.

The down-regulation of pyrimidine synthesis is a common repressed metabolism between the acid-nitrosative stress and the infection especially in the first where the synthesis is repressed by the *pyrR* regulator resulting in a down-regulation of *pyr* genes, perfectly correlated with the same mechanism of genic regulation occurred in previous experiments inherent *M. tuberculosis*'s response to inhibitors of translation (Boshoff et al., 2004) in which it was shown that the translational inhibition induced the bacterium to trigger a response that included both the repression of *de novo* nucleotides synthesis and the increase of the synthesis of ribosomes. The acid-nitrosative stress transcriptional profile, which includes a pattern of

expression that shows both the up-regulation of the *pyrR* repressor and the up-regulation of ribosomal structural proteins, could therefore suggest that the acid-nitrosative stress can act as an inhibitor of translational apparatus.

Finally, the situation appears very complex in the common metabolism of synthesis of vitamins and cofactors in which the up-regulation of folate synthesis occurs in both transcriptional profiles with the same entry *aminodeoxychorismate lyase protein* (MAP1079) as well as the synthesis of vitamin B12 (*cobT*) and the synthesis of porphyrins (*hemE*). In this case, the up-regulation of porphyrins synthesis may be due to the situation of starvation that requires *Map* to shift its energy metabolism from an aerobic condition to an anaerobic state using enzymes that cooperate with ferredoxines in the transfer of electrons in redox reactions as like as a metabolism pattern already identified in previous studies with the induction of slow growth and hypoxic cultures of *M. smegmatis* (Berney et al., 2010).

Further evidences about the switch of energy metabolism from aerobic pathway to anaerobic conditions are represented by the common up-regulation of the synthesis of menaquinone in both experiments, respectively with *menA* and *menB* in acid-nitrosative stress and in the cellular infection, since it could be an essential factor for the survival of non-replicating mycobacteria (Dhiman et al., 2009), thus corroborating the decrease of cell multiplication given by the down-regulation of functional genes for cell division. The only homology in the down-regulation profile of metabolism of cofactors is the repression of *pantothenate kinase* (*coaA*) probably in line with the down-regulation of lipid degradation.

As far as the energy metabolism is concerned, both transcriptomes are characterized by the up-regulation of the glyoxylate pathway in particular in

the acid-nitrosative stress with *isocitrate lyase* (*aceAb*), which was identified in many works as a factor expressed by mycobacteria to survive inside the macrophage and in other infection models as well as during growth with lipids as the sole sources of carbon (Russell et al., 2010). Nevertheless, the up-regulation of genes involved in the synthesis of lipids, especially in the construction of lipid membrane structures, is in contrast with previous works reporting that, inside the macrophage, mycobacteria such as *M. tuberculosis* shifted their energy metabolism to the use of fatty acids in beta-oxidation (Rohde et al., 2007).

However, the regime of anaerobic respiration is further confirmed by the down-regulation of oxidative phosphorylation both for subunits of *NADH dehydrogenase* and for other complexes involved in electron transport chain together with *F0F1 ATPase* subunits as already observed in experiments with *M. tuberculosis* under nutrient starvation (Betts et al., 2002), oxidative agents (Voskuil et al., 2011) and in infection of macrophages (Schnappinger et al., 2003) in addition to the common down-regulation of *nuoG,* which was identified in *M. tuberculosis* as an antiapoptotic factor for macrophages (Velmurugan et al., 2007).

With respect to the metabolism of transport, it is worth noting a common up-regulation of factors related to chloride (MAP3690) and nitrate (MAP1109) transport, where the latter gene may reflect the up-regulation of a certain type of anaerobic respiration during nitric stress or in infection by using nitrate as an alternative electron acceptor (Moreno-Vivian et al., 1999). The transition of energy generation from aerobic to anaerobic mechanism, however seems more like imposed on the bacterium rather than induced from the bacterium because of the nitrosative agent as noted in *M. bovis* (Boon et al., 2002).

On the other hand, in both down-regulated transcriptomes the phosphate uptake via *pho* system is repressed along with molybdenum uptake (*modD*) and the transport of lipids with several *mmpl* proteins, in addition to a common down-regulation of mycobactin production.

In the complex metabolism of cell wall and membrane, both transcriptomes show a common up-regulation of the synthesis of LPS (MAP3251) and membrane phospholipids (MAP3059c) while in the cell processing metabolism, a common up-regulation of resistance factors to multiple antibiotics (MAP3197, MAP1976, MAP3532c), together with a common down-regulation of some *tetR* factors (MAP3052c; MAP2262) involved in the suppression of the resistance to lipophilic antibiotics, is consistently present as similarly seen in *M. tuberculosis* with multiple stress experiments (Deb et al., 2009). Additionally, the detoxification metabolism underlines a common degradation pathway for reactive oxygen species with *superoxide dismutase* (*sodC*) which was also found to be significantly expressed in *M. tuberculosis* during oxidative stress (Voskuil et al., 2011) together with the up-regulation of *acid-resistance membrane protein* (MAP1317c) in order to cope with the acidic environment and *endonuclease IV* (*end*) required for the repair of DNA damage, and previously identified in *M. tuberculosis* after treatment with antibacterial agents (Waddell et al., 2004). Finally, *Map*'s virulence exhibits a common up-regulation of the *PE-PGRS family protein* (MAP4144) in both transcriptomes which might be a common response to the antigenic diversity profile.

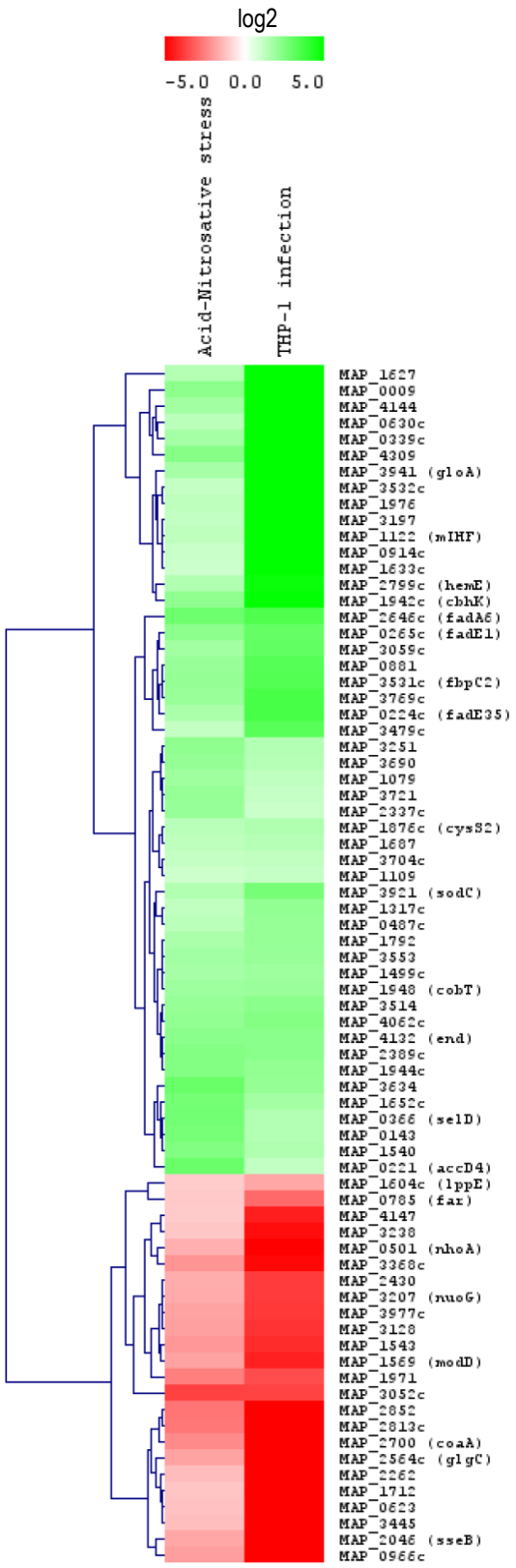

Figure 4. Functional clustering of common regulated *Map* genes under acid-nitrosative multi-stress and THP-1 infection. Expression ratios were log2-transformed, and displayed according to the color code at the top of the figure. The Euclidean average linkage clustering was performed to generate a gene tree shown at the left side of the figure. Venn diagrams showing the number of overlapping and unique genes modulated more than 2.0-fold under the two experimental conditions are on the right of each colored macrocluster. The number of induced or repressed overlapping genes is indicated in the green ellipse or red ellipse, respectively.

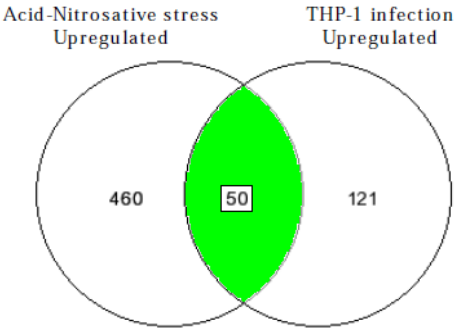

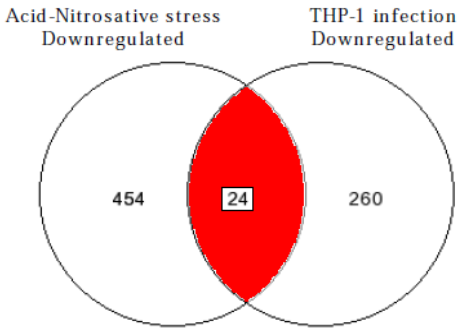

4.4 Cloning and expression of MAP3733c (MptD) and MAP3738c proteins

A gene encoding a putative bacterial integral membrane protein belonging to a *Map* ABC transporter was cloned. A 650 bp PCR product containing the *MAP3733c* ORF flanked by BamHI and PstI restriction sites was amplified and inserted into the pQE-30 expression vector, producing a construct that carried the *MAP3733c* ORF with upstream codons for a 6xHis tag which size was predicted in 24kDa. MptD recombinant protein was purified by Ni-NTA affinity chromatography under modified hybrid conditions because native purification with automated chromatography systems such as Profinia® failed. On PAGE analysis the 6xHis tagged MptD fusion protein migrated at the expected molecular mass of 24 kDa (Fig. 5). Due to the high content of hydrophobic amino acids (about 51%), the expression yield of this protein was low, nevertheless eluted fraction was found to be very high in purity without any non-specific band. Concentration and dialyzation gave an approximate yield of 300 µg/L of culture.

A second gene (*MAP3738c*) encoding a hypothetical protein was expressed. *In silico* analysis of *MAP3738c* has shown its involvement in mycolic acid biosynthesis as cyclopropanation enzyme or methyltransferase on methoxy-mycolic acids. *MAP3738c* was efficiently cloned into the pET-28a+vector. The cloned ORF was preceded at N-terminal by a sequence encoding for MGSSHHHHHHSSGLVPRGSH with a histidine tag and followed by a second 6xHis tag at the C-terminal. The expression of the 272 aa resulting protein was efficiently performed with high purity and optimal yield in native conditions. After concentration and dialyzation a yield of 600 µg/L culture was roughly assessed. SDS-PAGE analysis confirmed purity and an expected size of 31 kDa (Fig. 5).

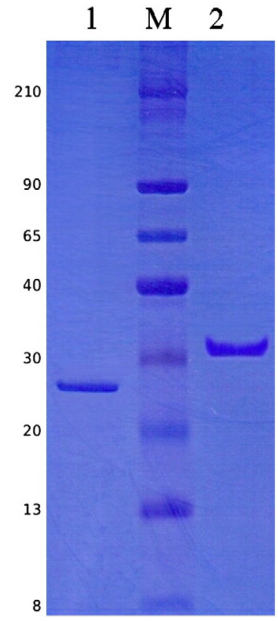

Figure 5. (SDS-PAGE) Purified recombinant proteins MAP3733c (MptD) and MAP3738c. Lane 1: purified protein MptD from induced *E.coli*: pQE30-*MAP3733c* at 24 kDa. Lane M: ColorBurst (Sigma) molecular weight marker. Lane 2: purified protein MAP3738c from induced *E.coli BL21(DE3)*: pET28a-*MAP3738c* at 31 kDa.

4.5 ELISA: Immunoreactivity of T1DM and T2DM patients′ sera against MAP3733c (MptD) and MAP3738c recombinant fusion proteins

Due to the lack of immunogenicity by the 6xHis tag, as these residues are uncharged at pH 7.2–7.4 and result in a poorly immunogenic action towards the majority of species (Crowe et al., 1996), both fusion proteins were tested in ELISA for evaluation of immune response in diabetic sera against MptD and MAP3738c proteins without removing tags as well. Moreover, T1DM and control sera were analyzed with a specific recombinant protein belonging to *Helicobacter pylori* (HP0986) tagged with 6xHis tag, which gave a negative result for the presence of a significant immune response against it (data not shown).

ELISA tests were performed with 43 T1DM sera, 56 T2DM sera and 48 healthy control sera against MAP3733c (MptD) and MAP3738c recombinant proteins to investigate the presence of humoral response against these

antigens. ELISA results showed an increased humoral response in T1 diabetic sera against both MAP3733c and MAP3738c proteins compared to healthy sera (Fig. 6) [MAP3733c (MptD); t student = 7.70; FD= 89; p=0.000000000017 (P<0.0001); 95%], [MAP3738c; t student= 6.49; FD=89; p=0.0000000045; (P<0.0001); 95%]. Area Under ROC Curve (AUC) (Fig. 6) confirmed the accuracy of the difference between averages for both proteins' experiments [MAP3733c (MptD); AUC=0.8576], [MAP 3738c; AUC=0.8278]. Assuming a cut-off value of 0.4 absorbance units at OD405 (average of healthy controls + 2SD) (Tab. 1), much greater than the ROC analysis curve's cut-off, set to approximately 0.2 absorbance units, MptD protein's ELISA results shown as a statistical analysis by the Chi-square with Yate's correction, generated χ equal to 21.657 with 1 degree of freedom and a two-tailed P value of 0.0001 showing a statistically significant difference between T1 diabetic patients and healthy controls. In the same way, data for MAP3738c recombinant protein with a 0.4 cut-off gave a Chi-square with Yate's correction equal to 12.344 with 1 degree of freedom and a two-tailed P value equals to 0.0004.

Data from T2 diabetic sera pool (Fig. 7) (Tab. 1) showed no difference between T2 sera and controls for both proteins: [(MAP3733c (MptD); t student=1.89; FD=102; p=0.0612; 95%; AUC=0.5822] and [MAP3738c; t student=0.11; FD=102; p=0.9108; 95%; AUC=0.5456]. Similarly, Chi-square analysis of T2DM ELISA data gave a χ value of 0.329 (MptD) and 1.581 (MAP3738c) with a P value of 0.5662 and 0.2086 respectively, showing no correlation between humoral immune response against *Map* and T2DM. In conclusion, both ELISA data showed an increased antibody presence against the two *Map* specific antigens in T1DM sera, unlike sera of healthy controls and T2DM patients.

Healthy control (sample name)	Sex	Age at blood sample (yr)	Family history of Diabetes (type)	Seropositivity for:	
				MAP3733c (MptD)	MAP3738c
1c	F	33	ND	-	-
2c	M	25	ND	-	++
3c	F	50	ND	-	-
4c	F	36	ND	-	-
5c	F	67	ND	-	-
6c	M	45	ND	-	-
7c	M	45	ND	-	-
8c	M	53	ND	-	-
9c	M	37	ND	-	-
10c	M	63	ND	-	-
11c	M	63	ND	-	-
12c	M	45	ND	-	-
13c	F	60	ND	-	-
14c	F	43	ND	-	-
15c	F	34	ND	-	-
16c	F	25	ND	-	-
17c	M	57	ND	-	-
18c	F	26	ND	-	-
19c	F	41	ND	-	+
20c	M	37	ND	-	-
21c	M	48	ND	-	-
22c	F	57	ND	-	-
23c	M	31	ND	-	++
24c	M	37	ND	-	-
25c	M	39	ND	-	-
26c	M	28	ND	-	-
27c	F	35	ND	-	+
28c	F	21	ND	-	-
29c	M	45	ND	-	-
30c	M	39	ND	-	-
31c	M	46	ND	-	+
32c	F	19	ND	-	-
33c	M	35	ND	-	-
34c	M	49	ND	-	-
35c	F	25	ND	-	-
36c	M	42	ND	-	-
37c	F	61	ND	-	++
38c	M	31	ND	-	-
39c	F	29	ND	-	-
40c	M	53	ND	-	-
41c	M	25	ND	+	+
42c	M	23	ND	-	-
43c	M	28	ND	-	-
44c	F	35	ND	-	-
45c	M	21	ND	-	-
46c	M	28	ND	+	-
47c	M	29	ND	-	-
48c	M	23	ND	-	-

Diabetic patient T1DM (sample name)	Sex	Age at blood sample (yr)	Family history of Diabetes (type)	Seropositivity for:	
				MAP3733c (MptD)	MAP3738c
1d1	M	21		-	-
2d1	F	31		++	++
3d1	M	36	I	+++	+++
4d1	F	36		-	-
5d1	M	37		-	-
6d1	M	26	II	-	-
7d1	M	30	I/II	+	+
8d1	F	37	I	-	-
9d1	F	37	I	+	++
10d1	F	27	I	+	+
11d1	M	31	I	-	-
12d1	M	40	I	-	+
13d1	M	38		++	-
14d1	F	37	I	+	++
15d1	F	35		+	+
16d1	F	40	II	-	-
17d1	F	34		-	+
18d1	M	41	I	-	-
19d1	F	36	I	-	-
20d1	F	37		+	-
21d1	F	32		+	+
22d1	M	43		-	-
23d1	F	33	I	++	++
24d1	F	33		+++	+++
25d1	M	38		+	+
26d1	M	33		++	++++
27d1	M	32		-	-
28d1	M	26	II	+	+++
29d1	F	32	I	++	+++
30d1	F	38		+	-
31d1	M	34		-	+
32d1	M	94		+++	++++
33d1	M	36		-	-
34d1	M	27	I	+++	++++
35d1	M	33	I	+	++
36d1	F	33		-	-
37d1	F	23	I	-	+
38d1	M	43	II	-	+
39d1	M	34		+++	-
40d1	F	59	I	-	-
41d1	F	42	I	-	-
42d1	F	47	II	-	-
43d1	ND	ND	ND	-	-

Diabetic patient T2DM (sample name)	Sex	Age at blood sample (yr)	Family history of Diabetes (type)	Seropositivity for:	
				MAP3733c (MptD)	MAP3738c
1d2	M	62		-	-
2d2	F	66		-	-
3d2	M	66	II	-	-
4d2	M	81		-	-
5d2	M	74	ND	-	-
6d2	M	62	II	-	-
7d2	F	50	II	-	-
8d2	M	53	II	-	-
9d2	M	75		-	-
10d2	F	72	ND	-	+
11d2	F	40	ND	-	-
12d2	F	76	ND	-	-
13d2	M	57	ND	-	-
14d2	M	62	II	-	-
15d2	F	77		-	-
16d2	M	56		-	-
17d2	M	71	I	-	-
18d2	M	65		-	-
19d2	F	66		-	-
20d2	M	69		-	-
21d2	M	75		-	-
22d2	M	63	ND	-	-
23d2	F	60		-	-
24d2	M	68	I	-	-
25d2	M	57	II	-	-
26d2	M	66	ND	-	++
27d2	M	76	II	-	-
28d2	F	74	ND	-	-
29d2	F	76	ND	-	-
30d2	F	64	ND	-	-
31d2	M	69		-	-
32d2	M	66	ND	-	-
33d2	F	65	ND	+	-
34d2	M	65	ND	-	-
35d2	F	73	II	-	-
36d2	M	80	ND	-	-
37d2	M	62	II	-	-
38d2	M	70	ND	-	-
39d2	M	74	ND	-	-
40d2	M	78		+	-
41d2	M	78	ND	-	-
42d2	F	53		-	-
43d2	F	49		-	-
44d2	M	69		-	-
45d2	M	70		-	-
46d2	M	72		++	-
47d2	M	60	II	-	-
48d2	F	67	ND	-	-
49d2	M	53	II	-	-
50d2	M	56		-	-
51d2	M	62	ND	+	+
52d2	F	73	ND	-	-
53d2	M	66		-	-
54d2	F	60		-	-
55d2	F	62	ND	+	-
56d2	F	55	ND	-	-

Table 1. Characteristics and ELISA results of healthy controls′ sera (left), type I diabetes patients′ sera (center), and type II diabetes patients′ sera (right) against recombinant antigens MAP3733c (MptD) and MAP3738c. M, male; F, female; ND, not determined; I, type I diabetes; II, type II diabetes. Arbitrary values were taken depending on the reading values in relation to a cut-off set at OD405=0.4 (control average plus 2 SD). Values are the following: – indicates a value less than 0.4, + indicates a value of 0.4–0.5, ++ indicates a value of 0.5–0.6, +++ indicates a value of 0.6–0.7, and ++++ indicates a value of 0.7–0.8.

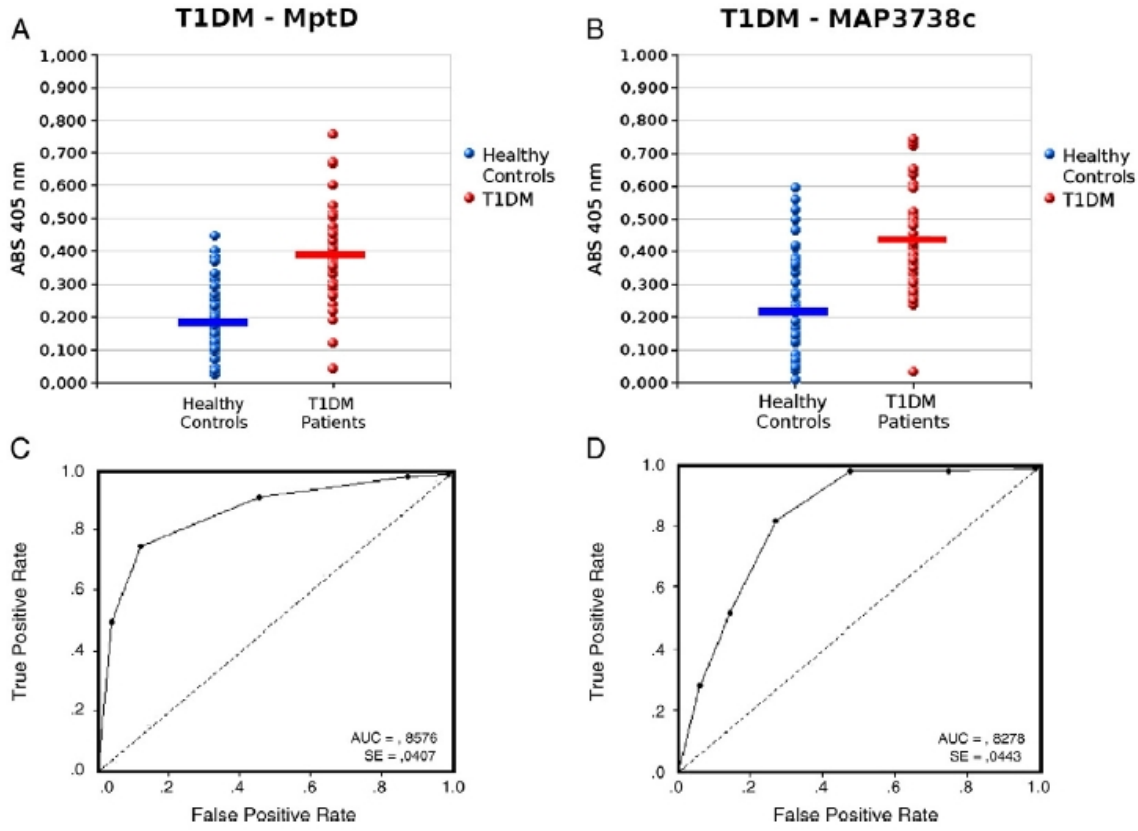

Figure 6. Evaluation of immunoreactivity against MAP3733c (MptD) recombinant protein (A), and MAP3738c recombinant protein (B) in sera from 43 patients with type I diabetes mellitus and 48 healthy controls. Data are shown as values of OD405 nm for each serum in performed ELISA. The average value for each population is indicated by the bolded horizontal line. ROC curve statistical analysis indicates the AUC value for experiments with MptD (C) and MAP3738c (D).

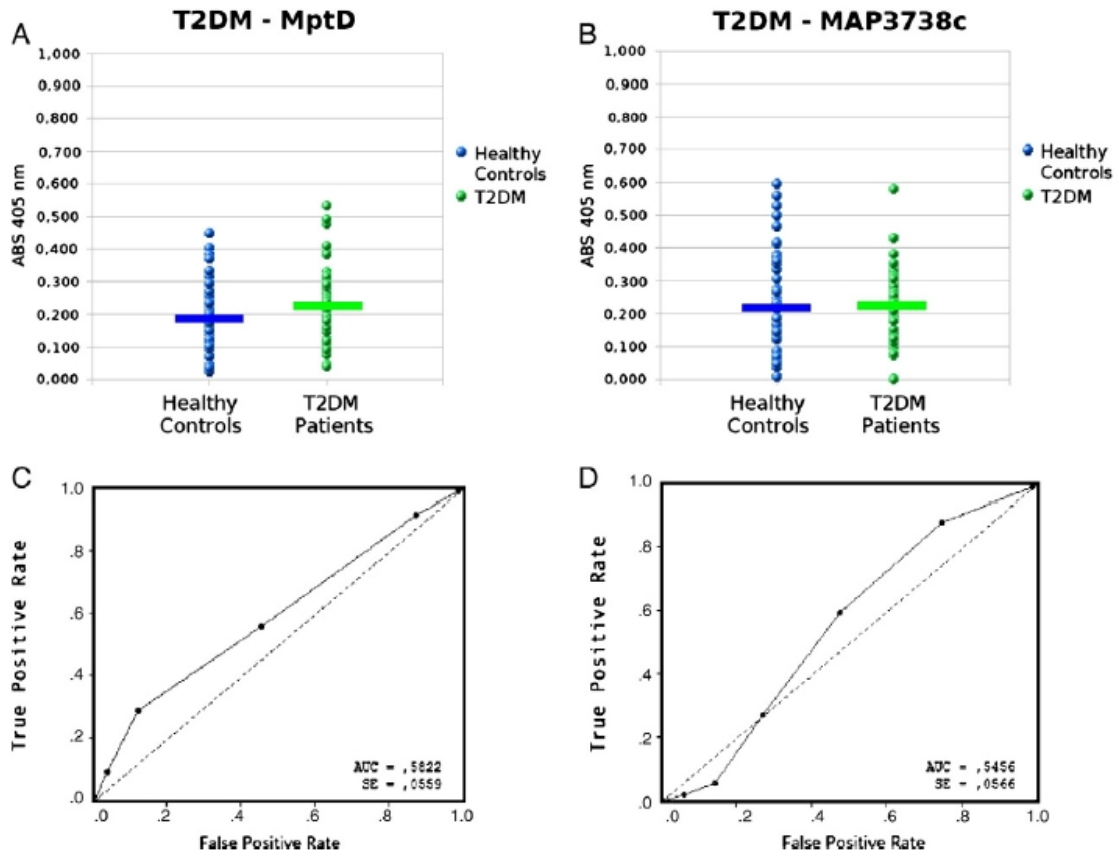

Figure 7. Evaluation of immunoreactivity against MAP3733c (MptD) recombinant protein (A), and MAP3738c recombinant protein (B) in sera from 56 patients with type II diabetes mellitus and 48 healthy controls. Data are shown as values of OD405 nm for each serum in performed ELISA. The average value for each population is indicated by the bolded horizontal line. ROC curve statistical analysis indicates the AUC value for experiments with MptD (C) and MAP3738c (D).

5. DISCUSSION

Most of the works present in the literature concerning studies on whole functional genomics in *in vitro* infection systems based on the interaction between mycobacteria and mammalian cell lines have focused on the transcriptional framework of the infected cell rather than the transcriptome belonging to the infecting bacteria (Murphy et al., 2006; Verschoor et al., 2010; MacHugh et al., 2009). The reason for this is due to the fact that obtaining sufficient quantities of RNA from mycobacteria in order to produce labeled products and to consequently perform microarray hybridization experiments, is difficult (Janagama et al., 2010). Furthermore, among the few studies that have addressed the involvement of *Map* transcriptome, no one has been focused on the *Map*-human system, but only on the definition of the *Map* transcriptome in bovine or murine cells (Zhu et al., 2008; Patel et al., 2006; Janagama et al., 2010). Certainly, this is due to the fact that bovine is the main host of *Map* and among ruminants cows are those in respect of which the most production losses caused by Paratuberculosis in the agricultural economic system are registered (Janagama et al., 2010). However, recent findings that have associated the mycobacterium potentially to intestinal diseases in humans such as Crohn's disease (Tanaka et al., 1991; Bull et al., 2003; Naser et al., 2004) or immune system disorders such as type I diabetes and multiple sclerosis (Sechi et al., 2008; Cossu et al., 2011), channel new research lines in the study of the bacterium's transcriptome during the infection of the potential human host.
For this reason this work has focused on studying the transcriptional profile of *Map* in two types of environmental conditions. The first one has been the simulation of the intraphagosomal environment through the creation of a

multiple stress system made by both the acid and the nitric components defining thus an acid-nitrosative environment with protonic and radicalic stressors, since the addition of nitrite to a growth medium at low pH, would have produced various anionic species of nitrogen oxides together with NO (Lundberg et al., 2005). Consequently, the experiment conducted in the acid-nitrosative stress would have served to highlight the transcriptional regulation of the bacterium in growth conditions reproduced in the standard growth medium with the simulation of the macrophage internalization probably encountered during *in vivo* infection. On the other hand, the second and last experimental approach has seen the preparation of the infection system *Map*-macrophage using the human macrophage/monocyte cell line THP-1 as host. By employing a simple and efficient protocol for the isolation of intracellular mycobacteria from infected cells (Butcher et al., 1998) it was possible to get a good starting amount of bacteria through the specific lysis of infected eukaryotic cells, surprisingly resulting in a very viable bacterial pellet (data not shown), sufficient for the continuation of all the downstream procedures starting from the extraction of bacterial RNA. Naturally, because of the low growth rate in the first experimental typology and the low yield of bacterial cells in the second, both experiments were carried out using large volumes of starting bacterial culture and wide infected cell layers with a multiplicity of infection (MOI) of 10:1 (10 bacteria / macrophage) for 24 h chosen for the optimal uptake of bacilli already shown (Murphy et al., 2006).

As far as the experimental transcriptomes are concerned, it could be noticed that under stress as well as in macrophage infection *Map* shifts its aerobic metabolism to a set of systems related to an energy metabolism based on the anaerobism, enabling nitrate respiration to generate ATP (Moreno-

Vivian et al., 1999), unlike mechanisms such as the oxidation of molecular hydrogen with the hydrogenase complex (Berney et al., 2010). This shift towards the nitrogen compound may be due in the case of multiple stress to the prevalence of nitrogen species in the culture medium ensuring that the bacterium utilizes the condition of excessive nitrate to its advantage, even though in a condition of starvation, using the nitrogen compound as an electron acceptor. Moreover, in the second case regarding the persistence of *Map* in macrophages, since the phagosome is known to be an anoxic environment (Loebel et al., 1933), in lack of molecular oxygen, the bacterium exploits oxidized nitrogen species in order to have an efficient anaerobic respiration. Common up-regulation of genes required for the synthesis of menaquinone in both experimental conditions along with the down-regulation of genes typical of the aerobic respiration, such as those for oxidative phosphorylation and synthesis of ubiquinone, corroborates this hypothesis since members of the menaquinone synthesis pathway have been found up-regulated four times in experiments of induced hypoxia with *M. smegmatis* (Berney et al., 2010). This would confirm the belief that, during infection, the environment inside the macrophage is dominated by a general condition of hypoxia as already demonstrated in *M. tuberculosis* (Wayne et al., 2001), and together with the here described down-regulation of *Map*'s TCA cycle would reflect a general slowing down of metabolism already found in *M. tuberculosis* under induced conditions of nutrient starvation (Betts et al., 2002). The general slowing down of metabolism could also have an impact in terms of replication of the bacterium in stress or infection conditions. As a matter of fact in the acid-nitrosative stress, the down-regulation of the cellular division could suggest a general slowdown of division and replication in the stress situation. This conclusion is in line

with experiments concerning *Map* infection of bovine macrophages (Janagama et al., 2010) where the bacterium up-regulated DNA repair genes, as emphasized in this work both in acid-nitrosative stress and in *Map* infection of THP-1 cell line. The perception of stress conditions in both experiments is emphasized by the up-regulation of several stress factors such as chaperonins and specific transcription factors among which it is worth to mention the *ad hoc* sigma factor *sigE* which is activated intracellularly or during oxidative stress (Graham et al., 1999). It is important to note the up-regulation of *oxyS* required for the response to general oxidative stress and *sodC* in the acid-nitrosative stress, along with the response for the resistance to acids (MAP1317c). Of particular interest in THP-1 infection is the down-regulation in *Map* transcriptome of the repressor of the glyoxylate cycle with the concomitant up-regulation of this pathway, which was identified as a characteristic feature of the persistence of mycobacteria inside the macrophage (McKinney et al., 2000), along with the down-regulation of genes involved in the synthesis of glycogen and pyrimidines, commonly down-regulated in both experiments. Ultimately, this set of regulated genes pertaining to this part of the transcriptional pattern shows, how in line with several works (Wu et al., 2007; Zhu et al., 2008), the bacterium expresses a specific defense against toxic compounds and an adequate response to the ongoing nutritional starvation.

However, although previous studies on mycobacteria highlighted a response to stressor conditions by up-regulating genes involved in the degradation of lipids or inhibiting lipid synthesis (Rengarajan et al., 2005; Betts et al., 2002), both in acid-nitrosative conditions and in macrophage infection, *Map* down-regulates the lipid degradation and up-regulates the synthesis of lipids. This is indeed complementary to the up-regulation of genes that

participates in the synthesis of LPS, phospholipids and mycolic acids especially in THP-1 infection with concomitant inhibition of genes coding for proteins required for the synthesis of cell wall polysaccharides, especially peptidoglycan. Therefore it can be inferred that, in presence of phagosomal environment, *Map* makes use of a kind of primary defense for its own surface that, from the structural point of view, is no longer strictly "rigid" such as found in the acid-nitrosative stress with the strengthening of peptidoglycan which reveals a typical physical-chemical stress, but rather “dynamic and interactive”. This could be explained as a sort of indirect spoliation of the bacterium by macrophage. *Map* would not repair degraded polysaccharides, however restores lipid structures, less xenogenic to host cell since hydrophobicity of lipids makes them less accessible to the immune system than are hydrophophilic molecules such as carbohydrates (Goding, 1996), thus implementing a kind of internal mimicry within intra-macrophage environment by appearing as “self compartment”. This could lead to an incomplete phagosomal acidification following the mycobacterial infection of macrophages (Sturgill-Koszycki et al., 1994), thereby avoiding the immune response which would confirm the identification of “cell wall deficient” *Map* as a way of persistence of the bacterium inside the host as described by several authors (Hines et al., 2003; Sechi et al., 2005). The different transcriptional response in the cell wall and membrane metabolism of *Map* between the acid-nitrosative stress and THP-1 infection would show the limits of the use of *in vitro* simulation for endo-phagosomal stress studies with physical and chemical agents indicating that simulation studies, albeit reproduced by multiple stressors and not by a single stress, are much different than the real conditions found in macrophage phagosomes that include still unknown environmental changes acting

within the interactive system defined by the bacterium and the phagosome. Finally, within the transcriptome of *Map* in macrophage infection, it is worth noting the up-regulation of the gene coding for *hemolysin A* (*tlyA*) while the *hbha* gene (MAP3968) is down-regulated. Whereas HBHA protein has been recognized as an important factor which is responsible for the adhesion and invasion in the host cell (Sechi et al., 2006b), hemolysin may be considered instead as an evasion factor (Rahman et al., 2010). In this way, it could be hypothesized that *Map* inside macrophage employs a virulence system devoted to escaping from the phagocytic cell, thus limiting invasion. This hypothesis could be consistent with the above-mentioned up-regulation of cell division in THP-1 infection, thus deducing an increased intracellular proliferation in anticipation of an impending escape from the phagosome, although this should be necessarily taken into account in relation to the temporal stage of *Map* infection. However, the concomitant down-regulation of *NADH deydrogenase subunit nuoG*, would reflect the repression of the antiapoptotic effect that bacteria have on the macrophage (Velmurugan et al., 2007) confirming the hypothesis of evasion and macrophage killing.

In line with this view, it is of particular importance to define and characterize the several virulence and pathogenic factors that *Map* may use during the infection of host cells. Some of these factors may be immunogenic proteins and, therefore, considered useful in the study of the host immune response to infection with the bacterium. Among these factors are several proteins involved in the acquisition of metals such as iron which is critical for the *in vivo* survival of *Map* since bacterial persistance is related to pathogenicity even in terms of the acquisition of metal micronutrients within the macrophage, which is generally considered as an iron-limiting environment (Rodriguez et al., 2002).

Iron uptake is essential for microbial growth because the acquisition of this metal is an important feature for the process of bacterial pathogenesis (Ratledge, 2004). Metal absorption is carried out by uptake factors such as the ABC transporters among which is numbered a specific operon denominated *Mpt*. The *Mpt* operon belongs to a specific 38 kb pathogenicity island of *Map* and a constitutive element of its sequence, the *MAP3733c* gene, encodes for the protein MptD that was firstly described as a membrane protein expressed during infection stages (Stratmann et al., 2004) and further identified as a virulent factor as well (Heinzmann et al., 2008). Because the process of iron acquisition might be a possible target for chemotherapeutic agents (Ratledge, 2004) or immunoprophylactic tools, Heinzmann and collegues cloned *Mpt* operon's fragments into the integrative pMV306 expression plasmid. Among these fragments also *mptD* ORF was present and has been expressed in BCG host with the aim of creating a vaccine candidate against *Map* (Heinzmann et al., 2008). Despite the authors were successfull to demonstrate a surface exposure, MptD protein was not purified.

Attempts were made to clone the single *mptD* ORF in a pMAL-series plasmid or in pMV261 vector with *M. smegmatis* as host; unfortunately, purification of expressed protein failed (data not shown). Subsequently, it was cloned into pQE-30 expression vector, with a 27°C expression temperature and a lesser IPTG concentration during induction to avoid the formation of inclusion bodies, making it easy to perform the 6xHis tag mediated purification although under modified hybrid conditions with Triton X-100 detergent which led to a low purification yield.

The second cloned protein, MAP3738c, seems to be the smallest among the hypothetical proteins of the specific 38 kb pathogenical island of *Map*

(Stratmann et al., 2004). The protein contains a putative cyclopropane mycolic acid synthase motif (CMAS) involved in biosynthesis of methoxy and cyclopropyl mycolic acids as for a similar domain found in *Mycobacterium tuberculosis* (Yuan et al., 1996). The analysis of the primary structure of MAP3738c showed a less hydrophobic character compared to the MptD protein, a detail that might explain the ease of its expression and purification. Enzymes involved in addition or degradation of mycolic acid components alter the lipidic composition and the hydrophobic balance of cell walls leading to a change in the ability to adhere to host cell surfaces (Miltner et al., 2005), furthermore cyclopropanated mycolic acid is involved in host cell entry. Miltner and collegues cloned an homologue of Rv3720, a cyclopropane fatty acyl-phospholipid synthase gene, assessing that its constitutive expression in *M. avium* host was fundamental for the invasion of epithelial cells (Miltner et al., 2005) while in a similar study the inactivation of *pcaA*, another cyclopropane synthase, dramatically decreased the virulence of *M. tuberculosis* (Glickman et al., 2000).

With the emergence of reports about the zoonotic danger of *Map*, many investigations had focused on the presence of humoral response against different *Map* antigens in patients afflicted by autoimmune diseases (Dow, 2008; Getts et al., 2010; Polymeros et al., 2006). In this study, a strong humoral immune response in T1DM sera against MAP3733c (MptD) and MAP3738c proteins was detected. An earlier study following a similar approach found this evidence using different specific antigens involved in bacteria survival and virulence (Sechi et al., 2008). The proteins of this study were not recognized by sera from patients with T2DM and controls. These results support the hypothesis proposed where *Map* is indicated as a potential trigger of the autoimmunity that characterize T1DM rather than to

a non-autoimmune disease as T2DM.

Immunological assays on autoimmune diseases have already focused on MptD protein using a small peptide called aMptD derived from a phage display study (Stratmann et al., 2004). This peptide mimed an ideotype sequence that recognized a small part of the MptD protein, and its use in serological assays for autoimmune diseases such as T1DM (Rosu et al., 2009) showed results similar to the present results. The direct identification of MptD protein has demonstrated the presence of intact *Map* cells in infected bulk milk (Stratmann et al., 2004), in addition electron microscopy experiments (Sechi et al., 2005) revealed that in human host *Map* is characterized as having a spheroplastic form with a partial degradation of cell wall, which is also corroborated by the loss of the Ziehl-Neelsen staining positiveness. This does not exclude the presence of the MptD antigen in *Map* infecting humans; therefore MptD remains a potential surface marker in the immunodiagnostic of *Map*.

Concerning immune response of T1DM patients against MAP3738c, proteins previously screened that are similar in function or cellular localization would make easier the understanding of these results. Wu and colleagues showed the importance of pstA protein in the addition of amino acids to the lipopeptidic core of *Map* demonstrating a significant role for pstA in the development of an immune response in infected cattle (Wu et al., 2009). Differently, Bannantine and Stabel had cloned the HspX protein of *Map* and revealed its immunogenicity in infected cows, although it was not a secreted antigen but rather a protein belonging to the soluble fraction (Bannantine et al, 2000). As for HspX antigen, MAP3738c protein may not be exposed, it is in any case involved in the biosynthesis of cell surface components as the pstA antigen. This line of evidence suggests that even if

MAP3738c is not exposed on the surface of *Map*, it could arouse a humoral response in T1DM patients as MptD, suggesting that the presence of the antigen on the outer surface of a cell is not an absolute prerequisite for the induction of an immune response by the host.

6. CONCLUSIONS

In conclusion, this work showed how *Map*'s transcriptome, both in the simulation of intraphagosomal stress and in macrophage infection, shifts towards an adaptive metabolism for anoxic environment and nutrient starvation, by up-regulating several response factors in order to cope with oxidative stress or intracellular permanence. However, along with the macroscopic transcriptional similarities between the two types of experiments, especially regarding the energy metabolism, the discovery of significant differences in cell wall metabolism, virulence and antigenical profile between *Map*'s transcriptomes under acid-nitrosative stress and macrophage infection, makes us understand how the *in vitro* simulation of intracellular stresses and the cell infection act differently in fine regulation of *Map*'s interactome with the host cell. Therefore, it is clear the importance of the need to construct apart from *in vitro* models, also appropriate *in vivo* models that could reveal further transcriptional differences to identify functional characteristics and particular transcriptional aspects regarding environmental stimuli to which the bacterium has to face, thus identifying genes involved in the molecular pathogenesis of *Map*-induced diseases.

Furthermore, data suggesting that two specific *Map* proteins, MptD (MAP3733c) and MAP3738c, are recognised only in T1DM patients and not in T2DM subjects, reinforce the hypothesis that the bacterium has a role, as an environmental factor in triggering T1DM and other autoimmune diseases. However, further studies should evaluate if infection is an etiological factor for the onset of the autoimmune disease or is merely a consequence of the pathology.

7. REFERENCES

Alaminos M., Ramos J.L., The methionine biosynthetic pathway from homoserine in Pseudomonas putida involves the metW, metX, metZ, metH and metE gene products, Arch. Microbiol. 176 (2001) 151-154.

Alonso S., Pethe K., Russell D.G., Purdy G.E., Lysosomal killing of Mycobacterium mediated by ubiquitin-derived peptides is enhanced by autophagy, Proc. Natl. Acad. Sci. USA 104 (2007), 6031-6036.

Arand M., Hallberg B.M., Zou J., Bergfors T., Oesch F., van der Werf M.J., de Bont J.A., Jones T.A., Mowbray S.L., Structure of Rhodococcus erythropolis limonene-1,2-epoxide hydrolase reveals a novel active site, EMBO J. 22 (2003) 2583-2592.

Bach H., Papavinasasundaram K.G., Wong D., Hmama Z., Av-Gay Y., Mycobacterium tuberculosis virulence is mediated by PtpA dephosphorylation of human vacuolar protein sorting 33B, Cell Host Microbe 3 (2008) 316-322.

Bacon J., James B.W., Wernisch L., Williams A., Morley K.A., Hatch G.J., Mangan J.A., Hinds J., Stoker N.G., Butcher P.D., Marsh P.D., The influence of reduced oxygen availability on pathogenicity and gene expression in Mycobacterium tuberculosis, Tuberculosis 84 (2004) 205-217.

Bannantine J.P., Stabel J.R., HspX is present within Mycobacterium paratuberculosis-infected macrophages and is recognized by sera from some infected cattle, Vet. Microbiol. 76 (2000) 343–358.

Bannantine J.P., Stabel J.R., Killing of Mycobacterium avium subspecies paratuberculosis within macrophages, BMC Microbiol. 2 (2002) 2.

Bateman R.L., Bhanumoorthy P., Witte J.F., McClard R.W., Grompe M., Timm D.E., Mechanistic inferences from the crystal structure of fumarylacetoacetate hydrolase with a bound phosphorus-based inhibitor, J. Biol. Chem. 276 (2001) 15284-15291.

Beard P.M., Henderson D., Daniels M., Pirie A., Buxton D., Greig A., Hutchings M.R., McKendrick I., Rhind S., Stevenson K., Sharp M., Evidence for paratuberculosis in fox (vulpes vulpes) and stoat (mustela erminea), Vet. Rec. 145 (1999) 612-613.

Begg K.J., Dewar S.J., Donachie W.D., A new Escherichia coli cell division gene, ftsK, J. Bacteriol. 177 (1995) 6211-6222.

Bera A., Biswas R., Herbert S., Gotz F., The presence of peptidoglycan O-acetyltransferase in various staphylococcal species correlates with lysozyme resistance and pathogenicity, Infect. Immun. 74 (2006) 4598-4604.

Berney M., Cook G.M., Unique flexibility in energy metabolism allows mycobacteria to combat starvation and hypoxia, PLoS One 5 (2010) e8614.

Bessman M.J., Frick D.N., O'Handley S.F., The MutT proteins or "Nudix" hydrolases, a family of versatile, widely distributed, "housecleaning" enzymes, J. Biol. Chem. 271 (1996) 25059-25062.

Betts J.C., Lukey P.T., Robb L.C., McAdam R.A., Duncan K., Evaluation of a nutrient starvation model of Mycobacterium tuberculosis persistence by gene and protein expression profiling, Mol. Microbiol. 43 (3) (2002) 717-731.

Boon C., Dick T., Mycobacterium bovis BCG response regulator essential for hypoxic dormancy, J. Bacteriol. 184 (2002) 6760-6767.

Boshoff H.I., Myers T.G., Copp B.R., McNeil M.R., Wilson M.A., Barry III C.E., The transcriptional responses of Mycobacterium tuberculosis to inhibitors of metabolism: novel insights into drug mechanisms of action. J. Biol. Chem. 279 (2004) 40174-40184.

Bull T.J., McMinn E.J., Sidi-Boumedine K., Skull A., Durkin D., Neild P., Rhodes G., Pickup R., Hermon-Taylor J., Detection and verification of Mycobacterium avium subsp. paratuberculosis in fresh ileocolonic mucosal biopsy specimens from individuals with and without Crohn's disease, J. Clin. Microbiol. 41 (2003) 2915-2923.

Butcher P.D., Mangan J., Monahan I.M., Intracellular gene expression: analysis of RNA from mycobacteria in macrophages using RT-PCR, Methods Mol. Biol. 101 (1998) 285-306.

Campbell J.W., Cronan Jr. J.E., Bacterial fatty acid biosynthesis: targets for antibacterial drug discovery, Annu. Rev. Microbiol. 55 (2001) 305-332.

Chiodini R.J., Crohn's disease and the mycobacteriosis: a review and comparison of two disease entities, Clin. Microbiol. Rev. 2 (1989) 90-117.

Chiodini R.J., Thayer W.R., Coutu J.A., Presence of Mycobacterium paratuberculosis antibodies in animal healthcare workers, in: R.J. Chiodini, M.E. Hines, M.T. Collins, M.A. Rehoboth (Eds.), Proceedings of the Fifth International Colloquium on Paratuberculosis, International Association of Paratuberculosis, 1996, pp. 324–328.

Cossu D., Cocco E., Paccagnini D., Masala S., Ahmed N., Frau J., Marrosu M.G., Sechi L.A., Association of Mycobacterium avium subsp. paratuberculosis with multiple sclerosis in Sardinian patients, PLoS One (2011) doi:10.1371/journal.pone.0018482.

Coussens P.M., Mycobacterium paratuberculosis and the bovine immune system, Anim. Health Res. Rev. 2 (2001) 141-161.

Crowe J., Masone B.S., Ribbe J., One-step purification of recombinant proteins with the 6xHis tag and Ni-NTA resin, Methods Mol. Biol. 58 (1996) 491–510.

Deb C., Lee C.M., Dubey V.S., Daniel J., Abomoelak B., Sirakova T.D., Pawar S., Rogers L., Kolattukudy P.E., A Novel In Vitro Multiple-Stress Dormancy Model for Mycobacterium tuberculosis Generates a Lipid-Loaded, Drug-Tolerant, Dormant Pathogen, PLoS One 4 (2009) e6077.

de Lisle G.W., Yates G.F., Joyce M.A., Cavaignac S.M., Hynes T.J., Collins D.M., Case report and DNA characterization of Mycobacterium avium isolates from multiple animals with lesions in a beef cattle herd, J. Vet. Diagn. Invest. 10 (1998) 283-284.

Delumeau O., Dutta S., Brigulla M., Kuhnke G., Hardwick S.W., Volker U., Yudkin M.D., Lewis R.J., Functional and structural characterization of RsbU, a stress signaling protein phosphatase 2C, J. Biol. Chem. 279 (2004) 40927-40937.

Dhiman R.K., Mahapatra S., Slayden R.A., Boyne M.E., Lenaerts A., Hinshaw J.C., Angala S.K., Chatterjee D., Biswas K., Narayanasamy P., Kurosu M., Crick D.C., Menaquinone synthesis is critical for maintaining mycobacterial viability during exponential growth and recovery from non-replicating persistence, Mol. Microbiol. 72 (2009) 85-97.

Djordjevic S., Stock A.M., Structural analysis of bacterial chemotaxis proteins: components of a dynamic signaling system, J. Struct. Biol. 124 (1998) 189-200.

Domenech P., Honore N., Heym B., Cole S.T., Role of OxyS of Mycobacterium tuberculosis in oxidative stress: overexpression confers increased sensitivity to organic hydroperoxides, Microbes Infect. 3 (2001) 713-721.

Donaghy J.A., Totton N.L., Rowe M.T., Persistence of Mycobacterium paratuberculosis during manufacture and ripening of cheddar cheese, Appl. Environ. Microbiol. 70 (2004) 4899-4905.

Dow C.T., Cows, Crohn's and more: is Mycobacterium paratuberculosis a superantigen? Med. Hypotheses 71 (2008) 858-861.

Fischer R., von Strandmann R.P., Hengstenberg W., Mannitol-specific phosphoenolpyruvate-dependent phosphotransferase system of Enterococcus faecalis: molecular cloning and nucleotide sequences of the enzyme IIIMtl gene and the mannitol-1-phosphate dehydrogenase gene, expression in Escherichia coli, and comparison of the gene products with similar enzymes, J. Bacteriol. 173 (1991) 3709-3715.

Gebhard S., Ekanayaka N., Cook G.M., The low-affinity phosphate transporter PitA is dispensable for in vitro growth of Mycobacterium smegmatis, BMC Microbiol. 9 (2009) 254.

Gerlach G.F., Paratuberculosis: the pathogen and routes of infection, Dtsch. Tieraerztl. Wochenschr. 109 (2002) 504-506.

Getts M.T., Miller S.D., 99th Dahlem conference on infection, inflammation and chronic inflammatory disorders: triggering of autoimmune diseases by infections, Clin. Exp. Immunol. 160 (2010) 15–21.

Glickman M.S., Cox J.S., Jacobs Jr. W.R., A novel mycolic acid cyclopropane synthetase is required for cording, persistence, and virulence of Mycobacterium tuberculosis, Mol. Cell 5 (2000) 717–727.

Goding J.W., Monoclonal antibodies: principles and practice, third ed., Academic Press, San Diego, 1996.

Graham J.E., Clark-Curtiss J.E., Identification of Mycobacterium tuberculosis RNAs synthesized in response to phagocytosis by human macrophages by selective capture of transcribed sequences (SCOTS), Proc. Natl. Acad. Sci. USA 96 (1999) 11554-11559.

Griffin H.G., Gasson M.J., The gene (aroK) encoding shikimate kinase I from Escherichia coli, DNA Seq. 5 (1995) 195-197.

Harris N.B., Barletta R.G., Mycobacterium avium subsp. paratuberculosis in veterinary medicine, Clin. Microbiol. Rev. 14 (2001) 489-512.

Heinzmann J., Wilkens M., Dohmann K., Gerlach G.F., Mycobacterium avium subsp. paratuberculosis-specific mpt operon expressed in M. bovis BCG as vaccine candidate, Vet. Microbiol. 130 (2008) 330-337.

Hestvik A.L.K., Hmama Z., Av-Gay Y., Mycobacterial manipulation of the host cell, FEMS Microbiol. Rev. (2005) doi:10.1016/j.femsre.2005.04.013.

Hines II M.E, Styer E.L., Preliminary characterization of chemically generated Mycobacterium avium subsp. paratuberculosis cell wall deficient forms (spheroplasts), Vet. Microbiol. 95 (4) (2003) 247-258.

Hu Y., Coates A.R.M., Increased levels of sigJ mRNA in late stationary phase cultures of Mycobacterium tuberculosis detected by DNA array hybridisation, FEMS Microbiol. Lett. 202 (2001) 59-65.

Hunter S., Apweiler R., Attwood T.K., Bairoch A., Bateman A., Binns D., Bork P., Das U., Daugherty L., Duquenne L., Finn R.D., Gough J., Haft D., Hulo N., Kahn D., Kelly E., Laugraud A., Letunic I., Lonsdale D., Lopez R., Madera M., Maslen J., McAnulla C., McDowall J., Mistry J., Mitchell A., Mulder N., Natale D., Orengo C., Quinn A.F., Selengut J.D., Sigrist C.J.A., Thimma M., Thomas P.D., Valentin F., Wilson D., Wu C.H., Yeats C., InterPro: the integrative protein signature database, Nucleic Acids Res. 37 (2009) D211-D215.

Ito T., Uozumi N., Nakamura T., Takayama S., Matsuda N., Aiba H., Hemmi H., Yoshimura T., The implication of YggT of Escherichia coli in osmotic regulation, Biosci. Biotechnol. Biochem. 73 (2009) 2698-2704.

Jackson M., Crick D.C., Brennan P.J., Phosphatidylinositol is an essential phospholipid of mycobacteria, J. Biol. Chem. 275 (2000) 30092-30099.

Janagama H., Lamont E.A., George S., Bannantine J.P., Xu W.W., Tu Z.J., Wells S.J., Schefers J., Sreevatsan S., Primary transcriptomes of Mycobacterium avium subsp. paratuberculosis reveal proprietary pathways in tissue and macrophages, BMC Genomics 11 (2010) 561.

Jitrapakdee S., Wallace J.C., The biotin enzyme family: conserved structural motifs and domain rearrangements, Curr. Protein Pept. Sci. 4 (2003) 217-229.

Kanehisa M., Goto S., KEGG: Kyoto Encyclopedia of Genes and Genomes, Nucleic Acids Res. 28 (2000) 27-30.

Kim S.K., Makino K., Amemura M., Shinagawa H., Nakata A., Molecular analysis of the phoH gene, belonging to the phosphate regulon in Escherichia coli, J. Bacteriol. 175 (1993) 1316-1324.

Kishida H., Wada T., Unzai S., Kuzuyama T, Takagi M., Terada T., Shirouzu M., Yokoyama S., Tame J.R., Park S.Y., Structure and catalytic mechanism of 2-C-methyl-D-erythritol 2,4-cyclodiphosphate (MECDP) synthase, an enzyme in the non-mevalonate pathway of isoprenoid synthesis, Acta Crystallogr. D Biol. Crystallogr. 59 (2003) 23-31.

Kisker C., Hinrichs W., Tovar K., Hillen W., Saenger W., The complex formed between Tet repressor and tetracycline-Mg2+ reveals mechanism of antibiotic resistance, J. Mol. Biol. 247 (1995) 260-280.

Kneidinger B., Graninger M., Adam G., Puchberger M., Kosma P., Zayni S., Messner P., Identification of two GDP-6-deoxy-D-lyxo-4-hexulose reductases synthesizing GDP-D-rhamnose in Aneurinibacillus thermoaerophilus L420-91T, J. Biol. Chem. 276 (2001) 5577-5583.

Kneidinger B., Marolda C., Graninger M., Zamyatina A., McArthur F., Kosma P., Valvano M.A., Messner P., Biosynthesis pathway of ADP-L-glycero-beta-D-manno-heptose in Escherichia coli, J. Bacteriol. 184 (2002) 363-369.

Körner H., Sofia H.J., Zumft W.G., Phylogeny of the bacterial superfamily of Crp-Fnr transcription regulators: exploiting the metabolic spectrum by controlling alternative gene programs, FEMS Microbiol. Rev. 27 (2003) 559-592.

Kuehnel M.P., Goethe R., Habermann A., Mueller E., Rohde M., Griffiths G., Valentin-Weigand P., Characterization of the intracellular survival of Mycobacterium avium ssp. paratuberculosis: phagosomal pH and fusogenicity in J774 macrophages compared with other mycobacteria, Cell. Microbiol. 3 (2001) 551-566.

Lam T.H.J., Yuen K.Y., Ho P.L., Wong K.C., Leong W.M., Law H.K.W., Weng X.H., Zhang W.H., Chen S., Yam W.C., Differential fadE28 expression associated with phenotypic virulence of Mycobacterium tuberculosis, Microb. Pathog. 45 (2008) 12-17.

Li L., Bannantine J.P., Zhang Q., Amonsin A., May B.J., Alt D., Banerji N., Kanjilal S., Kapur V., The complete genome sequence of Mycobacterium avium subspecies paratuberculosis, Proc. Natl. Acad. Sci. U. S. A. 102 (2005) 12344-12349.

Loebel R.O., Shorr E., Richardson H.B., The influence of adverse conditions upon the respiratory metabolism and growth of human tubercle bacilli, J. Bacteriol. 26 (1933) 167-200.

Long M.C., Escuyer V., Parker W.B., Identification and characterization of a unique adenosine kinase from Mycobacterium tuberculosis, J. Bacteriol. 185 (2003) 6548-6555.

Lundberg J.O., Weitzberg E., NO generation from nitrite and its role in vascular control arterioscler thromb, Arterioscler. Thromb. Vasc. Biol. 25 (2005) 915-922.

MacHugh D.E., Gormley E., Park S.D.E., Browne J.A., Taraktsoglou M., O'Farrelly C., Meade K.G., Gene expression profiling of the host response to Mycobacterium bovis infection in cattle, Transbound. Emerg. Dis. 56 (2009) 204-214.

Manganelli R., Dubnau E., Tyagi S., Kramer F.R., Smith I., Differential expression of 10 sigma factor genes in Mycobacterium tuberculosis, Mol. Microbiol. 31(2) (1999) 715-724.

McKinney J.D., Honer zu Bentrup K., Munoz-Elias E.J., Miczak A., Chen B., Chan W.T., Swenson D., Sacchettini J.C., Jacobs Jr. W.R., Russell D.G., Persistence of Mycobacterium tuberculosis in macrophages and mice requires the glyoxylate shunt enzyme isocitrate lyase, Nature 406 (2000) 735-738.

Mihara H., Esaki N., Bacterial cysteine desulfurases: their function and mechanisms, Appl. Microbiol. Biotechnol. 60 (2002) 12-23.

Miltner E., Daroogheh K., Mehta P.K., Cirillo S.L., Cirillo J.D., Bermudez L.E., Identification of Mycobacterium avium genes that affect invasion of the intestinal epithelium, Infect. Immun. 73 (2005) 4214-4221.

Mol C.D., Kuo C.F., Thayer M.M., Cunningham R.P., Tainer J.A., Structure and function of the multifunctional DNA-repair enzyme exonuclease III, Nature 374 (1995) 381-386.

Moreno-Vivian C., Cabello P., Martinez-Luque M., Blasco R., Castillo F., Prokaryotic nitrate reduction: molecular properties and functional distinction among bacterial nitrate reductases, J. Bacteriol. 181 (1999) 6573-6584.

Murphy J.T., Sommer S., Kabara E.A., Verman N., Kuelbs M.A., Saama P., Halgren R., Coussens P.M., Gene expression profiling of monocyte-derived macrophages following infection with Mycobacterium avium subspecies avium and Mycobacterium avium subspecies paratuberculosis, Physiol. Genomics 28 (2006) 67-75.

Naser S.A., Ghobrial G., Romero C., Valentine J.F., Culture of Mycobacterium avium subspecies paratuberculosis from the blood of patients with Crohn's disease, Lancet 364 (2004) 1039-1044.

Paccagnini D., Sieswerda L., Rosu V., Masala S., Pacifico A., Gazouli M., Ikonomopoulos J., Ahmed N., Zanetti S., Sechi L.A., Linking chronic infection and autoimmune diseases: Mycobacterium avium subspecies paratuberculosis, SLC11A1 polymorphisms and type-1 diabetes mellitus, PLoS One 4 (2009) e7109.

Passarino G., Underhill P.A., Cavalli-Sforza L.L., Semino O., Pes G.M., Carru C., Ferrucci L., Bonafe M., Franceschi C., Deiana L., Baggio G., De Benedictis G., Y chromosome binary markers to study the high prevalence of males in Sardinian centenarians and the genetic structure of the Sardinian population, Hum. Hered. 52 (2001) 136-139.

Patel D., Danelishvili L., Yamazaki Y., Alonso M., Paustian M.L., Bannantine J.P., Meunier-Goddik L., Bermudez L.E., The Ability of Mycobacterium avium subsp. paratuberculosis to enter bovine epithelial cells is influenced by preexposure to a hyperosmolar environment and intracellular passage in bovine mammary epithelial cells, Infect. Immun. 74 (2006) 2849-2855.

Payne S.M., Detection, isolation, and characterization of siderophores, Methods Enzymol. 235 (1994) 329-344.

Perez E., Samper S., Bordas Y., Guilhot C., Gicquel B., Martin C., An essential role for phoP in Mycobacterium tuberculosis virulence, Mol. Microbiol. 41 (2001) 179-187.

Pivetti C.D., Yen M.R., Miller S., Busch W., Tseng Y.H., Booth I.R., Saier Jr. M.H., Two families of mechanosensitive channel proteins, Microbiol. Mol. Biol. Rev. 67 (2003) 66-85.

Polymeros D., Bogdanos D.P., Day R., Arioli D., Vergani D., Forbes A., Does cross-reactivity between Mycobacterium avium paratuberculosis and human intestinal antigens characterize Crohn's disease? Gastroenterology 131 (2006) 85–96.

Rahman A., Srivastava S.S., Sneh A., Ahmed N., Krishnasastry M.V., Molecular characterization of tlyA gene product, Rv1694 of Mycobacterium tuberculosis: a non-conventional hemolysin and a ribosomal RNA methyl transferase, BMC Biochem. 11 (2010) 35.

Ratledge C., Iron, mycobacteria and tuberculosis, Tuberculosis 84 (2004) 110-130.

Rengarajan J., Bloom B.R., Rubin E.J., Genome-wide requirements for Mycobacterium tuberculosis adaptation and survival in macrophages, Proc. Natl. Acad. Sci. U S A 102 (2005) 8327-8332.

Rodriguez G.M., Voskuil M.I., Gold B., Schoolnik G.K., Smith I., IdeR, an essential gene in Mycobacterium tuberculosis: role of IdeR in iron-dependent gene expression, iron metabolism, and oxidative stress response, Infect. Imm. 70 (2002) 3371-3381.

Rohde K.H., Abramovitch R.B., Russell D.G., Mycobacterium tuberculosis invasion of macrophages: linking bacterial gene expression to environmental cues, Cell Host Microbe 2 (2007) 352-364.

Rosen B.P., The plasmid-encoded arsenical resistance pump: an anion-translocating ATPase, Res. Microbiol. 141 (1990) 336-341.

Rosu V., Ahmed N., Paccagnini D., Gerlach G., Fadda G., Hasnain S.E., Zanetti S., Sechi L.A., Specific immunoassays confirm association of Mycobacterium avium subsp. paratuberculosis with type-1 but not type-2 diabetes mellitus, PLoS One 4 (2009) e4386.

Russell D.G., VanderVen B.C., Lee W., Abramovitch R.B., Kim M.J., Homolka S., Niemann S., Rohde K.H., Mycobacterium tuberculosis wears what it eats, Cell Host Microbe 8 (2010) 68-76.

Sara M., Sleytr U.B., S-Layer proteins, J. Bacteriol. 182 (2000) 859-868.

Schinzel R., Nidetzky B., Bacterial alpha-glucan phosphorylases, FEMS Microbiol. Lett. 171 (1999) 73-79.

Schnappinger D., Ehrt S., Voskuil M.I., Liu Y., Mangan J.A., Monahan I.M., Dolganov G., Efron B., Butcher P.D., Nathan C., Schoolnik G.K., Transcriptional adaptation of Mycobacterium tuberculosis within macrophages: insights into the phagosomal environment, J. Exp. Med. 198 (5) (2003) 693-704.

Schue´ M., Maurin D., Dhouib R., Bakala N'Goma J.C., Delorme V., Lambeau G., Carriere F., Canaan S., Two cutinase-like proteins secreted by Mycobacterium tuberculosis show very different lipolytic activities reflecting their physiological function, FASEB J. 24 (2010) 1893-1803.

Sechi L.A., Scanu A.M., Molicotti P., Cannas S., Mura M., Dettori G., Fadda G., Zanetti S., Detection and isolation of Mycobacterium avium subspecies paratuberculosis from intestinal mucosal biopsies of patients with and without Crohn's disease in Sardinia, Am. J. Gastroenterol. 100 (2005) 1529-1536.

Sechi L.A., Gazouli M., Sieswerda L.E., Molicotti P., Ahmed N., Ikonomopoulos J., Scanu A.M., Paccagnini D., Zanetti S., Relationship between Crohn's disease, infection with Mycobacterium avium subspecies paratuberculosis and SLC11A1 gene polymorphisms in Sardinian patients, World J. Gastroenterol. 12 (2006a) 7161-7164.

Sechi L.A., Ahmed N., Felis G.E., Duprè I., Cannas S., Fadda G., Bua A., Zanetti S., Immunogenicity and cytoadherence of recombinant heparin binding haemagglutinin (HBHA) of Mycobacterium avium subsp. paratuberculosis: functional promiscuity or a role in virulence? Vaccine 24(3) (2006b) 236-243.

Sechi L.A., Felis G.E., Ahmed N., Paccagnini D., Usai D., Ortu S., Molicotti P., Zanetti S., Genome and transcriptome scale portrait of sigma factors in Mycobacterium avium subsp. paratuberculosis, Infect. Genet. Evol. 7 (2007) 424-432.

Sechi L.A., Rosu V., Pacifico A., Fadda G., Ahmed N., Zanetti S., Humoral immune responses of type 1 diabetes patients to Mycobacterium avium subsp. paratuberculosis lend support to the infectious trigger hypothesis, Clin. Vaccine Immunol. 15 (2008) 320-326.

Smith R.L., O'Toole J.F., Maguire M.E., Sanders II C.R., Membrane topology of Escherichia coli diacylglycerol kinase, J. Bacteriol. 176 (1994) 5459-5465.

Sohal J.S., Singh S.V., Tyagi P., Subhodh S., Singh P.K., Singh A.V., Narayanasamy K., Sheoran N., Singh S.K., Immunology of mycobacterial infections: with special reference to Mycobacterium avium subspecies paratuberculosis, Immunobiology 213 (2008) 585-598.

Sousa M.C., McKay D.B., Structure of the universal stress protein of Haemophilus influenzae, Structure 9 (2001) 1135-1141.

Stratmann J., Strommenger B., Goethe R., Dohmann K., Gerlach G.F., Stevenson K., Li L.L., Zhang Q., Kapur V., Bull T.J., A 38-kilobase pathogenicity island specific for Mycobacterium avium subsp. paratuberculosis encodes cell surface proteins expressed in the host, Infect. Immun. 72 (2004) 1265–1274.

Sturgill-Koszycki S., Schlesinger P., Chakraborty P., Haddix P.L., Collins H.L., Fok A.K., Allen R.D., Gluck S.L., Heuser J., Russell D.G., Lack of acidification in Mycobacterium phagosomes produced by exclusion of the vesicular proton-ATPase, Science 263 (1994) 678-681.

Sugahara M., Mikawa T., Kumasaka T., Yamamoto M., Kato R., Fukuyama K., Inoue Y., Kuramitsu S., Crystal structure of a repair enzyme of oxidatively damaged DNA, MutM (Fpg), from an extreme thermophile, Thermus thermophilus HB8, EMBO J. 19 (2000) 3857-3869.

Taylor B.L., Zhulin I.B., PAS domains: internal sensors of oxygen, redox potential, and light. Microbiol. Mol. Biol. Rev. 63 (1999) 479-506.

Tanaka K, Wilks M., Coates P.J., Farthing M.J., Walker-Smith J.A., Tabaqhali S., Mycobacterium paratuberculosis and Crohn's disease, Gut 32 (1991) 43-45.

Treuner-Lange A., Kuhn A., Durre P., The kdp system of Clostridium acetobutylicum: cloning, sequencing, and transcriptional regulation in response to potassium concentration, J. Bacteriol. 179 (1997) 4501-4512.

Uchiyama I., MBGD: a platform for microbial comparative genomics based on the automated construction of orthologous groups, Nucleic Acids Res. 35 (2007) D343-D346.

van Asselt E.J., Thunnissen A.M., Dijkstra B.W., High resolution crystal structures of the Escherichia coli lytic transglycosylase Slt70 and its complex with a peptidoglycan fragment, J. Mol. Biol. 291 (1999) 877-898.

Verschoor C.P., Pant S.D., You Q., Kelton D.F., Karrow N.A., Gene expression profiling of PBMCs from Holstein and Jersey cows sub-clinically infected with Mycobacterium avium ssp. paratuberculosis, Vet. Immunol. Immunopathol. (2010) doi:10.1016/j.vetimm.2010.03.026.

Velmurugan K., Chen B., Miller J.L., Azogue S., Gurses S., Hsu T., Glickman M., Jacobs Jr. W.R., Porcelli S.A., Briken V., Mycobacterium tuberculosis nuoG Is a Virulence Gene That Inhibits Apoptosis of Infected Host Cells, PLoS Pathog. 3 (2007) e110.

Voskuil M.I., Bartek I.L., Visconti K., Schoolnik G.K., The response of Mycobacterium tuberculosis to reactive oxygen and nitrogen species, Front. Microbiol. 2 (2011) 105.

Waddell S.J., Stabler R.A., Laing K., Kremer L., Reynolds R.C., Besra G.S., The use of microarray analysis to determine the gene expression profiles of Mycobacterium tuberculosis in response to anti-bacterial compounds, Tuberculosis 84 (2004) 263-274.

Wayne L.G., Sohaskey C.D., Nonreplicating persistence of mycobacterium tuberculosis, Annu. Rev. Microbiol. 55 (2001) 139-163.

Whittington R.J., Marshall D.J., Nicholls P.J., Marsh I.B., Reddacliff L.A., Survival and dormancy of Mycobacterium avium subsp. paratuberculosis in the environment, Appl. Environ. Microbiol. 70 (2004) 2989-3004.

Wu C.W., Schmoller S.K., Shin S.J., Talaat A.M., Defining the stressome of Mycobacterium avium subsp. paratuberculosis in vitro and in naturally infected cows, J. Bacteriol. 189 (2007) 7877-7886.

Wu C.W., Schmoller S.K., Bannantine J.P., Eckstein T.M., Inamine J.M., Livesey M., Albrecht R., Talaat A.M., A novel cell wall lipopeptide is important for biofilm formation and pathogenicity of Mycobacterium avium subspecies paratuberculosis, Microb. Pathog. 46 (2009) 222–230.

Yuan Y., Barry III C.E., A common mechanism for the biosynthesis of methoxy and cyclopropyl mycolic acids in Mycobacterium tuberculosis, Proc. Natl. Acad. Sci. U. S. A. 93 (1996) 12828-12833.

Zhu X.,Tu Z.J., Coussens P.M., Kapur V., Janagama H., Naser S., Sreevatsan S., Transcriptional analysis of diverse strains Mycobacterium avium subspecies paratuberculosis in primary bovine monocyte derived macrophages, Microbes Infect. 10 (2008) 1274-1282.

8. APPENDICES

Appendix 1

Genes of *Map* with significantly up-regulated expression levels in the acid-nitrosative stress

Gene ID	Gene Name	Gene Product	log2 [ratio (Exp/ctrl)]	P-value
MAP_0003	recF	recombination protein F	2,0725000000	0,0050406572
MAP_0009	-	Cytochrome P450	2,2425000000	0,0000963391
MAP_0011	ppiA	Peptidyl-prolyl cis-trans isomerase cyclophilin type	1,4549999000	0,0012625608
MAP_0017c	-	-	1,1750001000	0,0152715600
MAP_0025	-	-	1,0875001000	0,0002263457
MAP_0049c	-	Short-chain dehydrogenase/reductase SDR	1,6250000000	0,0076377704
MAP_0061c	-	Transcriptional regulator, PadR-like family	1,0150000000	0,0005740870
MAP_0065	-	Integral membrane protein	1,4849999000	0,0293643620
MAP_0071	dnaB	replicative DNA helicase dnaB	2,0549998000	0,0001034023
MAP_0082	-	transcriptional regulator, Crp/FNR family	1,0775001000	0,0159468780
MAP_0096c	-	Fatty acid desaturase	1,5074999000	0,0462325000
MAP_0101	-	Glutamate--cysteine ligase	1,8425000000	0,0045770737
MAP_0119c	-	-	1,0975000000	0,0029677076
MAP_0123	-	PPE family protein	1,5350001000	0,0040141013
MAP_0135	cmaA1	Cyclopropane-fatty-acyl-phospholipid synthase	1,1200000000	0,0083747560
MAP_0141	-	Luciferase-like protein alkanesulfonate monooxygenase	1,0300000000	0,0233765040
MAP_0143	-	-	2,6750000000	0,0000130400
MAP_0146	-	sulfonate/nitrate/taurine transport system permease protein	2,2649999000	0,0001725136
MAP_0152c	-	Transcription Regulatory protein, TetR	1,3475001000	0,0126857880
MAP_0155	-	Transcriptional regulator, TetR family	1,3875000000	0,0093981080
MAP_0171c	-	ATPase involved in chromosome partitioning-like protein	1,0225000000	0,0079415790
MAP_0175c	-	Luciferase-like monooxygenase	1,3425000000	0,0016505235
MAP_0183c	-	Nuclear export factor GLE1	1,6125001000	0,0153518760
MAP_0185c	-	transcriptional regulator, XRE family, Putative	1,4950000000	0,0002366803
MAP_0195c	-	Protein of unknown function DUF1025	1,1875000000	0,0058757067
MAP_0196c	-	Lipoprotein lppN	1,4200000000	0,0017361142
MAP_0201	-	Transcriptional regulator, TetR family	2,6499999000	0,0006519741
MAP_0211	glf	UDP-galactopyranose mutase	1,5400000000	0,0275330230
MAP_0213	-	-	1,3900000000	0,0015914425
MAP_0219	fadD32	AMP-dependent synthetase and ligase/ acyl-CoA synthase	1,0600000000	0,0125011740
MAP_0221	accD4	CoA carboxylase carboxyl transferase beta subunit AccD4_1	2,9400000000	0,0000671719
MAP_0223c	-	Transcriptional regulator, AraC family	1,6025000000	0,0048008147
MAP_0224c	fadE35	Acyl-CoA dehydrogenase domain protein	1,6500001000	0,0005759277
MAP_0225c	-	Transcriptional regulator, AsnC family	1,3250000000	0,0033265448
MAP_0236c	-	-	1,6650000000	0,0067528400
MAP_0263c	-	NAD(P)H quinone oxidoreductase, PIG3 family, Putative	1,4525000000	0,0186395760
MAP_0265c	fadE1	Acyl-CoA dehydrogenase protein	2,2649999000	0,0000021744
MAP_0267c	-	aminoglycoside phosphotransferase, Protein	1,0450001000	0,0118030040
MAP_0276	-	Protein of unknown function DUF1089	2,3525002000	0,0015591889
MAP_0277c	tyrA	prephenate dehydrogenase	1,0200000000	0,0104644075
MAP_0290	-	-	1,1025000000	0,0008893870
MAP_0296c	-	Isocitrate lyase protein	2,2525000000	0,0001277363
MAP_0301	-	-	1,7099999000	0,0000857997
MAP_0308c	-	Proline rich protein	1,4100001000	0,0008858651
MAP_0312	leuA	2-isopropylmalate synthase	1,0375000000	0,0051789060
MAP_0321	-	Cyclopropane-fatty-acyl-phospholipid synthase	1,4275000000	0,0004881796
MAP_0322c	dnaZX	DNA polymerase III subunits gamma and tau	1,3550001000	0,0010885537
MAP_0330	-	-	2,1250000000	0,0017354220
MAP_0332	-	dihydrodipicolinate reductase protein Hypothetical protein	1,0075000000	0,0309942300
MAP_0339c	-	-	1,7700000000	0,0135485240
MAP_0353	glpK	glycerol kinase	1,3675000000	0,0401876870
MAP_0366	selD	Selenide, water dikinase	2,7549999000	0,0002334216
MAP_0371	-	Luciferase-like protein alkanesulfonate monooxygenase	2,5750000000	0,0000712364
MAP_0386c	-	Response regulator receiver/ANTAR domain-containing protein	1,2225000000	0,0083139315
MAP_0391c	-	Metallophosphoesterase protein	1,8325000000	0,0007356053
MAP_0408	-	-	1,2850000000	0,0033231906
MAP_0430	rmlB2	NAD-dependent epimerase/dehydratase RmlB2	1,0750000000	0,0048756553
MAP_0434	-	Protein of unknown function DUF475	1,1800001000	0,0181230750
MAP_0445c	-	Luciferase-like monooxygenase	1,5025000000	0,0002862333
MAP_0449	folE	GTP cyclohydrolase I	2,1550002000	0,0000393257

Gene ID	Gene Name	Gene Product	log2 [ratio (Exp/ctrl)]	P-value
MAP_0450	folP	Dihydropteroate synthase	1,6000000000	0,0025908388
MAP_0484c	arsB2	Arsenical pump membrane protein	1,0749999000	0,0040716906
MAP_0487c	-	ABC transporter, permease protein	1,3600000000	0,0004245808
MAP_0522	-	Cytochrome P450	1,3000000000	0,0173356780
MAP_0539	-	-	1,4324999000	0,0004688749
MAP_0545	-	Luciferase-like protein alkanesulfonate monooxygenase	1,6324999000	0,0023789853
MAP_0569	-	ABC-type transport system involved in resistance to organic solvents, periplasmic component, Ttg2C	1,1625000000	0,0010028183
MAP_0571	-	-	1,8799999000	0,0101176580
MAP_0573c	otsA	Alpha,alpha-trehalose-phosphate synthase (UDP-forming)	2,6575000000	0,0000360541
MAP_0579c	cpsA	Cell envelope-related protein transcriptional attenuator	2,8075000000	0,0001768436
MAP_0580c	-	-	1,8675000000	0,0001425728
MAP_0591	phoP	Two-component response transcriptional regulator PhoP	2,8200000000	0,0068628006
MAP_0627c	-	-	2,3775000000	0,0000339942
MAP_0630c	-	Linocin_M18 bacteriocin protein	1,3700000000	0,0036361117
MAP_0632	pepC	Aminopeptidase 2, Putative	1,3199999000	0,0030983374
MAP_0637	-	-	1,5600000000	0,0001968081
MAP_0644c	sseC	Protein of unknown function DUF1416	2,4924998000	0,0004359854
MAP_0649	-	acetolactate synthase catalytic subunit	1,4000001000	0,0002379634
MAP_0672c	-	Short chain dehydrogenase/reductase	1,2400000000	0,0002094371
MAP_0697	-	Luciferase-like monooxygenase family protein	1,8075001000	0,0001008071
MAP_0705	-	-	1,1775001000	0,0220368820
MAP_0712c	-	-	1,9225000000	0,0001284230
MAP_0730c	-	cytochrome p450	1,6800000000	0,0010236306
MAP_0743c	-	-	1,7500000000	0,0029171908
MAP_0766c	-	-	2,0950000000	0,0083767240
MAP_0767c	-	Mce associated membrane protein	1,1150000000	0,0241534470
MAP_0768c	-	-	2,7224998000	0,0003861249
MAP_0779	-	-	1,0500000000	0,0055032680
MAP_0781	fadD16	Fatty-acid-CoA ligase	1,6175000000	0,0040252074
MAP_0792c	-	F420-dependent methylene-tetrahydromethanopterin reductase	1,3600000000	0,0457243800
MAP_0803	mog	Molybdenum cofactor biosynthesis protein/molybdopterin protein	2,0825000000	0,0005828945
MAP_0810	cspB	Cold-shock DNA-binding domain protein	1,4950000000	0,0197783020
MAP_0829	gltA2	citrate synthase type II	1,2325001000	0,0146878260
MAP_0833c	-	two-component system, OmpR family, sensor histidine kinase PrrB	2,0850000000	0,0000791309
MAP_0841	-	Zn-dependent hydrolase of the beta-lactamase fold protein	1,2625000000	0,0009969390
MAP_0843	ctpE	ATPase, P-type (transporting), HAD superfamily, subfamily IC	1,2750000000	0,0148161490
MAP_0860c	-	-	1,6925001000	0,0000206248
MAP_0879c	-	Mannitol dehydrogenase domain protein	1,0550000000	0,0059210820
MAP_0881	-	Fumarylacetoacetate hydrolase protein	2,0375000000	0,0002762598
MAP_0885c	-	-	2,1550002000	0,0001943799
MAP_0886c	-	Flavin binding monooxygenase	1,2225000000	0,0078532975
MAP_0889	-	formamidopyrimidine-DNA glycosylase	1,4900000000	0,0022844200
MAP_0894c	-	-	1,0375000000	0,0163787680
MAP_0895c	-	Peptidase M23B protein	1,9275000000	0,0003807703
MAP_0898	-	acetyl-CoA acetyltransferase	1,3975000000	0,0140511720
MAP_0904	-	D-alanyl-D-alanine carboxypeptidase, Putative	2,3950000000	0,0008638823
MAP_0914c	-	Protein of unknown function DUF1446	1,0775000000	0,0078347990
MAP_0924	galU	UTP-glucose-1-phosphate uridylyltransferase	1,2774999000	0,0091977800
MAP_0940	-	-	1,5000000000	0,0019370900
MAP_0951	-	S-layer domain protein	1,3500000000	0,0001843221
MAP_0952	-	Exopolysaccharide biosynthesis tyrosine-protein kinase	1,4750000000	0,0025587426
MAP_0953	-	-	1,0825000000	0,0092551100
MAP_0957c	-	-	1,3175001000	0,0101455380
MAP_0972c	metS	methionyl-tRNA synthetase	1,4675000000	0,0010264454
MAP_0982c	arsC	Arsenate reductase	1,2075000000	0,0014775922
MAP_0990	eno	phosphopyruvate hydratase	2,4400000000	0,0001118282
MAP_1000c	kdpA	potassium-transporting ATPase subunit	2,4025000000	0,0001601638
MAP_1003c	PE	PPE family protein	1,8024999000	0,0006630175
MAP_1013c	lpqV	Lipoprotein LpqV	1,6725000000	0,0059816640
MAP_1019	-	Protein of unknown function DUF1112	1,5525000000	0,0006307425
MAP_1025	pra	Pra	1,0450000000	0,0011868657
MAP_1044	secF	preprotein translocase subunit	1,0025000000	0,0178291690
MAP_1059	dapA	Dihydrodipicolinate synthase DapA_1	1,0799999000	0,0133477850
MAP_1065	-	Hemerythrin HHE cation binding domain protein	1,1600001000	0,0013121874
MAP_1071c	-	Integral membrane protein	2,1399999000	0,0002954648
MAP_1079	-	Aminodeoxychorismate lyase protein	1,8975000000	0,0003375133
MAP_1092	aroK	shikimate kinase	1,4725001000	0,0201177350
MAP_1101	-	Sensor signal transduction histidine kinase	1,2975001000	0,0050914740

Gene ID	Gene Name	Gene Product	log2 [ratio (Exp/ctrl)]	P-value
MAP_1109	-	sulfonate/nitrate/taurine transport system permease protein	1,0150000000	0,0008763704
MAP_1114	pyrR	bifunctional pyrimidine regulatory protein	1,6700001000	0,0008886508
MAP_1115	pyrB	aspartate carbamoyltransferase catalytic subunit	2,9750000000	0,0000125614
MAP_1122	mIHF	integration host factor, Putative	1,2850000000	0,0103321410
MAP_1156	-	Diacylglycerol O-acyltransferase	1,2875000000	0,0098131090
MAP_1162	-	Transmembrane protein	1,9000001000	0,0002713248
MAP_1178c	tkt	transketolase	1,7125001000	0,0012441662
MAP_1181	-	-	2,1400000000	0,0000868713
MAP_1206	-	Protein of unknown function DUF58	1,5274999000	0,0064902785
MAP_1214	-	membrane protein, SPFH/band 7 family, Putative	1,2025000000	0,0026633318
MAP_1216c	lpqQ	LpqQ	2,0125000000	0,0003749799
MAP_1217c	-	Transmembrane protein	1,1650001000	0,0037654848
MAP_1220c	-	-	1,1800000000	0,0194101840
MAP_1233	-	-	1,7124999000	0,0026315502
MAP_1265	-	Phosphoesterase, PA-phosphatase related protein	1,4200001000	0,0178254680
MAP_1266c	-	Pyridoxamine 5'-phosphate oxidase-related FMN-binding protein	1,3425001000	0,0001481004
MAP_1271c	-	Acyltransferase 3	1,9700000000	0,0451373050
MAP_1289	nadA	quinolinate synthetase	1,3349999000	0,0162663120
MAP_1292c	-	-	1,6675000000	0,0032135164
MAP_1298	impA	Phosphatase, inositol monophosphatase ImpA	1,3675000000	0,0127297050
MAP_1301	chaA	H+/Ca2+ exchanger Ca2+ sodium/calcium/Ca2+ antiporter	2,9075000000	0,0031610043
MAP_1303	trpE	anthranilate synthase component I	1,3850000000	0,0035876576
MAP_1306	trpB	tryptophan synthase subunit	1,8950000000	0,0002976290
MAP_1317c	-	Acid-resistance membrane protein	1,2300000000	0,0007438008
MAP_1331c	-	ABC transporter ATP-binding protein	1,5125000000	0,0084859500
MAP_1334	-	-	1,1350000000	0,0023435878
MAP_1341	uvrA	excinuclease ABC subunit	1,6075001000	0,0007039704
MAP_1358	-	Transmembrane protein	1,3150000000	0,0001199998
MAP_1365	argF	ornithine carbamoyltransferase	1,6775000000	0,0016360738
MAP_1368	argH	argininosuccinate lyase	1,6775000000	0,0466726160
MAP_1384c	-	Glycoside hydrolase 15-related protein	1,0174999000	0,0159603930
MAP_1385c	-	glucose-methanol-choline oxidoreductase, Putative	1,5225000000	0,0024294062
MAP_1386c	-	-	2,3474998000	0,0003248178
MAP_1393c	-	ABC transporter, ATP-binding protein	3,1875000000	0,0005276490
MAP_1405	-	-	1,8675000000	0,0012897949
MAP_1428c	-	Mitochondrial cell death effector	1,4825001000	0,0004492579
MAP_1430c	-	Luciferase-like monooxygenase	2,1550000000	0,0000126805
MAP_1442	-	Short chain dehydrogenase/reductase	2,3450000000	0,0004896303
MAP_1443c	-	Stress responsive alpha-beta barrel domain-containing protein	1,4625000000	0,0037918240
MAP_1455c	-	Short-chain dehydrogenase/reductase SDR	1,0500001000	0,0025029164
MAP_1464	fadD1	AMP-dependent synthetase and ligase	1,4275000000	0,0297849640
MAP_1481c	-	DEAD/DEAH box ATP-dependent RNA helicase	1,9100000000	0,0003892671
MAP_1493c	-	Integral membrane protein	1,4800000000	0,0074160450
MAP_1499c	-	Luciferase-like monooxygenase	1,7524999000	0,0005558299
MAP_1500c	-	4-alpha-glucanotransferase	1,0325000000	0,0438455900
MAP_1502	-	Cell divisionFtsK/SpoIIIE	2,0375000000	0,0040666326
MAP_1509	-	-	1,4675000000	0,0028539747
MAP_1516	-	PPE family protein	1,3924999000	0,0024430244
MAP_1519	-	PPE family protein	1,2824999000	0,0002611624
MAP_1540	-	FHA domain-containing protein	2,4625000000	0,0003162386
MAP_1544	-	-	1,3625001000	0,0015725979
MAP_1551c	-	Hemolysin / protein of unknown function DUF21:transporter	1,4599999000	0,0015776351
MAP_1553c	fadE14	Acyl-CoA dehydrogenase domain protein FadE14	2,2300000000	0,0000693578
MAP_1560	-	Thioesterase superfamily protein	1,5200000000	0,0030213287
MAP_1563c	-	Luciferase-like monooxygenase	1,3300000000	0,0027700912
MAP_1564c	-	FadB domain-containing protein	1,5124999000	0,0001478045
MAP_1570	-	-	1,7075000000	0,0084866930
MAP_1580c	-	Protein of unknown function DUF72	1,4200001000	0,0010466208
MAP_1584c	-	ATP-dependent protease La	1,6175001000	0,0028445001
MAP_1599	glnA3	Glutamine synthetase GlnA3	1,9850000000	0,0099208360
MAP_1607c	-	Transglycosylase domain protein	1,7650000000	0,0035731874
MAP_1624	-	Protein of unknown function DUF77	1,3500000000	0,0018368526
MAP_1627	-	-	1,4900000000	0,0099014165
MAP_1633c	-	-	1,0200000000	0,0128553230
MAP_1641c	-	Transcriptional regulator, ArsR family	2,0225000000	0,0000471365
MAP_1643	aceAb	isocitrate lyase	2,8125000000	0,0005298370
MAP_1645	-	Luciferase-like monooxygenase	2,2000000000	0,0007049181
MAP_1646c	-	Alkyl hydroperoxide reductase/ Thiol specific antioxidant/ Mal allergen	1,0100000000	0,0113976120
MAP_1650	-	-	1,1250000000	0,0024178268

Gene ID	Gene Name	Gene Product	log2 [ratio (Exp/ctrl)]	P-value
MAP_1652c	-	Transcriptional regulator, AraC family	2,7400000000	0,0006331192
MAP_1654c	-	2-nitropropane dioxygenase, NPD	2,1250000000	0,0010881502
MAP_1666c	-	Glycosyl transferase group 1	1,1550000000	0,0207543000
MAP_1668c	katG	Catalase/peroxidase HPI KatG	1,6500001000	0,0003273020
MAP_1670c	lppS	LppS_1	2,5450000000	0,0002459700
MAP_1687	-	Glucose-6-phosphate 1-dehydrogenase	1,2925000000	0,0000936669
MAP_1688	-	Citrate lyase beta subunit	1,1175000000	0,0082225890
MAP_1695c	-	Chaperone protein DnaJ	1,4775000000	0,0410531240
MAP_1697	-	Transcriptional regulator, MerR family	2,0100000000	0,0006146544
MAP_1698c	hsp18	Heat shock protein Hsp20	1,8775000000	0,0006374138
MAP_1701c	-	Biotin carboxylase-like protein	1,3275000000	0,0018568153
MAP_1702c	-	Thioredoxin-like / Protein of unknown function DUF899	1,6050000000	0,0001230650
MAP_1719c	-	Transcriptional regulator, TetR family	1,2325000000	0,0006087652
MAP_1724c	-	Cytochrome B561	2,1475000000	0,0001127255
MAP_1727	-	Dienelactone hydrolase domain protein	1,2275000000	0,0004360967
MAP_1746c	-	UBA/THIF-type NAD/FAD binding family protein	1,2400000000	0,0348788350
MAP_1756c	-	-	1,2200000000	0,0011886474
MAP_1757c	-	ECF RNA polymerase sigma factor	1,0075000000	0,0479090250
MAP_1764	-	-	1,3500000000	0,0026398690
MAP_1774c	pncA	nicotinamidase/pyrazinamidase	2,1850000000	0,0009406482
MAP_1776c	-	-	2,3475000000	0,0001070423
MAP_1792	-	-	1,6550000000	0,0000859932
MAP_1802c	-	-	1,1675000000	0,0027576599
MAP_1805c	cobN	cobaltochelatase subunit	1,2700000000	0,0017080626
MAP_1809c	-	sulfonate/nitrate/taurine transport system permease protein	1,7049999000	0,0018453558
MAP_1848c	-	Transcriptional regulator, TetR family	1,2825000000	0,0085097720
MAP_1857	-	Mce associated membrane protein	1,3625000000	0,0008964753
MAP_1864c	-	Siderophore interacting FAD binding protein	1,4050000000	0,0021761700
MAP_1876c	cysS2	cysteinyl-tRNA synthetase	1,3850000000	0,0006524210
MAP_1879c	-	-	1,2950001000	0,0002398120
MAP_1885c	-	PBP family phospholipid-binding protein	1,1475000000	0,0058751083
MAP_1890c	-	Protein of unknown function YGGT	1,5925000000	0,0143253930
MAP_1902c	murE	UDP-N-acetylmuramoylalanyl-D-glutamate--2,6-diaminopimelate ligase	2,1299999000	0,0011212980
MAP_1907c	-	Membrane protein	1,1975000000	0,0475580020
MAP_1909	lppM	Lipoprotein lppM	1,4650000000	0,0037105617
MAP_1914	pknL	Serine/threonine protein kinase	1,0125000000	0,0474694860
MAP_1918c	-	Integral membrane protein	2,2649999000	0,0000447764
MAP_1925	fadD15	Long-chain fatty acid--CoA ligase and synthetase FadD15	3,0700002000	0,0000672031
MAP_1936c	-	-	1,9675000000	0,0000253275
MAP_1939c	-	integral membrane protein, Putative	3,6675000000	0,0002339631
MAP_1942c	cbhK	adenosine kinase CbhK	2,1875000000	0,0024008380
MAP_1944c	-	HesB/YadR/YfhF iron-sulfur cluster assembly accessory protein	2,4450000000	0,0000112712
MAP_1948	cobT	nicotinate-nucleotide--dimethylbenzimidazole phosphoribosyltransferase	1,9399999000	0,0003043933
MAP_1956	sucB	dihydrolipoamide acetyltransferase dlaT	2,7075000000	0,0002450934
MAP_1973	-	-	1,4575000000	0,0458843260
MAP_1976	-	Prolyl 4-hydroxylase, alpha subunit	1,2850001000	0,0049559446
MAP_1986	-	Surfeit locus 1 family protein	1,0900000000	0,0008421072
MAP_2015	-	Cytochrome P450	1,6525002000	0,0057939750
MAP_2019c	-	-	1,6300000000	0,0012649082
MAP_2025c	-	Carboxymuconolactone decarboxylase protein	1,0925000000	0,0122062580
MAP_2032c	-	transcriptional regulator, TetR family, Putative	2,2200000000	0,0000147371
MAP_2037	-	Cobalamin biosynthesis CbiX protein	1,0900000000	0,0066804100
MAP_2042c	-	-	1,0525000000	0,0361689800
MAP_2082	-	Aminoglycoside phosphotransferase	1,2525000000	0,0052952450
MAP_2095c	-	Arginine deiminase protein	1,2475000000	0,0118860590
MAP_2106c	-	-	1,7375000000	0,0000454356
MAP_2130c	dnaG	DNA primase	1,3775000000	0,0027256594
MAP_2133	-	Protein of unknown function DUF477	1,1900000000	0,0131294485
MAP_2139	furB	Ferric uptake regulator, Fur family protein	1,3650000000	0,0020055613
MAP_2149c	-	-	1,6300000000	0,0026899215
MAP_2166	-	ECF subfamily RNA polymerase sigma-24 factor	2,1225000000	0,0000687486
MAP_2170c	mbtG	mycobactin lysine-N-oxygenase mbtG	1,7700000000	0,0114627630
MAP_2176c	-	Thioesterase	2,1950002000	0,0000082137
MAP_2181c	-	-	2,0600000000	0,0000356389
MAP_2215	-	Glycoside hydrolase 15-related protein	3,2100000000	0,0001540688
MAP_2248c	-	Mechanosensitive ion channel/cyclic nucleotide-binding domain-containing protein	1,9175000000	0,0090251690
MAP_2260	-	NAD-dependent deacetylase SIR2 information regulator	1,0500000000	0,0024388367
MAP_2263c	proB	gamma-glutamyl kinase	1,1875000000	0,0228405370

Gene ID	Gene Name	Gene Product	log2 [ratio (Exp/ctrl)]	P-value
MAP_2273c	-	-	1,7950000000	0,0003317051
MAP_2303c	-	-	1,8125000000	0,0000519878
MAP_2308c	pdhB	Pyruvate dehydrogenase E1 component, beta subunit	2,2425000000	0,0010577611
MAP_2310c	citE	Citrate lyase beta subunit	1,9150000000	0,0002246805
MAP_2314c	accD1	CoA carboxylase carboxyl transferase beta subunit AccD1	1,1175001000	0,0006759415
MAP_2337c	-	-	2,0424998000	0,0007720905
MAP_2353	-	Acyl-CoA dehydrogenase domain protein	1,0400000000	0,0293775740
MAP_2357	-	Amidohydrolase 2	1,7925000000	0,0000008705
MAP_2372	accD4	CoA carboxylase carboxyl transferase beta subunit	2,0324998000	0,0133087660
MAP_2389c	-	-	2,4400000000	0,0012341700
MAP_2392c	-	dihydrodipicolinate synthase	1,9525000000	0,0002252108
MAP_2393c	-	Short-chain dehydrogenase/reductase SDR	1,6275000000	0,0180422700
MAP_2401	fadD35	AMP-dependent synthetase and ligase	1,5700000000	0,0046542315
MAP_2405c	fadE3	Acyl-CoA dehydrogenase protein FadE3_1	2,5525000000	0,0153948140
MAP_2432c	glgP	Glycogen/alpha-glucan phosphorylase	1,8749999000	0,0001705070
MAP_2433	-	Alpha amylase, catalytic region	1,6824999000	0,0205620150
MAP_2436c	fadA4	acetyl-CoA acetyltransferase	1,6550000000	0,0085018760
MAP_2446c	-	-	1,3125000000	0,0054688230
MAP_2447c	murA	UDP-N-acetylglucosamine 1-carboxyvinyltransferase	2,3700001000	0,0003568890
MAP_2452c	atpG	F0F1 ATP synthase subunit	1,0550001000	0,0093816090
MAP_2453c	atpA	F0F1 ATP synthase subunit	3,3725000000	0,0027557872
MAP_2463c	rpmE	50S ribosomal protein L31	1,5699999000	0,0013207616
MAP_2475	-	Metalloendopeptidase-like membrane protein	2,0700002000	0,0000213747
MAP_2482	-	Glyoxalase/bleomycin resistance protein/dioxygenase	1,6700001000	0,0005865668
MAP_2488	oppB	peptide/nickel transport system permease protein	1,7075000000	0,0000151870
MAP_2506c	-	CopG/DNA-binding domain-containing protein	3,2350001000	0,0437428580
MAP_2521c	deaD	DEAD/DEAH box ATP-dependent RNA helicase DeaD	1,4175000000	0,0000625496
MAP_2525c	-	cytochrome p450	1,1800000000	0,0114331950
MAP_2539c	lpqZ	LpqZ	2,1675000000	0,0000949819
MAP_2549c	-	Transmembrane protein	1,2200000000	0,0012623320
MAP_2556c	-	anti-sigma factor transmembrane, Putative	1,1000000000	0,0120012990
MAP_2557c	sigE	RNA polymerase sigma factor SigE	1,0649999000	0,0079590560
MAP_2574c	dapE	succinyl-diaminopimelate desuccinylase	1,9549999000	0,0134257560
MAP_2579c	-	MFS permease, Putative	1,0725000000	0,0017859801
MAP_2580c	fadD36	AMP-dependent synthetase and ligase	2,3725000000	0,0001047601
MAP_2584	-	cytochrome p450	1,4649999000	0,0003087983
MAP_2585	fadE26	Acyl-CoA dehydrogenase domain protein FadE26_2	2,1050000000	0,0005646771
MAP_2595	-	PPE family protein	1,0975000000	0,0060879174
MAP_2598c	sat	sulfate adenylyltransferase	2,5800000000	0,0003152069
MAP_2603c	-	Beta-ketoacyl synthase	1,0200000000	0,0020625766
MAP_2609	-	-	1,1000000000	0,0040383020
MAP_2627c	-	-	1,5124999000	0,0213186260
MAP_2642	-	Naringenin-chalcone synthase	1,1150000000	0,0003819241
MAP_2646c	fadA6	Acetyl-CoA acetyltransferase FadA6_3	2,8800000000	0,0004880775
MAP_2698c	desA2	acyl-[acyl-carrier-protein] desaturase DesA2	1,6725000000	0,0037323134
MAP_2719c	-	-	1,0475000000	0,0229568350
MAP_2721	-	A3(2) glycogen metabolism cluster I	1,0675001000	0,0177128200
MAP_2742	-	-	1,1900000000	0,0041630090
MAP_2773c	-	Acetoacetate decarboxylase	1,5700000000	0,0445106850
MAP_2780	-	Short chain dehydrogenase/reductase	1,1424999000	0,0153765480
MAP_2790c	-	ATPase, AFG1 family protein	1,0075000000	0,0163356160
MAP_2799c	hemE	uroporphyrinogen decarboxylase	1,5400000000	0,0033781782
MAP_2809	trkB	Potassium transporter peripheral membrane component	2,4924998000	0,0169722870
MAP_2812	-	-	1,2175001000	0,0439784600
MAP_2824c	-	-	1,7425001000	0,0000917543
MAP_2828c	-	-	1,0300001000	0,0010940962
MAP_2836	lexA	SOS transcriptional repressor, LexA	1,4725001000	0,0103696950
MAP_2842c	-	-	1,1200000000	0,0013458235
MAP_2846c	-	MiaB-like tRNA modifying enzyme	3,1625000000	0,0000349758
MAP_2851c	-	Glycosyl transferase family protein	1,9825001000	0,0067490470
MAP_2865c	ThyX	FAD-dependent thymidylate synthase	1,0325000000	0,0066112736
MAP_2870	-	carboxymethylenebutenolidase	1,2674999000	0,0478827020
MAP_2877c	-	TPR repeat-containing protein	1,2725000000	0,0003993435
MAP_2878c	dapB	dihydrodipicolinate reductase	1,0125000000	0,0158137810
MAP_2883	-	transcriptional regulator, Putative	1,9600002000	0,0040528630
MAP_2888	ald	Alanine dehydrogenase	1,6450000000	0,0004943677
MAP_2889c	-	Nitropropane dioxygenase	1,1225001000	0,0023561544
MAP_2901	-	-	1,6374999000	0,0008724672
MAP_2911	-	-	1,7100000000	0,0025816222

Gene ID	Gene Name	Gene Product	log2 [ratio (Exp/ctrl)]	P-value
MAP_2912	-	-	1,2475000000	0,0024896923
MAP_2922	-	Alpha/beta hydrolase fold protein	1,1125000000	0,0259674700
MAP_2929c	aldC	Aldehyde dehydrogenase (acceptor) AldC	1,4050001000	0,0044339670
MAP_2937c	-	GCN5-related protein N-acetyltransferase	1,9400000000	0,0050425977
MAP_2941c	-	-	1,1025000000	0,0049209814
MAP_2967c	-	NAD-dependent epimerase/dehydratase	1,7850001000	0,0000883732
MAP_2971c	lepB	signal peptidase I	1,3125000000	0,0022739992
MAP_2974c	trmD	TRNA (guanine-N(1)-)-methyltransferase	1,3100000000	0,0005722088
MAP_2975c	rimM	16S rRNA processing protein RimM	1,2075000000	0,0004890945
MAP_3000c	-	Acetolactate synthase 2 catalytic subunit	1,4024999000	0,0069691944
MAP_3030c	-	2-2,4-1,7 isomerase/5-carboxymethyl-2-3-ene-1,7 protein	1,5899999000	0,0057150940
MAP_3033c	serA	D-3-phosphoglycerate dehydrogenase	1,0124999000	0,0285434690
MAP_3035	-	NADPH-dependent FMN reductase flavodoxin	1,6200000000	0,0080182390
MAP_3045c	gatA	aspartyl/glutamyl-tRNA amidotransferase subunit	1,9350000000	0,0026628730
MAP_3046c	gatC	aspartyl/glutamyl-tRNA amidotransferase subunit	1,8500000000	0,0012669208
MAP_3048c	-	-	1,4950000000	0,0000041659
MAP_3055c	-	Methionine synthase, vitamin-B12 independent	1,7850001000	0,0030931898
MAP_3059c	-	Phospholipid/glycerol acyltransferase, hemolysin	1,8299999000	0,0010197446
MAP_3074	crtT	CrtT	1,1550000000	0,0147550330
MAP_3086c	-	Phosphatidylethanolamine N-methyltransferase	1,2300000000	0,0074214340
MAP_3088c	-	Hydrolase, NUDIX protein	1,2499999000	0,0047687967
MAP_3092	fecB	iron complex transport system substrate-binding protein	1,5825000000	0,0015043084
MAP_3094c	-	-	1,5950000000	0,0000081476
MAP_3097	-	Transcriptional regulator, TetR family protein	3,5050000000	0,0006391874
MAP_3098c	-	flavin monooxygenase, Putative	2,3825002000	0,0000202245
MAP_3101c	nrdI	Ribonucleotide reductase stimulatory protein	1,3575000000	0,0010618047
MAP_3110c	-	2-isopropylmalate synthase	1,6099999000	0,0075200670
MAP_3119	-	Molecular chaperone	1,6950000000	0,0009186266
MAP_3120c	-	Luciferase-like protein alkanesulfonate monooxygenase	1,2700000000	0,0005329691
MAP_3122	fadE1	Acyl-CoA dehydrogenase protein	1,5025000000	0,0082465720
MAP_3123c	-	-	1,4850000000	0,0000488097
MAP_3129	-	-	1,0475000000	0,0078368490
MAP_3131	-	Transmembrane transport protein	1,1300000000	0,0004430940
MAP_3133c	-	Enolase phosphopyruvate hydratase	1,3575000000	0,0034587465
MAP_3134c	-	Carboxymuconolactone decarboxylase protein	1,3175000000	0,0047130412
MAP_3147	-	Camphor resistance CrcB protein	1,3375001000	0,0000115400
MAP_3148	-	Camphor resistance protein CrcB	1,2975000000	0,0023804600
MAP_3171c	ftsX	cell division transport system permease protein	1,3100001000	0,0039095840
MAP_3173c	-	-	1,2350000000	0,0067595040
MAP_3176	fprA	glutamate synthase subunit beta, putative	1,9825000000	0,0014059596
MAP_3185	-	PPE family protein	1,0125000000	0,0017792591
MAP_3189	fadE23	Acyl-CoA dehydrogenase protein FadE23	2,9900000000	0,0005859005
MAP_3194	-	hydroxymethylglutaryl-CoA lyase	1,5200000000	0,0010485813
MAP_3197	-	aminoglycoside phosphotransferase, Protein	1,2025000000	0,0113684490
MAP_3221	-	Protein of unknown function DUF222	1,0925000000	0,0004881667
MAP_3237c	-	-	1,3275000000	0,0012728857
MAP_3241	-	-	1,4849999000	0,0017848172
MAP_3251	-	D,d-heptose 1,7-bisphosphate phosphatase protein	2,2075000000	0,0000436674
MAP_3254	-	UDP-glucose 6-dehydrogenase	1,3300000000	0,0073233503
MAP_3256c	-	Uracil-DNA glycosylase:Phage SPO1 DNA polymerase-related protein	1,9625000000	0,0000196362
MAP_3262c	glgX	Glycogen debranching enzyme GlgX	1,6975000000	0,0049726310
MAP_3276c	-	Acyltransferase 3	2,4450000000	0,0000723535
MAP_3283c	-	Metal-dependent hydrolase, putative	1,8075000000	0,0056104166
MAP_3285c	-	Diacylglycerol kinase catalytic region	1,1325000000	0,0192023760
MAP_3306c	moeZ	UBA/THIF-type NAD/FAD binding/MoeB protein	1,2750000000	0,0367836900
MAP_3311c	-	-	1,6850000000	0,0021963823
MAP_3314c	-	Cobyrinic acid a,c-diamide synthase	1,2624999000	0,0016933962
MAP_3316	entC	isochorismate synthase	1,1200000000	0,0067685830
MAP_3317	-	GCN5-related N-acetyltransferase	1,8549999000	0,0008015444
MAP_3323c	-	Anti-sigma factor	1,5750000000	0,0048882870
MAP_3340	-	-	1,3824999000	0,0019316667
MAP_3345c	-	-	2,2675000000	0,0001492522
MAP_3365c	-	Amino acid transporter permease protein	1,7300000000	0,0023958394
MAP_3380c	rmlD	DTDP-4-dehydrorhamnose reductase RmlD	2,5250000000	0,0004862597
MAP_3386	-	L-carnitine dehydratase/bile acid-inducible protein F	1,4649999000	0,0222147220
MAP_3424c	lpdA	flavoprotein disulfide reductase	2,6125002000	0,0000092242
MAP_3441	sdhC	Succinate dehydrogenase, cytochrome b subunit	1,7725000000	0,0286496930
MAP_3453c	trpS	tryptophanyl-tRNA synthetase	1,3900000000	0,0003915478
MAP_3454	-	hydrolase, Putative	1,7225001000	0,0009745324

Gene ID	Gene Name	Gene Product	log2 [ratio (Exp/ctrl)]	P-value
MAP_3456c	icd2	Isocitrate dehydrogenase, NADP-dependent Icd2	1,1850000000	0,0160359480
MAP_3458	metA	homoserine O-acetyltransferase	1,4675000000	0,0031262755
MAP_3466	-	ABC transporter ATP-binding protein	1,4900000000	0,0005410654
MAP_3479c	-	MaoC domain protein dehydratase	1,1925000000	0,0000683353
MAP_3481	lpqD	LpqD	1,4675000000	0,0045344005
MAP_3482	acrA1	Short-chain dehydrogenase/reductase SDR	2,1349998000	0,0001024358
MAP_3488c	-	-	2,2675002000	0,0001111764
MAP_3492	-	Trehalose/maltose hydrolase phosphorylase	1,0250000000	0,0070481943
MAP_3495c	-	Cutinase	1,1075001000	0,0392470100
MAP_3507	-	3-oxoacyl-carrier reductase / Short-chain dehydrogenase/reductase SDR	1,0025000000	0,0041529993
MAP_3509	-	flavin monooxygenase, Putative	2,3475000000	0,0013562891
MAP_3514	-	Acyltransferase 3	2,0700000000	0,0003856171
MAP_3519	-	-	1,5325000000	0,0437973370
MAP_3522	oxyS	Transcriptional regulator, oxyS	2,0075002000	0,0006526395
MAP_3526c	-	Pyridoxamine 5'-phosphate oxidase-related protein FMN-binding	2,1475000000	0,0000199788
MAP_3530	-	Protein of unknown function DUF1275	1,1850000000	0,0226328520
MAP_3531c	fbpC2	esterase protein Putative	2,0800002000	0,0000502361
MAP_3532c	-	antibiotic transport system permease protein	1,1675000000	0,0052665790
MAP_3537c	bpoC	Alpha/beta hydrolase fold protein	1,4000001000	0,0208113680
MAP_3541c	-	Luciferase-like monooxygenase	1,3775000000	0,0030403854
MAP_3547c	-	-	1,7000000000	0,0006634501
MAP_3549	-	Sulfotransferase	1,6150000000	0,0030243520
MAP_3553	-	Cytochrome P450 family protein	1,8100000000	0,0006854780
MAP_3555	-	-	2,7550000000	0,0001919022
MAP_3564	-	O-methyltransferase protein	1,6850000000	0,0011204770
MAP_3569c	-	-	1,2650000000	0,0009582668
MAP_3572	pntAA	NAD(P) transhydrogenase subunit alpha PntAA	1,6500000000	0,0031528962
MAP_3577	fabG3	Short-chain dehydrogenase/reductase SDR	1,6075000000	0,0015010898
MAP_3595	-	Alpha/beta hydrolase fold-3 domain protein	2,0975000000	0,0000676856
MAP_3609	-	Virulence factor Mce family protein	2,3100000000	0,0000186439
MAP_3634	-	ErfK/YbiS/YcfS/YnhG family protein	2,9800000000	0,0002231324
MAP_3639c	-	Integral membrane protein	1,9550000000	0,0009995231
MAP_3645	-	-	1,0375000000	0,0156952070
MAP_3661c	-	-	1,8700001000	0,0011160263
MAP_3671	-	Transcriptional regulator, TetR family	3,0900002000	0,0001464092
MAP_3673c	gabD2	succinic semialdehyde dehydrogenase	1,8275000000	0,0010268257
MAP_3686c	-	Transmembrane protein	2,2500000000	0,0001263330
MAP_3690	-	Chloride channel protein	2,0925002000	0,0006064777
MAP_3692c	fabG4	3-ketoacyl-(acyl-carrier-protein) reductase	1,7775002000	0,0010823614
MAP_3699c	-	Integral membrane protein	1,5450001000	0,0031674649
MAP_3703	nirD	Nitrite reductase (NAD(P)H), small subunit NirD	1,1300000000	0,0183401100
MAP_3704c	-	-	1,1650000000	0,0002474365
MAP_3714	fadD2	AMP-dependent Acyl-CoA synthetase and ligase	1,0225000000	0,0005223693
MAP_3720	-	-	1,0975000000	0,0006466091
MAP_3721	-	Non-ribosomal peptide synthetase/polyketide synthase	2,0700002000	0,0066001510
MAP_3727	-	iron complex transport system ATP-binding protein	1,1525000000	0,0019790910
MAP_3732c	-	cobalt/nickel transport system permease protein	1,4900000000	0,0011624069
MAP_3747c	-	-	1,9599999000	0,0438222030
MAP_3769c	rpmG	50S ribosomal protein L33	2,0124998000	0,0000264146
MAP_3771	-	50S ribosomal protein L31 type B	1,5275000000	0,0059453086
MAP_3772c	-	Cobalamin synthesis protein/P47K:cobalamin synthesis CobW	1,2800000000	0,0014668887
MAP_3774c	-	ABC transporter, permease protein	1,5525000000	0,0012708929
MAP_3778	-	AAA ATPase central domain protein	1,2600000000	0,0052375710
MAP_3802c	-	threonine rich protein, Putative	1,7450000000	0,0007118210
MAP_3820	dcd	deoxycytidine triphosphate deaminase	1,7350001000	0,0003347720
MAP_3829c	-	YibE/F family protein	1,2100000000	0,0026670133
MAP_3832c	-	-	1,3025000000	0,0060234710
MAP_3875c	-	-	1,6225000000	0,0052190350
MAP_3876c	-	Transcriptional regulator, TetR family	1,3824999000	0,0001945882
MAP_3883c	-	Beta-lactamase domain protein	1,4575000000	0,0060264010
MAP_3890	mmpL4	Transmembrane transport protein	1,0975001000	0,0148874280
MAP_3893c	pknG	Serine/threonine protein kinase	1,4000000000	0,0007950174
MAP_3916c	xthA	exodeoxyribonuclease III xthA	1,4550000000	0,0010947422
MAP_3921	sodC	Copper/zinc superoxide dismutase	1,5350001000	0,0003390060
MAP_3930c	psd	phosphatidylserine decarboxylase	1,5225000000	0,0099302550
MAP_3941	gloA	Glyoxalase/bleomycin resistance protein/dioxygenase	1,7550000000	0,0027071900
MAP_3942	-	chorismate synthase, Putative	1,5200000000	0,0017159957
MAP_3959c	-	Transcriptional regulator, XRE family	1,8775000000	0,0006845295
MAP_3962	fadB2	3-hydroxybutyryl-CoA dehydrogenase	1,5550000000	0,0104773950

Gene ID	Gene Name	Gene Product	log2 [ratio (Exp/ctrl)]	P-value
MAP_4017c	-	Mandelate racemase/muconate lactonizing protein	1,4799999000	0,0025598616
MAP_4020	hemL	glutamate-1-semialdehyde aminotransferase	1,0500000000	0,0091982230
MAP_4030	pnp	5'-methylthioadenosine phosphorylase	2,2675000000	0,0014776918
MAP_4038c	menE	O-succinylbenzoic acid--CoA ligase	2,6925000000	0,0013745648
MAP_4039c	-	-	2,0200000000	0,0004667851
MAP_4040c	-	Transmembrane protein	1,8925000000	0,0020597307
MAP_4048c	fadD8	AMP-dependent synthetase and ligase	1,6200000000	0,0022107728
MAP_4050	menC	O-succinylbenzoate synthase	1,6450000000	0,0098629830
MAP_4062c	-	flavin monooxygenase, Putative	2,1500000000	0,0002384940
MAP_4069c	-	Protein of unknown function DUF88	3,6900000000	0,0001962086
MAP_4082	-	ABC transporter, permease protein, Putative	1,1700001000	0,0005611124
MAP_4100c	-	Periplasmic nitrate reductase	1,0425000000	0,0085807340
MAP_4104c	-	hydroxyacylglutathione hydrolase	1,3775000000	0,0065530030
MAP_4113	rplA	50S ribosomal protein L1	1,5600001000	0,0028919121
MAP_4118c	lipG	LipG	2,5825000000	0,0000581790
MAP_4122	fabD2	Malonyl CoA-acyl carrier protein transacylase FabD2	1,1475000000	0,0046455050
MAP_4132	end	endonuclease IV	2,2875001000	0,0000338965
MAP_4134	echA4	enoyl-CoA hydratase	1,8174999000	0,0009052228
MAP_4143	tuf	Translation elongation factor Tu	1,5375001000	0,0056276890
MAP_4144	-	PE-PGRS family protein	1,8375000000	0,0007451880
MAP_4160	rpsJ	30S ribosomal protein S10	1,2075000000	0,0328515900
MAP_4164	rplB	50S ribosomal protein L2	2,2424998000	0,0084264080
MAP_4167	rpsC	30S ribosomal protein S3	1,8625000000	0,0003398198
MAP_4181	rpsH	30S ribosomal protein S8	1,1850000000	0,0020913598
MAP_4198	secY	preprotein translocase subunit	1,9850001000	0,0062607755
MAP_4199	adk	adenylate kinase	2,4575000000	0,0009185638
MAP_4207c	-	ABC transporter, ATP-binding protein	1,1175001000	0,0051100450
MAP_4208	-	Acetolactate synthase 2 catalytic subunit	2,0049999000	0,0004703861
MAP_4211	-	Histidinol-phosphate aminotransferase	1,1225000000	0,0013347695
MAP_4237c	-	Cutinase	2,0375000000	0,0348042850
MAP_4264	groES	Co-chaperonin GroES/Cpn10	1,7325001000	0,0007796757
MAP_4265	groEL1	chaperonin GroEL	1,4800000000	0,0007399050
MAP_4307	-	Protein of unknown function DUF190	1,6925000000	0,0001190738
MAP_4309	-	Anti-sigma factor antagonist	2,3625000000	0,0000567120
MAP_4311c	-	-	1,2100000000	0,0004070295
MAP_4325c	-	-	2,1650000000	0,0029231699
MAP_4342c	-	GCN5-related N-acetyltransferase	1,7500000000	0,0279211010
MAP_4348c	-	Protein of unknown function DUF37	1,2050000000	0,0015875059

Appendix 2

Genes of *Map* with significantly down-regulated expression levels in the acid-nitrosative stress

Gene ID	Gene Name	Gene Product	log2 [ratio (Exp/ctrl)]	P-value
MAP_0005	gyrB	DNA gyrase / DNA topoisomerase subunit B	-2,3925000000	0,0058077774
MAP_0013c	-	septation inhibitor protein, Putative	-1,2075000000	0,0458532460
MAP_0014	-	Protein of unknown function DUF881	-2,1775000000	0,0099504390
MAP_0015	pabA	para-aminobenzoate synthase component II	-1,1425000000	0,0030562868
MAP_0030c	-	Acetyltransferase protein	-2,3025000000	0,0151999565
MAP_0035	-	transcriptional regulator, Cro/CI family	-1,1275000000	0,0233057530
MAP_0042	-	-	-1,9174999000	0,0019406064
MAP_0086	-	-	-1,6400000000	0,0005019327
MAP_0097c	-	-	-1,4175000000	0,0049146520
MAP_0138c	-	-	-1,2575000000	0,0014697160
MAP_0147c	-	-	-4,2850000000	0,0359841620
MAP_0150c	fadE25	Acyl-CoA dehydrogenase protein FadE25_2	-1,2300000000	0,0092442630
MAP_0160	-	ESAT-6 like protein EsxD	-2,9050000000	0,0370159150
MAP_0172	gltB	Glutamate synthase large subunit	-2,3900000000	0,0107736580
MAP_0179c	-	Transcriptional regulator, TetR family	-1,5400000000	0,0144979470
MAP_0181c	menG	Ribonuclease activity regulator protein RraA	-1,0725000000	0,0141933290
MAP_0184c	-	-	-2,3350000000	0,0134405850
MAP_0190	glpQ1	glycerophosphoryl diester phosphodiesterase GlpQ1	-1,2225000000	0,0064321607
MAP_0231c	-	-	-1,4024999000	0,0007934986
MAP_0241c	-	lipopolysaccharide transport system ATP-binding protein	-1,7850001000	0,0038250715
MAP_0247c	-	-	-1,7200000000	0,0369250770
MAP_0249c	echA21	enoyl-CoA hydratase	-2,3125000000	0,0111323330
MAP_0252c	hisC2	histidinol-phosphate aminotransferase	-1,5975001000	0,0003585100
MAP_0253	-	Integrase catalytic region	-1,0300000000	0,0383113470
MAP_0255c	-	aminoglycoside phosphotransferase, Protein:	-1,1925000000	0,0203524290
MAP_0274	proW	osmoprotectant transport system permease protein ProW	-1,1950000000	0,0361494160
MAP_0286	-	Protein of unknown function DUF2237	-2,0775000000	0,0152987250
MAP_0292	-	L-carnitine dehydratase/bile acid-inducible protein F	-1,9600000000	0,0177689140
MAP_0297c	-	2-methylcitrate dehydratase	-1,4124999000	0,0017225882
MAP_0324	-	Transmembrane protein	-1,2700000000	0,0056507340
MAP_0336c	-	cytochrome p450	-2,1250000000	0,0425314980
MAP_0362c	-	Integral membrane protein	-1,8350000000	0,0007550442
MAP_0363	-	GatB/Yqey domain-containing protein	-1,9425000000	0,0185696430
MAP_0364c	-	Translation elongation factor Tu	-1,4275000000	0,0137458120
MAP_0368	-	Formate dehydrogenase alpha subunit	-3,2050002000	0,0310679500
MAP_0383	-	-	-1,3600000000	0,0218026700
MAP_0385	-	-	-1,1725000000	0,0419407930
MAP_0393	whiB4	Transcription regulator factor WhiB	-1,9800000000	0,0129480180
MAP_0400	nth	endonuclease III nth	-1,4399999000	0,0014698601
MAP_0401	-	Alkyl hydroperoxide reductase/ Thiol specific antioxidant/ Mal allergen	-1,3275000000	0,0052549630
MAP_0404c	ephE	Alpha/beta hydrolase fold protein	-1,0124999000	0,0207343210
MAP_0407c	acs	acetyl-CoA synthetase	-1,4800000000	0,0478959000
MAP_0426c	-	adenylate cyclase	-2,3300000000	0,0001467458
MAP_0433c	-	Polysaccharide biosynthesis protein	-1,6850001000	0,0373493060
MAP_0438	mesJ	TRNA(Ile)-lysidine synthetase protein	-1,4175000000	0,0112098060
MAP_0439	hpt	hypoxanthine-guanine phosphoribosyltransferase	-1,0725000000	0,0180952100
MAP_0458	-	pantothenate kinase	-1,5675000000	0,0189214220
MAP_0466c	lpqF	LpqF	-1,5175000000	0,0468478800
MAP_0473c	radA	DNA repair protein RadA	-1,8000000000	0,0143046980
MAP_0474c	lpqE	Protein of unknown function DUF461	-1,7475001000	0,0094520510
MAP_0476	ispD	2-C-methyl-D-erythritol 4-phosphate cytidylyltransferase	-2,2575000000	0,0048905946
MAP_0479	-	TRNA/rRNA methyltransferase	-1,7600000000	0,0335827800
MAP_0480	-	glycerophosphoryl diester phosphodiesterase	-2,0650000000	0,0108500020
MAP_0501	nhoA	arylamine N-acetyltransferase NhoA	-1,5675000000	0,0000598163
MAP_0512c	-	-	-1,4900000000	0,0231949220
MAP_0519c	-	Hemerythrin HHE cation binding domain protein	-1,5999999000	0,0033964713
MAP_0533	-	4-hydroxy-2-ketovalerate aldolase	-1,1475000000	0,0081188790
MAP_0537	-	Sulfotransferase	-1,0475000000	0,0471092720
MAP_0547	-	Cytochrome P450	-2,1924999000	0,0005216567
MAP_0553	ilvX	Acetolactate synthase 2 catalytic subunit	-1,6949999000	0,0302063110
MAP_0581c	-	Aspartyl/glutamyl-tRNA amidotransferase subunit A	-1,2775000000	0,0026426080
MAP_0587	-	-	-1,7950000000	0,0119087230
MAP_0621	-	FAD-binding dehydrogenase, Putative	-1,9100001000	0,0450279680
MAP_0623	-	-	-1,2100000000	0,0006202053
MAP_0660	-	Protein of unknown function DUF2236	-1,7225000000	0,0125997085

Gene ID	Gene Name	Gene Product	log2 [ratio (Exp/ctrl)]	P-value
MAP_0661c	-	Transcriptional regulator, ArsR family protein	-1,1925000000	0,0433349870
MAP_0663	-	O-methyltransferase protein	-1,1850000000	0,0417493700
MAP_0682	-	Acyl-CoA dehydrogenase domain protein	-2,9200000000	0,0243216080
MAP_0686	-	Acetyl-CoA acetyltransferase	-1,1325000000	0,0015843532
MAP_0691c	-	Fumarate reductase/succinate dehydrogenase flavoprotein domain protein	-1,4375000000	0,0336179360
MAP_0714c	-	-	-3,2575002000	0,0313614940
MAP_0719c	-	-	-4,5400000000	0,0080584750
MAP_0721c	-	Carboxymuconolactone decarboxylase protein	-1,0350000000	0,0308042900
MAP_0727	-	cytochrome p450	-1,1775000000	0,0045255665
MAP_0728	-	Protein of unknown function DUF1330	-2,2950000000	0,0114302740
MAP_0742c	-	-	-1,1625000000	0,0047105090
MAP_0753c	-	-	-1,5550001000	0,0234625730
MAP_0757	-	ABC transporter, permease protein, Putative	-3,2525000000	0,0211034300
MAP_0763	-	-	-2,1900000000	0,0045246254
MAP_0785	far	L-carnitine dehydratase/bile acid-inducible protein F	-1,0424999000	0,0103612170
MAP_0791c	-	-	-1,0825000000	0,0266461860
MAP_0805c	-	Transglycosylase domain protein	-2,6900000000	0,0077739405
MAP_0807c	-	molybdenum cofactor biosynthesis protein	-1,7974999000	0,0372407470
MAP_0818c	-	Transmembrane protein	-3,2875000000	0,0094517930
MAP_0821	-	-	-2,2775000000	0,0014945079
MAP_0827c	citA	citrate synthase 2	-1,2125001000	0,0071171387
MAP_0828	pdxH	pyridoxamine 5'-phosphate oxidase	-2,2975001000	0,0067578990
MAP_0831c	-	-	-2,3225000000	0,0465741100
MAP_0840	echA6	enoyl-CoA hydratase	-1,2925000000	0,0003368283
MAP_0847	-	Carbohydrate-binding protein	-1,3075001000	0,0252421050
MAP_0852	-	-	-2,4900000000	0,0004345498
MAP_0858	-	-	-1,2375000000	0,0248232260
MAP_0876c	-	Ribokinase:Carbohydrate kinase	-2,1675000000	0,0187579060
MAP_0878c	-	HAD superfamily hydrolase	-2,5024998000	0,0020885738
MAP_0882c	-	O-methyltransferase protein	-1,5500001000	0,0483964200
MAP_0891c	pgi	glucose-6-phosphate isomerase	-1,9350000000	0,0014580024
MAP_0892c	-	Chorismate mutase	-1,9549999000	0,0020530522
MAP_0909c	echA7	enoyl-CoA hydratase	-2,3725000000	0,0000404741
MAP_0910c	fadE12	Acyl-CoA dehydrogenase domain protein FadE12_2	-3,3375000000	0,0042062346
MAP_0925	moeA	Molybdenum cofactor biosynthesis protein MoeA	-1,1825000000	0,0146945070
MAP_0928	-	-	-1,9625001000	0,0356411520
MAP_0934	-	Peptidase M42 family protein	-4,5875000000	0,0037615085
MAP_0944	-	-	-2,0975000000	0,0052845940
MAP_0954	-	-	-3,2375000000	0,0225107430
MAP_0955	-	Aldo-keto reductase-like protein	-1,3699999000	0,0057555423
MAP_0966c	-	PPE family protein	-1,8875000000	0,0390864350
MAP_0969	cprA	Transcriptional regulator, TetR family	-1,5350000000	0,0078193275
MAP_0974	-	Transglycosylase domain-containing protein	-3,0525000000	0,0387174100
MAP_0984c	glmU	bifunctional UDP-N-acetylglucosamine pyrophosphorylase	-1,0174999000	0,0141938840
MAP_0995c	kdpE	two-component system, OmpR family, KDP operon response regulator KdpE	-2,8750000000	0,0156908050
MAP_0997c	kdpC	K+-transporting ATPase ATPase C chain KdpC	-1,1925000000	0,0016568177
MAP_1007	-	40-residue YVTN family beta-propeller repeat protein	-2,2300000000	0,0031619936
MAP_1011	-	Patatin protein	-1,1300000000	0,0482924400
MAP_1014	-	Cysteine dioxygenase type I protein	-2,6374998000	0,0000003560
MAP_1022c	-	Lipolytic protein G-D-S-L family	-2,2850000000	0,0012433183
MAP_1038	ruvB	Holliday junction DNA helicase	-1,8024999000	0,0161203720
MAP_1045	-	peptide/nickel transport system substrate-binding protein	-1,6374999000	0,0099869220
MAP_1053	-	13E12 repeat family protein	-1,2125000000	0,0491788800
MAP_1070c	-	Protein of unknown function DUF404	-1,9925000000	0,0067073640
MAP_1117	-	Integral membrane protein	-2,5200000000	0,0160836060
MAP_1120	pyrF	orotidine 5'-phosphate decarboxylase	-1,0025000000	0,0484161100
MAP_1123	gmk	guanylate kinase	-1,0400000000	0,0074082003
MAP_1138c	lprG	Protein of unknown function DUF1396	-1,8750000000	0,0103064220
MAP_1142	-	Protein of unknown function DUF2581	-1,0825000000	0,0063078813
MAP_1148	-	LPPG:FO 2-phospho-L-lactate transferase	-1,1775000000	0,0485836750
MAP_1149	-	Protein of unknown function DUF199	-1,6625000000	0,0304975860
MAP_1151c	-	-	-1,4750001000	0,0192846840
MAP_1154	-	Lipoprotein LprJ	-1,9150000000	0,0149126090
MAP_1170	-	integral membrane protein, Putative	-1,0400000000	0,0221366340
MAP_1183c	-	antibiotic transport system permease protein	-2,7574997000	0,0220363550
MAP_1195c	fadE15	Acyl-CoA dehydrogenase domain protein	-2,1675000000	0,0458662900
MAP_1197	echA12	enoyl-CoA hydratase	-1,2300000000	0,0320947500
MAP_1202	-	-	-2,9724998000	0,0478076100
MAP_1210	inhA	2-trans-enoyl-acyl carrier protein reductase (inhA)	-2,7000000000	0,0324308130

Gene ID	Gene Name	Gene Product	log2 [ratio (Exp/ctrl)]	P-value
MAP_1228	lipL	Esterase beta-lactamase	-1,6999999000	0,0094365245
MAP_1238c	drrA	antibiotic transport system ATP-binding protein DrrA	-1,7175000000	0,0031210098
MAP_1249c	ansA	L-asparaginase AnsA	-1,0775000000	0,0027757210
MAP_1262	-	-	-3,3500001000	0,0356400160
MAP_1279c	-	methyl-accepting chemotaxis sensory, Putative	-1,1550000000	0,0389974640
MAP_1282c	-	-	-1,7500000000	0,0374181680
MAP_1283	bioB	biotin synthase	-2,0950003000	0,0361941900
MAP_1288c	-	NUDIX hydrolase	-2,2150002000	0,0060003390
MAP_1297	hisA	phosphoribosyl isomerase A	-1,3175001000	0,0076827550
MAP_1320c	-	Acetyl-CoA acetyltransferase protein	-2,0325000000	0,0497234900
MAP_1347c	-	-	-1,3500000000	0,0254021660
MAP_1349c	-	-	-1,3125000000	0,0427595820
MAP_1354	rplT	50S ribosomal protein L20	-1,7375000000	0,0002594108
MAP_1356c	-	Protein of unknown function DUF2236	-1,8850000000	0,0190906640
MAP_1359	pheS	phenylalanyl-tRNA synthetase subunit	-1,3475001000	0,0429007630
MAP_1361	argC	N-acetyl-gamma-glutamyl-phosphate reductase	-1,1099999000	0,0182239560
MAP_1367	argG	argininosuccinate synthase	-2,9800000000	0,0158213250
MAP_1377	-	-	-1,1075001000	0,0219476390
MAP_1379	-	-	-1,0250000000	0,0121354420
MAP_1382c	-	Mandelate racemase/muconate lactonizing protein	-1,3275000000	0,0051175640
MAP_1389	-	Poly-beta-hydroxybutyrate polymerase acid synthase	-3,1475000000	0,0105121825
MAP_1402	ppnk	inorganic polyphosphate/ATP-NAD kinase	-3,2424998000	0,0087208680
MAP_1406	pyrG	CTP synthetase	-2,2975001000	0,0189212450
MAP_1427	-	Multicopper oxidase/copper protein	-1,7825000000	0,0268352740
MAP_1437c	-	-	-2,2775002000	0,0360939800
MAP_1454	-	TolA protein	-1,8824999000	0,0131456840
MAP_1463	-	flavin monooxygenase, Putative	-2,5150000000	0,0226506740
MAP_1469c	-	cytochrome p450	-1,4600000000	0,0143126180
MAP_1476c	-	Cutinase	-1,2200000000	0,0184304380
MAP_1477c	-	Transcriptional regulator, TetR family	-2,4900000000	0,0179127030
MAP_1486c	-	-	-3,2150002000	0,0064454367
MAP_1489c	-	-	-1,0375000000	0,0272910730
MAP_1501	-	Protein of unknown function DUF690	-1,2350001000	0,0373935140
MAP_1503c	-	Cytochrome P450	-1,1925001000	0,0026701784
MAP_1504	-	-	-1,9950000000	0,0116843640
MAP_1510	-	Secretion protein snm4	-1,2800000000	0,0379524680
MAP_1521	-	PPE family protein	-1,0375000000	0,0465329550
MAP_1524	mgtC	Transporter, MgtC/SapB family	-1,5450001000	0,0308741480
MAP_1526	-	-	-2,6925000000	0,0013203417
MAP_1541	-	Transcriptional regulator, MerR family	-2,0125000000	0,0032306835
MAP_1543	-	Transcriptional regulator, MerR family	-2,0300000000	0,0049986100
MAP_1555c	-	-	-4,3025000000	0,0053641936
MAP_1569	modD	modD	-1,8149999000	0,0089464550
MAP_1572c	-	Abortive infection protein	-2,0725000000	0,0289714020
MAP_1574c	-	Short-chain dehydrogenase/reductase SDR	-1,1800000000	0,0442772360
MAP_1604c	lppE	Lipoprotein LppE	-1,0100000000	0,0014394172
MAP_1606c	-	Polyketide cyclase/dehydrase	-1,2974999000	0,0287426470
MAP_1611	-	-	-1,7775000000	0,0175574180
MAP_1630c	-	-	-1,0325000000	0,0021417753
MAP_1635c	-	3-octaprenyl-4-hydroxybenzoate carboxy-lyase UbiX	-1,7000000000	0,0329585400
MAP_1640c	-	Activator of Hsp90 ATPase 1 family protein	-3,3775000000	0,0392128040
MAP_1653	tpx	Thiol peroxidase protein	-1,7950001000	0,0019395581
MAP_1658	-	Aldehyde dehydrogenase (acceptor)	-1,8325000000	0,0024761330
MAP_1679c	-	Protein of unknown function DUF1345	-1,0074999000	0,0000049003
MAP_1708	-	Metal-dependent phosphohydrolase	-1,3850000000	0,0326277300
MAP_1712	-	L-carnitine dehydratase/bile acid-inducible protein F	-1,1375000000	0,0403606740
MAP_1721c	-	Transcriptional regulator, TetR family	-1,1375000000	0,0036664167
MAP_1741c	-	Universal stress protein, UspA	-1,2875000000	0,0092614490
MAP_1744	-	-	-1,4150000000	0,0171469340
MAP_1755c	-	Formate/nitrite transporter protein	-1,7450000000	0,0034605270
MAP_1758c	nrtC	Acyl-CoA dehydrogenase protein, putative	-1,2375000000	0,0276806800
MAP_1777c	-	-	-1,3550000000	0,0468005280
MAP_1796c	pks12	Type I modular polyketide synthase	-1,8225000000	0,0031739632
MAP_1821c	-	-	-1,0275000000	0,0049501457
MAP_1824c	-	IS30 family transposase	-1,5224999000	0,0183240800
MAP_1826c	-	-	-1,2275000000	0,0220108050
MAP_1833c	-	proteasome component/protein of unknown function, DUF275, Putative	-1,6125001000	0,0060145436
MAP_1839	-	-	-1,2975000000	0,0277660710
MAP_1844c	lpd	Pyridine nucleotide-disulphide oxidoreductase	-2,7200000000	0,0146146660

Gene ID	Gene Name	Gene Product	log2 [ratio (Exp/ctrl)]	P-value
MAP_1855	-	-	-1,0250000000	0,0142223970
MAP_1867c	pks5	Beta-ketoacyl synthase	-1,8924999000	0,0013954911
MAP_1868c	efpA	Major facilitator superfamily transporter	-2,1500000000	0,0144234780
MAP_1870c	-	Non-ribosomal peptide synthetase	-1,5225000000	0,0023782493
MAP_1874c	-	Transcriptional regulator, LuxR family	-1,5749999000	0,0081545105
MAP_1889c	wag31	Cell-division initiation protein DivIVA	-1,8325001000	0,0180892390
MAP_1904c	-	-	-1,5525000000	0,0123370320
MAP_1912	-	Glycosyl transferase, group 2 family protein	-1,4399999000	0,0108081850
MAP_1935	qcrB	ubiquinol-cytochrome c reductase cytochrome b subunit QcrB	-1,4675000000	0,0110568125
MAP_1954c	-	Polyketide cyclase / dehydrase and lipid transport	-2,4275000000	0,0239679980
MAP_1959	lipA	lipoyl synthase	-1,7425000000	0,0224995740
MAP_1971	-	Mannan endo-1,4-beta-mannosidase	-2,5175000000	0,0029622766
MAP_1981c	-	zinc ribbon domain, protein / Protein of unknown function DUF164	-2,7000000000	0,0154358630
MAP_1983c	cobC	L-threonine-O-3-phosphate decarboxylase	-1,3149999000	0,0070156422
MAP_1985	ptpA	Protein tyrosine phosphatase	-1,7599999000	0,0012256114
MAP_1999	kasB	3-oxoacyl-(acyl carrier protein) synthase II	-1,2525000000	0,0387020670
MAP_2003c	-	Transcriptional regulator, TetR family	-1,0050001000	0,0156229030
MAP_2005	-	Diacylglycerol kinase, catalytic region	-1,9250000000	0,0213282850
MAP_2012c	-	-	-1,1950000000	0,0021857086
MAP_2023c	-	Transcriptional regulator, TetR family	-1,3249999000	0,0089859900
MAP_2046	sseB	Thiosulfate sulfurtransferase SseB	-1,7099999000	0,0078082043
MAP_2062	-	Integral membrane protein	-1,9250000000	0,0012646823
MAP_2074c	-	-	-1,9150000000	0,0311049350
MAP_2085	-	-	-1,9125000000	0,0185360900
MAP_2086c	-	-	-1,6400000000	0,0057756430
MAP_2099	-	Transcriptional regulator, MarR family	-2,3175000000	0,0163931720
MAP_2102c	narK3	Nitrate/nitrite transporter/facilitator	-2,1850000000	0,0164274930
MAP_2110c	-	-	-2,2875000000	0,0281802270
MAP_2127	-	monooxygenase, Putative	-2,0475001000	0,0042230100
MAP_2140c	-	-	-1,8250000000	0,0116612250
MAP_2154c	-	-	-1,8275000000	0,0009543235
MAP_2161c	-	16S ribosomal RNA methyltransferase RsmE	-1,5350000000	0,0303555520
MAP_2167c	-	-	-1,2924999000	0,0272364370
MAP_2175c	mbtC	mycobactin polyketide synthetase MbtC	-2,1750000000	0,0425198600
MAP_2178	mbtA	mycobactin salicyl-AMP ligase MbtA	-3,7900000000	0,0330420400
MAP_2180c	-	-	-1,8249999000	0,0165652860
MAP_2208	nirA	Nitrite/sulfite reductase beta subunit NirA_2	-1,4449999000	0,0304918600
MAP_2212c	cysT	sulfate transport system permease protein CysT	-1,2175000000	0,0089931080
MAP_2223c	-	Protein of unknown function DUF404	-2,3000002000	0,0033452369
MAP_2230c	-	Type I modular polyketide synthase	-1,5874999000	0,0015443376
MAP_2231	papA3	Non-ribosomal peptide synthetase/polyketide synthase	-2,2500000000	0,0452030380
MAP_2232	mmpL10	Transmembrane transport protein	-1,2375000000	0,0228799820
MAP_2237	-	dihydrodipicolinate reductase protein, Hypothetical protein	-1,1350000000	0,0471044030
MAP_2240c	-	DegV family protein	-1,4750000000	0,0459297700
MAP_2242c	-	Phosphoglycerate mutase	-1,4250000000	0,0227254780
MAP_2247c	proA	gamma-glutamyl phosphate reductase	-1,5900000000	0,0245714840
MAP_2262	-	Transcriptional regulator, TetR family	-1,3125000000	0,0150107300
MAP_2285c	rpi	ribose-5-phosphate isomerase B	-2,2224998000	0,0380816420
MAP_2289c	-	-	-1,1300000000	0,0010042387
MAP_2292	-	Alpha amylase, catalytic region	-1,5450001000	0,0356236730
MAP_2297c	-	copper resistance protein D, Putative	-2,3325000000	0,0025407034
MAP_2299c	-	1-acyl-sn-glycerol-3-phosphate acyltransferase	-1,1300000000	0,0380092150
MAP_2302	-	Integrase catalytic region	-1,2550000000	0,0000195355
MAP_2305	-	-	-3,8799999000	0,0410033300
MAP_2307c	pdhC	branched-chain alpha-keto acid dehydrogenase subunit	-2,7800002000	0,0385057030
MAP_2319c	-	NPT hydrolase putative, Protein of unknown function DUF853	-1,2700000000	0,0014550403
MAP_2321	-	-	-4,3050000000	0,0433959700
MAP_2324c	-	exporter RND superfamily protein, Putative	-1,5600000000	0,0001722701
MAP_2329	bcp	Bacterioferritin comigratory protein, alkyl hydroperoxide reductase/thiol specific antioxidant	-4,4175000000	0,0202388480
MAP_2335c	-	Transcriptional regulator	-1,5849999000	0,0070750520
MAP_2338	-	Aldehyde dehydrogenase (acceptor)	-1,8400000000	0,0038316974
MAP_2345c	-	-	-2,7250000000	0,0379370820
MAP_2351	-	Acyl-CoA dehydrogenase domain protein	-1,2625000000	0,0155414900
MAP_2352	-	Acyl-CoA dehydrogenase domain protein	-3,3975000000	0,0189711200
MAP_2361	rsbU	anti-sigma regulatory factor, serine/threonine protein kinase rsbU, Putative	-2,3175000000	0,0071685240
MAP_2364c	-	Alpha/beta hydrolase fold-3 domain protein	-1,4150000000	0,0244416520
MAP_2382	-	cytochrome p450	-1,5600001000	0,0321235020
MAP_2394	-	Transcriptional regulator, TetR family	-3,0000000000	0,0116067670

Gene ID	Gene Name	Gene Product	log2 [ratio (Exp/ctrl)]	P-value
MAP_2400	-	Acyl-CoA synthetase medium-chain family member 1	-1,3975000000	0,0092541350
MAP_2423c	-	Beta-lactamase domain protein	-1,3250000000	0,0173750310
MAP_2430	-	nicotinate phosphoribosyltransferase	-1,6150000000	0,0156515860
MAP_2434	glgB	glycogen branching enzyme	-2,0350000000	0,0104751390
MAP_2450c	atpC	F0F1 ATP synthase subunit	-2,0825000000	0,0059991600
MAP_2468c	thrA	homoserine dehydrogenase	-1,0825000000	0,0040326770
MAP_2480c	-	-	-1,5700000000	0,0132031970
MAP_2485c	cysD	sulfate adenylyltransferase subunit	-1,3924999000	0,0300035900
MAP_2490	oppD	peptide/nickel transport system ATP-binding protein OppD	-2,0025000000	0,0028264548
MAP_2508	-	G:T/U mismatch-specific uracil DNA-glycosylase	-2,0700002000	0,0213328580
MAP_2518	-	Cytochrome P450	-1,0150001000	0,0002220944
MAP_2530	-	Short-chain dehydrogenase/reductase SDR	-3,4875000000	0,0018459195
MAP_2545c	sugC	Spermidine/putrescine ABC transporter ATP-binding subunit	-1,7525000000	0,0162020340
MAP_2552	-	Membrane-bound lytic murein transglycosylase B-like protein	-1,3075000000	0,0417875300
MAP_2554c	-	sec-independent translocase	-1,0650000000	0,0138544090
MAP_2555c	htrA	DO serine protease htrA	-1,6999999000	0,0136116800
MAP_2561	-	antibiotic transport system permease protein	-2,1625001000	0,0304509600
MAP_2564c	glgC	glucose-1-phosphate adenylyltransferase	-1,8225000000	0,0399640900
MAP_2572c	-	Rossmann fold nucleotide-binding protein, Putative	-1,1175001000	0,0002497403
MAP_2602	-	-	-1,6225000000	0,0155674820
MAP_2607c	fdxC	4Fe-4S ferredoxin iron-sulfur binding domain protein	-2,6400000000	0,0103534530
MAP_2619c	narH	nitrate reductase 1, beta subunit NarH	-1,4225000000	0,0000410190
MAP_2628c	-	HhH-GPD family protein	-1,3699999000	0,0368894700
MAP_2630c	-	Pyridoxamine 5'-phosphate oxidase-related protein FMN-binding	-2,7100000000	0,0185485990
MAP_2637c	-	Short-chain dehydrogenase/reductase SDR:3 dehydrogenase	-1,6000000000	0,0085829700
MAP_2649c	-	cytochrome p450	-2,9000000000	0,0384020320
MAP_2653c	nirQ	nitric-oxide reductase NorQ protein NirQ	-3,5975000000	0,0014199215
MAP_2655	-	Acyl-CoA dehydrogenase domain protein	-1,8950000000	0,0128908550
MAP_2656	-	Acyl-CoA dehydrogenase domain protein	-1,4250001000	0,0135301990
MAP_2662c	-	Transmembrane protein	-1,6400000000	0,0009496614
MAP_2667c	ephC	Short chain dehydrogenase ephC	-1,3850000000	0,0305054630
MAP_2672	-	Adenylate cyclase protein	-2,4924998000	0,0022497391
MAP_2681c	-	HNH endonuclease protein	-1,7700000000	0,0116946600
MAP_2693	fum	fumarate hydratase	-2,2325000000	0,0191334710
MAP_2694	-	-	-2,0949998000	0,0093699900
MAP_2697c	phoH2	PhoH family protein	-1,4275000000	0,0362982450
MAP_2700	coaA	pantothenate kinase	-2,2900000000	0,0031315007
MAP_2708c	-	glutamine amidotransferase	-1,6825000000	0,0025626768
MAP_2717	-	Na+/H+ exchanger; sodium:hydrogen antiporter	-1,4175000000	0,0234532490
MAP_2718c	-	hippurate hydrolase	-2,4325001000	0,0187551320
MAP_2724c	-	Transmembrane protein	-1,1100000000	0,0418727300
MAP_2747	-	AMP-dependent Acyl-CoA synthetase and ligase	-1,1000000000	0,0314568700
MAP_2753	-	-	-1,5025000000	0,0389824360
MAP_2758	-	-	-1,7450000000	0,0158918970
MAP_2768c	-	Integrase	-1,4200001000	0,0148177120
MAP_2782	-	Aldehyde dehydrogenase	-1,6300000000	0,0139399930
MAP_2784	-	Cation diffusion facilitator family transporter	-1,1949999000	0,0002151367
MAP_2793	-	Protein of unknown function DUF2029	-1,9000000000	0,0184393930
MAP_2796c	-	-	-1,3850001000	0,0182317300
MAP_2813c	-	-	-2,6600000000	0,0261916280
MAP_2820	sigA	RNA polymerase sigma factor sigA	-1,7750001000	0,0125489770
MAP_2822	-	-	-1,2600000000	0,0198017550
MAP_2844	-	Protein of unknown function DUF349	-2,0325000000	0,0107991140
MAP_2852	-	limonene-1,2-epoxide hydrolase	-2,7250001000	0,0439100080
MAP_2860	-	-	-1,4700000000	0,0210955590
MAP_2873c	-	Acetyl CoA carboxylase, biotin carboxylase subunit	-1,9750000000	0,0060010077
MAP_2886c	-	Metal-dependent hydrolase, putative	-1,0525000000	0,0121614910
MAP_2891c	gpsI	polynucleotide phosphorylase/polyadenylase	-1,6625000000	0,0317527950
MAP_2893c	ribF	bifunctional riboflavin kinase/FMN adenylyltransferase	-1,7275000000	0,0010547766
MAP_2909c	nusA	Transcription elongation factor NusA	-1,6525000000	0,0229981000
MAP_2917c	cobB	cobyrinic acid a,c-diamide synthase	-1,7425001000	0,0128780320
MAP_2921c	-	malate:quinone oxidoreductase	-1,4025000000	0,0158656650
MAP_2943c	-	Radical SAM enzyme, Cfr family protein	-1,1625000000	0,0451911300
MAP_2944c	cdsA	phosphatidate cytidylyltransferase	-1,9925000000	0,0407454070
MAP_2949c	-	Phospholipid/glycerol acyltransferase	-1,7600001000	0,0398456680
MAP_2950c	-	Immunogenic protein MPT63 (16 kDa immunoprotective extracellular protein)	-1,4075000000	0,0207138430
MAP_2973	lppW	alanine rich lipoprotein LppW, Putative	-3,3525000000	0,0016263869
MAP_2993	-	-	-1,7900000000	0,0008606784
MAP_2997c	-	Vacuolar-type H+-ATPase subunit H	-1,3525000000	0,0035752063

Gene ID	Gene Name	Gene Product	log2 [ratio (Exp/ctrl)]	P-value
MAP_3013c	-	Oxidoreductase, short-chain dehydrogenase/reductase protein	-2,4075000000	0,0427859700
MAP_3018	-	Secreted protein	-1,6850000000	0,0198505930
MAP_3027	-	-	-1,4150000000	0,0132832650
MAP_3028	-	Pyridoxamine 5'-phosphate oxidase-related protein FMN-binding	-4,0175000000	0,0039991937
MAP_3032c	leuB	3-isopropylmalate dehydrogenase	-1,2574999000	0,0240014530
MAP_3040c	-	-	-1,2600000000	0,0008230781
MAP_3043c	-	ATPase involved in chromosome partitioning-like protein	-1,8125001000	0,0296364900
MAP_3050c	-	-	-1,3050001000	0,0087347460
MAP_3052c	-	Transcriptional regulator, TetR family	-3,7224998000	0,0184491840
MAP_3058c	-	cysteine desulfurase	-1,6399999000	0,0090415210
MAP_3075	-	isorenieratene synthase	-1,6274999000	0,0004547367
MAP_3079c	-	isopentenyl pyrophosphate isomerase	-2,0850000000	0,0217884830
MAP_3128	-	-	-1,8575000000	0,0406074450
MAP_3136c	-	Dioxygenase, alpha subunit:Rieske	-1,0800000000	0,0024245614
MAP_3140c	-	Amidohydrolase protein	-1,5949999000	0,0026418236
MAP_3143	-	Aldehyde dehydrogenase protein	-1,5200000000	0,0437913460
MAP_3150c	-	Protein of unknown function DUF488	-1,9825000000	0,0009373041
MAP_3158c	-	Lipoprotein LprJ	-2,7375000000	0,0144867610
MAP_3170c	smpB	SsrA-binding protein	-2,8525000000	0,0221831460
MAP_3175c	prfB	Peptide chain release factor 1	-1,1300000000	0,0177076720
MAP_3177	-	Pyridoxamine 5'-phosphate oxidase-related FMN- binding protein	-1,4849999000	0,0007985896
MAP_3180	-	Cytochrome b subunit of nitric oxide reductase	-3,6825000000	0,0354471540
MAP_3183	-	SPFH domain-containing protein/band 7 family protein	-1,0175000000	0,0024787890
MAP_3207	nuoG	NADH dehydrogenase subunit	-1,6275000000	0,0011622205
MAP_3231c	-	-	-3,4950000000	0,0230569700
MAP_3238	-	acyl-CoA dehydrogenase-related protein, Putative	-1,1000000000	0,0168962460
MAP_3244	-	DNA topoisomerase I protein, Putative	-1,3799999000	0,0155238295
MAP_3263c	-	-	-1,3900000000	0,0177940730
MAP_3293	-	-	-1,0250000000	0,0229707470
MAP_3310	-	Membrane protein	-1,0950000000	0,0086391130
MAP_3312	rhlE	DEAD/DEAH box ATP-dependent RNA helicase	-2,7400002000	0,0015395508
MAP_3324c	sigH	RNA polymerase sigma factor RpoE SigH	-1,0150000000	0,0132252040
MAP_3339c	-	ZK899.2	-1,0600000000	0,0347291640
MAP_3341	-	-	-1,1450000000	0,0196217220
MAP_3342	-	-	-3,2350001000	0,0281073940
MAP_3346c	pvdS	Protein of unknown function DUF344	-1,0475000000	0,0321872000
MAP_3363c	-	-	-2,1875000000	0,0159141200
MAP_3368c	-	Bifunctional phosphoglucose/phosphomannose isomerase	-2,0800000000	0,0246661080
MAP_3371	-	cytoplasmic protein, Putative	-1,5699999000	0,0074622550
MAP_3394c	purK	phosphoribosylaminoimidazole carboxylase ATPase subunit	-1,3075000000	0,0038021830
MAP_3427c	amiB	Amidohydrolase protein	-3,7800002000	0,0072668693
MAP_3439c	deoA	thymidine phosphorylase	-1,0174999000	0,0431707580
MAP_3440c	cdd	cytidine deaminase	-5,0474997000	0,0005472814
MAP_3443	sdhA	succinate dehydrogenase flavoprotein subunit	-1,4000000000	0,0213117100
MAP_3445	-	-	-1,2675000000	0,0477673700
MAP_3470c	-	Protein of unknown function DUF742	-1,3725000000	0,0419953580
MAP_3472c	-	Membrane sensor signal transduction histidine kinase	-1,4875001000	0,0231373100
MAP_3486	-	L-lactate dehydrogenase/FMN-dependent alpha-hydroxy acid dehydrogenase	-1,5575001000	0,0170162040
MAP_3500c	-	-	-1,2625000000	0,0467167000
MAP_3539c	fadE1	Acyl-CoA dehydrogenase protein FadE1_3	-2,0175000000	0,0455302370
MAP_3559	-	DNA--protein / DNA-3-methyladenine glycosylase II	-1,7950001000	0,0044738260
MAP_3565	-	Cell envelope-related protein transcriptional attenuator	-1,8725000000	0,0315721800
MAP_3570c	fadE2	Acyl-CoA dehydrogenase protein FadE2	-1,0200000000	0,0235688350
MAP_3579c	-	-	-1,2975000000	0,0467580070
MAP_3580c	-	cytoplasmic protein, Putative	-1,6925000000	0,0150051000
MAP_3584	-	Luciferase-like monooxygenase	-1,7300000000	0,0003970711
MAP_3605	-	MCE-family protein MCE1B	-1,8749999000	0,0119604040
MAP_3617c	-	Pirin domain protein	-1,2650001000	0,0159269530
MAP_3622	-	Alpha/beta hydrolase fold protein	-1,2774999000	0,0241178850
MAP_3651c	fadE3	Acyl-CoA dehydrogenase protein FadE3_2	-1,6375000000	0,0435297750
MAP_3659	-	AMP-dependent synthetase and ligase	-1,4925000000	0,0154368080
MAP_3662c	-	Aldehyde dehydrogenase (acceptor)	-1,8374999000	0,0441309400
MAP_3674	-	-	-2,2425000000	0,0003776424
MAP_3683	-	catalase	-2,0875000000	0,0029331122
MAP_3684	-	Glucose-methanol-choline oxidoreductase	-1,5274999000	0,0443041660
MAP_3689	-	Transcriptional regulator, TetR family	-1,0475000000	0,0025172967
MAP_3695	-	Oxidoreductase, 2OG-Fe(II) oxygenase family protein	-1,1250000000	0,0016768635
MAP_3702	nirB	Nitrite reductase (NAD(P)H), large subunit	-1,0600000000	0,0269976520
MAP_3708c	-	Allophanate hydrolase/urea amidolyase-related protein	-1,0125000000	0,0225835070

Gene ID	Gene Name	Gene Product	log2 [ratio (Exp/ctrl)]	P-value
MAP_3710c	fecB2	iron complex transport system substrate-binding protein	-1,1550000000	0,0386322850
MAP_3738c	-	Methyltransferase type 12 / Cyclopropane-fatty-acyl-phospholipid synthase	-1,4775000000	0,0021631715
MAP_3764c	pks2	Beta-ketoacyl synthase	-1,7175000000	0,0049018010
MAP_3770	-	-	-2,3100002000	0,0210987050
MAP_3800	-	-	-1,6100000000	0,0005328486
MAP_3801	-	-	-1,3075000000	0,0272810700
MAP_3807	-	Integral membrane protein	-2,2425000000	0,0090337620
MAP_3813	-	-	-1,2100000000	0,0053242133
MAP_3822	-	-	-2,3274999000	0,0107425920
MAP_3826	-	Protein of unknown function DUF1503	-1,5300000000	0,0214752100
MAP_3827	-	-	-1,3275000000	0,0050340950
MAP_3836c	-	-	-1,8750000000	0,0222396200
MAP_3843	hspR	Transcriptional regulator, MerR family	-1,5875000000	0,0465048400
MAP_3849	-	-	-2,2050000000	0,0257382780
MAP_3852c	-	threonine rich protein, Putative	-1,0100000000	0,0089580850
MAP_3854	-	IS30 family transposase	-1,5300000000	0,0343996100
MAP_3865c	-	Cation diffusion facilitator family transporter	-1,9225001000	0,0159389620
MAP_3879c	-	2-hydroxycyclohexanecarboxyl-CoA dehydrogenase	-1,1575000000	0,0051762280
MAP_3891	-	Transcriptional regulator, TetR family	-1,3500000000	0,0073654640
MAP_3905	-	transmembrane protein, Putative	-1,0400000000	0,0412072540
MAP_3907	lpqL	Peptidase, M28 protein	-2,9325000000	0,0185010540
MAP_3915c	-	-	-1,9000001000	0,0368294530
MAP_3936	groEL2	chaperonin GroEL	-1,3125001000	0,0301781000
MAP_3955	-	-	-1,8824999000	0,0202891980
MAP_3961	aceA	isocitrate lyase	-3,4074998000	0,0235934870
MAP_3965c	-	-	-1,5000000000	0,0468538000
MAP_3977c	-	Short-chain dehydrogenase/reductase SDR	-1,8050001000	0,0253895800
MAP_3993	galE1	UDP-glucose 4-epimerase GalE1	-1,3675001000	0,0151495360
MAP_3996c	-	MaoC domain protein dehydratase	-1,3600000000	0,0160989220
MAP_3999c	-	-	-1,1925000000	0,0242378000
MAP_4001	-	Glutaredoxin 2	-1,8950001000	0,0225827150
MAP_4007c	-	-	-1,4675001000	0,0166178960
MAP_4010c	-	Acyltransferase 3	-1,0225000000	0,0220075530
MAP_4024	-	Cytochrome c biogenesis protein ResB	-1,3125000000	0,0191882600
MAP_4027	-	-	-1,7375000000	0,0007245111
MAP_4029c	menA	1,4-dihydroxy-2-naphthoate octaprenyltransferase	-1,4200001000	0,0146104300
MAP_4032	-	UDP-glucose 4-epimerase	-1,5375000000	0,0026939362
MAP_4049	-	Amidohydrolase 3	-1,5450001000	0,0024812096
MAP_4065	-	Manganese transport protein MntH	-1,7050000000	0,0041898554
MAP_4080c	-	Transcriptional regulator, CopG/Arc/MetJ family, Putative	-2,1875000000	0,0006173553
MAP_4103c	-	-	-1,9950000000	0,0176426250
MAP_4111	nusG	Transcription antitermination protein nusG	-4,1875000000	0,0170589690
MAP_4116c	mmaA4	Cyclopropane-fatty-acyl-phospholipid synthase	-2,5150000000	0,0412096270
MAP_4135	-	Transcriptional regulator, PaaX family	-1,0650000000	0,0024944313
MAP_4147	-	FAD-dependent pyridine nucleotide-disulphide oxidoreductase	-1,0275000000	0,0002454193
MAP_4154	lldD1	L-lactate dehydrogenase/FMN-dependent alpha-hydroxy acid dehydrogenase	-2,1500000000	0,0018687053
MAP_4155	-	Creatininase protein	-1,7324998000	0,0082740400
MAP_4169	rpmC	50S ribosomal protein L29	-1,5750000000	0,0096378140
MAP_4175	-	Transmembrane protein	-2,3350000000	0,0445678120
MAP_4176	-	13E12 repeat family protein	-1,6050000000	0,0301955160
MAP_4179	rplE	50S ribosomal protein L5	-1,9324999000	0,0075750044
MAP_4183	rplR	50S ribosomal protein L18	-1,0975000000	0,0236751960
MAP_4187c	-	Luciferase-like monooxygenase family protein	-1,6225000000	0,0021084328
MAP_4191c	-	O-methyltransferase protein	-1,3975000000	0,0059860363
MAP_4218	-	Rieske iron sulfur protein, putative	-1,2700001000	0,0003597415
MAP_4249	-	-	-2,2425000000	0,0287646840
MAP_4267	-	-	-3,0874999000	0,0046230042
MAP_4283	-	-	-2,0500000000	0,0317114850
MAP_4290	-	Transcriptional regulator, TetR family	-1,3000000000	0,0254209540
MAP_4305	-	-	-1,3924999000	0,0330497100
MAP_4312	-	-	-3,3150000000	0,0370880630
MAP_4314	-	Adenine deaminase protein	-3,3500000000	0,0131417870
MAP_4316	-	-	-1,0100000000	0,0088289490
MAP_4319	-	-	-1,5175000000	0,0093556450
MAP_4321c	-	Cell divisionFtsK/SpoIIIE	-1,5675000000	0,0107074360
MAP_4324c	-	Lytic transglycosylase catalytic	-3,9775000000	0,0335854200
MAP_4326c	-	-	-1,4600000000	0,0370298850
MAP_4340	trxC	Thioredoxin	-1,2125001000	0,0013323367
MAP_4347c	-	inner membrane protein translocase component, putative	-1,1424999000	0,0206814020

Appendix 3

Genes of *Map* with significantly up-regulated expression levels in the infection of THP-1 cells

Gene ID	Gene Name	Gene Product	log2 [ratio (Exp/ctrl)]	P-value
MAP_0009	-	Cytochrome P450	7,2125000000	0,0207695640
MAP_0026	fadD33	AMP-dependent synthetase and ligase/ acyl-CoA synthase	5,1324997000	0,0434645400
MAP_0029c	-	HNH endonuclease protein	1,3399999000	0,0128770310
MAP_0053c	-	-	5,8475000000	0,0209919080
MAP_0080c	-	Integral membrane protein	5,8900000000	0,0012928207
MAP_0094	-	-	1,5225000000	0,0414180350
MAP_0143	-	-	1,4925001000	0,0117405780
MAP_0176	-	Integral membrane protein	7,7600000000	0,0000936609
MAP_0209c	csp	N-acetylmuramoyl-L-alanine amidase domain protein	6,7875004000	0,0172869940
MAP_0212	-	Glycosyl transferase protein	4,8075000000	0,0214458310
MAP_0221	accD4	propionyl-CoA carboxylase beta chain accD4	1,2049999000	0,0212881400
MAP_0224c	fadE35	Acyl-CoA dehydrogenase domain protein	3,6100001000	0,0412252000
MAP_0234c	-	Short-chain dehydrogenase/reductase SDR	6,2250000000	0,0262615960
MAP_0265c	fadE1	Acyl-CoA dehydrogenase protein	3,0250000000	0,0004099883
MAP_0297c	-	2-methylcitrate dehydratase	2,3750000000	0,0348027160
MAP_0303c	-	Methyltransferase	5,9525003000	0,0240094550
MAP_0316c	recR	recombination protein RecR	6,2350000000	0,0061582050
MAP_0339c	-	-	6,0175000000	0,0090723530
MAP_0366	selD	selenide, water dikinase	1,5024999000	0,0382095500
MAP_0373	-	methyltransferase, Putative	1,4449999000	0,0477139280
MAP_0428	-	Integrase catalytic subunit	3,1600000000	0,0043508470
MAP_0487c	-	ABC transporter, permease protein	2,0650000000	0,0251688900
MAP_0488c	-	ABC transporter ATP-binding protein	3,1850002000	0,0287775140
MAP_0526	-	-	2,9375000000	0,0368672400
MAP_0533	-	4-hydroxy 2-oxovalerate aldolase	1,4200000000	0,0485457930
MAP_0589c	-	Integrase catalytic subunit	2,6699998000	0,0014183925
MAP_0620	-	Deacetylase-like protein	5,5475000000	0,0347601470
MAP_0630c	-	Linocin_M18 bacteriocin protein	6,3475000000	0,0182118860
MAP_0678c	-	-	5,3800000000	0,0129413780
MAP_0684c	-	Proline iminopeptidase	3,7550000000	0,0003213855
MAP_0694	mphA	3-(3-hydroxyphenyl)propionate hydroxylase	4,9300003000	0,0344308170
MAP_0733c	-	Acetyl-CoA acetyltransferase-like protein	5,1475000000	0,0318203570
MAP_0740c	-	-	6,2050000000	0,0068302983
MAP_0771	-	Integral membrane protein	5,3675000000	0,0027626026
MAP_0772	-	-	5,8424997000	0,0249243680
MAP_0814c	-	-	1,0274999000	0,0058911527
MAP_0820	-	TRNA/rRNA methyltransferase	1,6075000000	0,0199733700
MAP_0830c	-	Phytoene dehydrogenase oxidoreductase	1,6900000000	0,0477921960
MAP_0847	-	Carbohydrate-binding protein	5,0150000000	0,0463599530
MAP_0850c	-	Integrase catalytic subunit	2,3274999000	0,0059462725
MAP_0881	-	Fumarylacetoacetate hydrolase protein	3,3225002000	0,0396981760
MAP_0899c	-	Luciferase-like monooxygenase	5,1174994000	0,0211969800
MAP_0914c	-	Protein of unknown function DUF1446	5,1925000000	0,0335478700
MAP_0998c	-	K+-transporting ATPase ATPase B chain	4,6175003000	0,0130341975
MAP_1015	-	Rhodanese domain protein	6,4125004000	0,0079477895
MAP_1036	ruvC	Holliday junction resolvase	4,5850005000	0,0250094140
MAP_1066	-	Membrane protein-like protein	6,4725000000	0,0137952090
MAP_1079	-	Aminodeoxychorismate lyase protein	1,2550000000	0,0066615680
MAP_1087	-	peptide/nickel transport system permease protein	5,8650000000	0,0093260430
MAP_1088	-	peptide/nickel transport system permease protein	5,1475000000	0,0090535500
MAP_1102c	tcrA	Two-component response transcriptional regulator	3,0775000000	0,0427127330
MAP_1109	-	sulfonate/nitrate/taurine transport system permease protein	1,1274999000	0,0372465180
MAP_1122	mIHF	integration host factor, Putative	5,2100000000	0,0316669120
MAP_1129	-	YhhN family protein	3,6075000000	0,0047971616
MAP_1151c	-	-	3,6250002000	0,0407747000
MAP_1160c	-	Phospholipid/glycerol acyltransferase	2,1975000000	0,0457255430
MAP_1167	secG	preprotein translocase subunit	3,9125000000	0,0327946660
MAP_1187	-	Cysteine desulfurase activator complex subunit SufB	7,6099997000	0,0081206710
MAP_1190	-	cysteine desulfurase / selenocysteine lyase	4,9800000000	0,0136102410
MAP_1201c	acn	aconitate hydratase 1	6,6575000000	0,0179230220
MAP_1211	hemZ	ferrochelatase	7,6900005000	0,0142862730
MAP_1249c	ansA	L-asparaginase AnsA	1,2925000000	0,0210066210
MAP_1275	bioF	8-amino-7-oxononanoate synthase	5,5900000000	0,0230494720
MAP_1280c	-	-	1,7450000000	0,0421722700
MAP_1314c	cydD	ATP-binding cassette, subfamily C, bacterial	4,7850000000	0,0276521780

Gene ID	Gene Name	Gene Product	log2 [ratio (Exp/ctrl)]	P-value
MAP_1317c	-	Acid-resistance membrane protein	2,1375000000	0,0035157793
MAP_1401	tlyA	Hemolysin A	4,8650000000	0,0475476980
MAP_1407	-	ADP-ribose pyrophosphatase	6,1175000000	0,0425594340
MAP_1414	cmk	cytidylate kinase	3,7900002000	0,0058572720
MAP_1429	-	-	3,2300003000	0,0012365552
MAP_1496c	-	-	1,9875001000	0,0019214510
MAP_1499c	-	Holliday junction resolvase-like protein	1,9175000000	0,0041509396
MAP_1535	pgsA2	CDP-diacylglycerol--glycerol-3-phosphate 3-phosphatidyltransferase	2,6799998000	0,0016632862
MAP_1540	-	FHA domain-containing protein	1,5600000000	0,0459475780
MAP_1578	-	-	2,3300000000	0,0016716373
MAP_1627	-	-	8,4625000000	0,0017399573
MAP_1633c	-	-	5,3275000000	0,0499747400
MAP_1652c	-	Transcriptional regulator, AraC family	1,7900000000	0,0082960130
MAP_1687	-	glucose-6-phosphate 1-dehydrogenase	1,4499999000	0,0199980380
MAP_1737	mmpS5	Membrane protein	6,5399995000	0,0064323100
MAP_1754c	-	Universal stress protein, UspA	3,4750001000	0,0041128676
MAP_1792	-	-	2,0625000000	0,0359757730
MAP_1815c	cobK	cobalt-precorrin-6x reductase	6,6700000000	0,0013724100
MAP_1876c	cysS2	cysteinyl-tRNA synthetase	1,5550001000	0,0195564370
MAP_1891c	-	Protein of unknown function DUF552	1,3600000000	0,0018672752
MAP_1901c	murF	UDP-N-acetylmuramoylalanyl-D-glutamyl-2,6-diaminopimelate--D -alanyl-D-alanine ligase	8,5525000000	0,0099505590
MAP_1920c	-	1-acyl-sn-glycerol-3-phosphate acyltransferase	6,6325000000	0,0007279405
MAP_1942c	cbhK	adenosine kinase	4,9525003000	0,0485895900
MAP_1943	-	-	4,5050000000	0,0413518100
MAP_1944c	-	HesB/YadR/YfhF iron-sulfur cluster assembly accessory protein	2,1275000000	0,0278204830
MAP_1945c	-	glycerate kinase	5,4550000000	0,0185406170
MAP_1948	cobT	nicotinate-nucleotide--dimethylbenzimidazole phosphoribosyltransferase	1,9975000000	0,0314154550
MAP_1960	-	Integral membrane protein	4,4900000000	0,0104052540
MAP_1972c	-	-	4,7550000000	0,0044379374
MAP_1976	-	Prolyl 4-hydroxylase, alpha subunit	5,7675004000	0,0056681484
MAP_1981c	-	zinc ribbon domain, protein / Protein of unknown function DUF164	5,7025000000	0,0018806965
MAP_2007c	-	Methyltransferase type 12	1,1350000000	0,0022897911
MAP_2061	-	Membrane protein-like protein	2,3450000000	0,0345124970
MAP_2114c	-	-	2,6399999000	0,0067271990
MAP_2129	-	Secreted protein	1,6400001000	0,0071303174
MAP_2150	-	Transposase, Mutator family	1,9449999000	0,0173648260
MAP_2214c	-	-	5,3675000000	0,0168646000
MAP_2259	entB	Isochorismatase hydrolase protein	4,2750000000	0,0466061980
MAP_2280c	clpP2	ATP-dependent Clp protease proteolytic subunit	7,4600000000	0,0086016870
MAP_2294c	-	NAD-glutamate dehydrogenase	6,3424993000	0,0376893500
MAP_2327	-	Transmembrane protein	2,7225000000	0,0434326120
MAP_2337c	-	-	1,0475000000	0,0263204400
MAP_2349c	-	Luciferase-like monooxygenase	2,1800000000	0,0043700820
MAP_2389c	-	-	2,2824998000	0,0023960348
MAP_2406c	-	L-carnitine dehydratase/bile acid-inducible protein F	1,6775000000	0,0101971375
MAP_2408c	fabG2	3-ketoacyl-(acyl-carrier-protein) reductase	2,5149999000	0,0312107480
MAP_2546c	sugB	Binding-protein-dependent transport systems inner membrane component	7,2400000000	0,0184804500
MAP_2562	-	S-isoprenylcysteine-methyltransferase CARBOXYL; protein-	7,2799997000	0,0005084410
MAP_2565	-	Glycosyl transferase, group 1	4,8250000000	0,0449158660
MAP_2640c	-	Abortive infection protein	4,1150002000	0,0262062010
MAP_2646c	fadA6	Acetyl-CoA acetyltransferase	3,4724998000	0,0332470400
MAP_2706c	-	Protein of unknown function DUF255	1,8525000000	0,0488347080
MAP_2799c	hemE	uroporphyrinogen decarboxylase	4,8050003000	0,0326381300
MAP_2814c	dut	deoxyuridine 5'-triphosphate nucleotidohydrolase	7,8700000000	0,0106179940
MAP_2857c	pgsA3	CDP-diacylglycerol--glycerol-3-phosphate 3-phosphatidyltransferase	6,4100000000	0,0150372170
MAP_2868c	dfrA	dihydrofolate reductase	1,5350001000	0,0420838300
MAP_2871c	-	glycosyl transferase UDP-glucuronosyltransferase, Putative	2,7075000000	0,0296103970
MAP_3001	-	HNH endonuclease protein	1,2049999000	0,0088569460
MAP_3059c	-	Phospholipid/glycerol acyltransferase, hemolysin	3,1075000000	0,0277983230
MAP_3109	-	Cytochrome P450 family protein	4,9375000000	0,0035043438
MAP_3111c	-	Sensory transduction histidine kinase	4,0625000000	0,0331948060
MAP_3197	-	aminoglycoside phosphotransferase, Protein:	5,4375000000	0,0055615166
MAP_3212	nuoL	NADH dehydrogenase subunit	7,5225000000	0,0120867650
MAP_3215c	-	-	1,1150000000	0,0072993604
MAP_3251	-	D,d-heptose 1,7-bisphosphate phosphatase protein	1,5000000000	0,0326151920
MAP_3267c	-	Transcriptional regulator, MerR family	2,0200000000	0,0110821380
MAP_3290c	mpt64	mpt64	1,5775000000	0,0157641170
MAP_3327c	-	Sulfotransferase	6,1325000000	0,0327295250

Gene ID	Gene Name	Gene Product	log2 [ratio (Exp/ctrl)]	P-value
MAP_3462c	-	integral membrane protein, Putative	2,1000000000	0,0018468513
MAP_3479c	-	MaoC domain protein dehydratase	3,2825000000	0,0039609075
MAP_3514	-	Acyltransferase 3	2,2775000000	0,0060172053
MAP_3531c	fbpC2	esterase protein Putative	3,3850002000	0,0296529300
MAP_3532c	-	antibiotic transport system permease protein	5,8000000000	0,0057898764
MAP_3534c	-	Phosphodiesterase, MJ0936 family	4,6499996000	0,0158086680
MAP_3542	-	N-acetyltransferase, Related	4,4725000000	0,0345446730
MAP_3553	-	Cytochrome P450 family protein	2,0375000000	0,0048316885
MAP_3583	-	Acyl-CoA thioesterase II	8,0300010000	0,0018416113
MAP_3599c	-	Transcriptional regulator, GntR family	4,4050000000	0,0459034900
MAP_3623	-	-	7,4150000000	0,0054009976
MAP_3634	-	ErfK/YbiS/YcfS/YnhG family protein	2,0950000000	0,0050395555
MAP_3688	lpqI	Beta-glucosidase lpqI	4,7750000000	0,0345299400
MAP_3689	-	Transcriptional regulator, TetR family	4,5725000000	0,0272052250
MAP_3690	-	Chloride channel protein	1,4449999000	0,0439660100
MAP_3704c	-	-	1,2425000000	0,0293238830
MAP_3721	-	Non-ribosomal peptide synthetase/polyketide synthase	1,1350000000	0,0218950270
MAP_3758c	-	Transcriptional regulator, AraC family	4,6425000000	0,0348644200
MAP_3766	-	Permease protein	3,4824998000	0,0119400040
MAP_3769c	rpmG	50S ribosomal protein L33	3,6000000000	0,0240467840
MAP_3845	-	-	3,6575000000	0,0318172830
MAP_3862c	-	DedA family membrane-associated protein	4,3900003000	0,0346829500
MAP_3921	sodC	Copper/zinc superoxide dismutase	2,6875000000	0,0016061538
MAP_3941	gloA	Glyoxalase/bleomycin resistance protein/dioxygenase	5,4874997000	0,0227282420
MAP_3954	-	-	2,5525000000	0,0175629150
MAP_4035	-	Glycosyl transferase 2 family protein	3,3925000000	0,0131530270
MAP_4041c	pitA	Phosphate transporter	3,8800000000	0,0409213860
MAP_4044c	menB	naphthoate synthase	2,4350000000	0,0462299730
MAP_4062c	-	flavin monooxygenase, Putative	2,4250000000	0,0433575320
MAP_4071	galT	UDPglucose--hexose-1-phosphate uridylyltransferase galT	2,4950001000	0,0245072790
MAP_4077c	-	Integral membrane protein	3,0400000000	0,0123806140
MAP_4128	-	Lignostilbene-alpha,beta-dioxygenase	7,0874996000	0,0071025263
MAP_4132	end	endonuclease IV	2,2775000000	0,0031315035
MAP_4144	-	PE-PGRS family protein	6,6675000000	0,0445232540
MAP_4152	-	-	8,7550000000	0,0043432354
MAP_4246	rpsI	30S ribosomal protein S9	4,4750000000	0,0270679500
MAP_4261	-	Peptidase M22 glycoprotease	5,6575003000	0,0125848250
MAP_4309	-	Anti sigma factor antagonist	6,0325003000	0,0387834300

Appendix 4

Genes of *Map* with significantly down-regulated expression levels in the infection of THP-1 cells

Gene ID	Gene Name	Gene Product	log2 [ratio (Exp/ctrl)]	P-value
MAP_0006	gyrA	DNA gyrase / DNA topoisomerase subunit A	-7,2950000000	0,0039188303
MAP_0017c	-	-	-3,3700000000	0,0331364420
MAP_0018c	pknA	Serine/threonine protein kinase	-5,6700000000	0,0040729404
MAP_0036	-	NLP/P60 protein	-3,21	0,0180560500
MAP_0101	-	Glutamate--cysteine ligase	-4,8900000000	0,0270537530
MAP_0113	-	-	-5,4049997000	0,0106181230
MAP_0155	-	Transcriptional regulator, TetR family	-1,0375000000	0,0466666560
MAP_0156	-	Glyoxalase/bleomycin resistance protein/dioxygenase	-6,5750000000	0,0471630770
MAP_0170	sigI	ECF subfamily RNA polymerase sigma-24 factor SigI	-1,3250000000	0,0132190480
MAP_0245c	-	NAD(P)H quinone oxidoreductase, PIG3 family, Putative	-5,0225000000	0,0191811320
MAP_0250	-	-	-6,2200003000	0,0029793372
MAP_0295c	gltA1	citrate synthase	-6,2400002000	0,0010372063
MAP_0305c	-	Protein of unknown function DUF323	-5,7425000000	0,0421303920
MAP_0335	-	Transcriptional regulator, TetR family	-4,2925000000	0,0037779050
MAP_0344c	-	Cytochrome P450	-6,3500004000	0,0000277004
MAP_0376c	-	Anti-sigma regulatory factor, serine/threonine protein kinase phosphatase	-4,5299997000	0,0261629910
MAP_0396	-	Endoribonuclease L-PSP protein	-7,1425000000	0,0036533838
MAP_0402	-	Hydrolase, NUDIX family protein	-5,8174996000	0,0002236711
MAP_0408	-	-	-1,2700000000	0,0393177300
MAP_0414c	-	HAD-superfamily subfamily IB hydrolase	-6,8875003000	0,0065472634
MAP_0420	-	-	-7,8775000000	0,0076522140
MAP_0445c	-	Luciferase-like monooxygenase	-2,0225000000	0,0176091340
MAP_0454	-	Transmembrane protein	-4,7149997000	0,0326922400
MAP_0501	nhoA	arylamine N-acetyltransferase nhoA	-5,1150000000	0,0042851097
MAP_0515c	-	3-oxoacid CoA-transferase, A subunit	-7,2500000000	0,0001884913
MAP_0549c	echA19	enoyl-CoA hydratase	-6,1700000000	0,0003316083
MAP_0555c	-	-	-3,7300000000	0,0017556121
MAP_0560	fdxD	fdxD	-6,9249997000	0,0026599800
MAP_0563	-	ABC transporter	-5,6700000000	0,0170298240
MAP_0590	-	-	-7,9499993000	0,0185306670
MAP_0613c	-	transmembrane protein, Putative	-5,2275000000	0,0035099345
MAP_0622c	-	Zn-dependent hydrolase of beta-lactamase fold protein, Predicted	-4,8900000000	0,0013851977
MAP_0623	-	-	-6,2150000000	0,0158092750
MAP_0638	purF	amidophosphoribosyltransferase	-5,0550003000	0,0190038120
MAP_0653	pstA1	phosphate transport system permease protein PstA1_1	-4,1050000000	0,0258710600
MAP_0654	phoT	phosphate transporter ATP-binding protein	-5,4075000000	0,0239244570
MAP_0662c	-	CMP/dCMP deaminase zinc-binding protein	-6,3175000000	0,0008889569
MAP_0770c	-	-	-5,5299997000	0,0054162326
MAP_0785	far	L-carnitine dehydratase/bile acid-inducible protein F	-2,9299998000	0,0202354880
MAP_0801	-	Fumarate reductase iron-sulfur subunit	-3,0375000000	0,0005640677
MAP_0812	-	glutathione S-transferase protein, Putative	-6,1000000000	0,0032953343
MAP_0874	pstA1	phosphate transport system permease protein PstA1_2	-5,2575000000	0,0009273010
MAP_0885c	-	-	-3,0200000000	0,0191570730
MAP_0917	-	two-component system, OmpR family, sensor histidine kinase MprB	-6,2175000000	0,0000279134
MAP_0963c	-	-	-8,3525000000	0,0059994670
MAP_0966c	-	PPE family protein	-7,2675000000	0,0003220790
MAP_0973	-	TatD-related deoxyribonuclease family protein	-3,4675002000	0,0405528660
MAP_0975	ksgA	Dimethyladenosine transferase	-4,9275000000	0,0005567338
MAP_0982c	arsC	Arsenate reductase	-6,4150000000	0,0028105592
MAP_1018c	echA9	3-hydroxyisobutyryl-CoA hydrolase	-8,1800000000	0,0000557431
MAP_1027c	greA	Transcription elongation factor GreA	-6,1450000000	0,0072568753
MAP_1028c	-	-	-3,9350000000	0,0369685300
MAP_1031c	speE	spermidine synthase	-4,2875000000	0,0113238790
MAP_1084c	-	-	-4,8775000000	0,0062009185
MAP_1124	-	DNA-directed RNA polymerase subunit	-5,9625006000	0,0005208299
MAP_1126	metK	S-adenosylmethionine synthetase	-6,4825000000	0,0012453169
MAP_1217c	-	Transmembrane protein	-2,7050000000	0,0024441762
MAP_1230	-	Glycosyl transferase, group 1	-6,5050000000	0,0031061016
MAP_1231	gmdA	GDPmannose 4,6-dehydratase GmdA	-4,3425000000	0,0311309600
MAP_1293	hisD	histidinol dehydrogenase	-5,4500000000	0,0033175852
MAP_1326	-	dephospho-CoA kinase/protein folding accessory domain-containing protein	-6,2524996000	0,0074937367
MAP_1334	-	-	-4,2200000000	0,0311174260
MAP_1346c	-	Diguanylate cyclase/phosphodiesterase with PAS/PAC sensor(s)	-6,9249997000	0,0085452350
MAP_1353	rpmI	50S ribosomal protein L35	-4,5375004000	0,0064728560
MAP_1384c	-	Glycoside hydrolase 15-related protein	-4,7400000000	0,0092542540

Gene ID	Gene Name	Gene Product	log2 [ratio (Exp/ctrl)]	P-value
MAP_1387c	-	membrane protein, Hypothetical	-5,1150000000	0,0023205160
MAP_1388	-	-	-5,2574997000	0,0173434820
MAP_1400	-	-	-5,0924997000	0,0299618190
MAP_1419	mbtH	MbtH domain protein	-4,7950000000	0,0060191294
MAP_1433c	-	Fumarate reductase/succinate dehydrogenase flavoprotein domain protein	-8,0925000000	0,0068030027
MAP_1445c	-	Alpha/beta hydrolase fold-3 domain protein	-5,8775005000	0,0006213110
MAP_1446c	-	Transcriptional regulator, IclR family	-4,4300000000	0,0473135400
MAP_1468c	-	Oxidoreductase, short-chain dehydrogenase/reductase protein	-5,3525000000	0,0016088889
MAP_1484c	-	Dioxygenase, alpha subunit:Rieske	-6,5625000000	0,0002149928
MAP_1512	-	-	-4,7100000000	0,0184586570
MAP_1515	-	PPE family protein	-5,3275000000	0,0001684795
MAP_1537	-	Small basic protein	-4,6300000000	0,0232227840
MAP_1543	-	Transcriptional regulator, MerR family	-4,1250000000	0,0062550150
MAP_1550c	-	protein of unknown function DUF21:transporter CBS:	-3,1175000000	0,0123136490
MAP_1561c	ndh	NADH dehydrogenase	-3,4800000000	0,0050599840
MAP_1568	modC	molybdate transport system ATP-binding protein	-6,3175000000	0,0004670557
MAP_1569	modD	modD	-4,3525000000	0,0044640163
MAP_1580c	-	Protein of unknown function DUF72	-3,0600000000	0,0302326640
MAP_1594c	-	-	-3,7325000000	0,0003958648
MAP_1598	-	-	-2,2824998000	0,0091053190
MAP_1604c	lppE	Lipoprotein LppE	-1,7325001000	0,0490233080
MAP_1614c	-	Cytochrome P450	-1,7199999000	0,0027916154
MAP_1618c	-	2-nitropropane dioxygenase, NPD	-6,8400000000	0,0048796157
MAP_1642	-	Beta-lactamase domain-containing protein	-4,4800000000	0,0069350870
MAP_1643	aceAb	isocitrate lyase	-1,0300000000	0,0016311094
MAP_1663	-	Glycosyl transferase family 2	-3,8599997000	0,0276869520
MAP_1682c	-	Ribonuclease BN	-2,0900000000	0,0015772793
MAP_1695c	-	Chaperone protein DnaJ	-2,4400000000	0,0210470280
MAP_1700c	-	Beta-lactamase, putative	-5,2800000000	0,0068153315
MAP_1712	-	L-carnitine dehydratase/bile acid-inducible protein F	-6,1650000000	0,0000148670
MAP_1728c	yfnB	2-haloacid dehalogenase	-5,6300000000	0,0109462200
MAP_1766c	-	cellobiose transport system ATP-binding protein	-6,4674997000	0,0000878424
MAP_1772	-	Integral membrane protein	-5,0825000000	0,0011047763
MAP_1773c	-	Steroid delta-5-3-ketosteroid isomerase	-5,5275000000	0,0192079150
MAP_1791	norQ	ATPase associated with various cellular activities	-5,6725000000	0,0000244614
MAP_1805c	cobN	cobaltochelatase subunit	-9,8799990000	0,0001799652
MAP_1841	-	Protein of unknown function DUF503	-4,8350000000	0,0401649400
MAP_1843	-	RecB family exonuclease-like protein	-1,9975000000	0,0157155800
MAP_1847c	hisI	phosphoribosyl-ATP pyrophosphatase	-4,4375000000	0,0069538727
MAP_1859c	metH	B12-dependent methionine synthase	-5,2950000000	0,0048572575
MAP_1877c	cysQ	CysQ_1	-6,7574997000	0,0000763721
MAP_1897c	murG	undecaprenyldiphospho-muramoylpentapeptide beta-N-acetylglucosaminyltransferase	-5,4425000000	0,0166127270
MAP_1900c	murX	phospho-N-acetylmuramoyl-pentapeptide-transferase	-5,5699997000	0,0084653220
MAP_1902c	murE	UDP-N-acetylmuramoylalanyl-D-glutamate--2,6-diaminopimelate ligase	-3,9374998000	0,0335265140
MAP_1907c	-	Membrane protein	-6,3150000000	0,0086511580
MAP_1911	idsA2	geranylgeranyl diphosphate synthase, type I IdsA2_1	-6,4475000000	0,0048116060
MAP_1966c	glnA2	glutamine synthetase	-3,9950001000	0,0209978820
MAP_1971	-	Mannan endo-1,4-beta-mannosidase	-3,4875000000	0,0202826650
MAP_1988	-	Protein of unknown function DUF2236	-3,8100000000	0,0000626826
MAP_1990	-	Protein of unknown function DUF105	-5,1450000000	0,0210919450
MAP_1998	kasA	3-oxoacyl-(acyl carrier protein) synthase II	-4,3125000000	0,0080870330
MAP_2008	adhE2	Alcohol dehydrogenase protein	-7,2324996000	0,0009434574
MAP_2013c	-	dihydrodipicolinate reductase protein, Hypothetical protein	-6,1674995000	0,0003557315
MAP_2027c	-	PilT domain-containing protein	-1,9325000000	0,0443386030
MAP_2041	lipM	Esterase/lipase protein	-6,5499997000	0,0088187030
MAP_2046	sseB	thiosulfate/3-mercaptopyruvate sulfurtransferase sseB	-6,7050000000	0,0006584607
MAP_2047	-	-	-5,9175000000	0,0074732658
MAP_2055	-	cystathione beta-lyase	-3,1775000000	0,0000497177
MAP_2068c	-	-	-4,7500000000	0,0018951072
MAP_2075c	-	Methyltransferase type 11	-4,7050000000	0,0075473510
MAP_2081	-	-	-7,3650000000	0,0007612520
MAP_2083c	-	Protein of unknown function DUF477	-3,4100000000	0,0257737580
MAP_2104	fdhF	Oxidoreductase / formate dehydrogenase, alpha subunit	-4,1075000000	0,0014155690
MAP_2107c	-	-	-3,4000000000	0,0433718670
MAP_2125	-	Luciferase-like protein alkanesulfonate monooxygenase	-5,7450000000	0,0020287375
MAP_2135c	-	-	-3,0675000000	0,0105140340
MAP_2142c	-	DNA repair protein RecO	-6,1949997000	0,0208583360
MAP_2144	-	lysine decarboxylase	-1,6475000000	0,0199204870

Gene ID	Gene Name	Gene Product	log2 [ratio (Exp/ctrl)]	P-value
MAP_2153	-	-	-5,1475000000	0,0029363430
MAP_2158	-	-	-5,0000000000	0,0126712990
MAP_2160c	phoH	PhoH family protein	-4,7250000000	0,0097967370
MAP_2172c	-	Non-ribosomal peptide synthetase synthase	-7,0225000000	0,0005256854
MAP_2207c	hemN	coproporphyrinogen III oxidase	-5,1974998000	0,0155317670
MAP_2215	-	Glycoside hydrolase 15-related protein	-1,9424999000	0,0205648450
MAP_2233	-	MMPL domain-containing protein	-4,6825000000	0,0023783646
MAP_2248c	-	Mechanosensitive ion channel/cyclic nucleotide-binding domain-containing protein	-4,4275002000	0,0009303714
MAP_2262	-	Transcriptional regulator, TetR family	-5,9800005000	0,0016204334
MAP_2279	-	homocysteine methyltransferase	-4,0525002000	0,0023970578
MAP_2288c	-	Protein of unknown function DUF477	-3,7400000000	0,0011199882
MAP_2298c	plsB2	glycerol-3-phosphate acyltransferase	-4,5325003000	0,0169177600
MAP_2314c	accD1	3-methylcrotonyl-CoA carboxylase beta subunit accD1	-3,3100000000	0,0224303960
MAP_2336	-	Dioxygenase, alpha subunit:Rieske	-5,4775000000	0,0000234449
MAP_2383	-	L-carnitine dehydratase/bile acid-inducible protein F	-5,7549996000	0,0226868130
MAP_2409	fadE25	acyl-CoA dehydrogenase	-3,8050000000	0,0006474985
MAP_2430	-	nicotinate phosphoribosyltransferase	-3,8250000000	0,0095294425
MAP_2456c	atpE	F0F1 ATP synthase subunit	-9,2575000000	0,0006368514
MAP_2458c	-	ATP synthase I	-1,5100000000	0,0008212169
MAP_2467c	thrC	threonine synthase	-5,2325000000	0,0079713210
MAP_2471	-	-	-4,1250000000	0,0207998880
MAP_2472	-	Transmembrane protein	-4,4650000000	0,0406590200
MAP_2475	-	Metalloendopeptidase-like membrane protein	-1,6375000000	0,0003298114
MAP_2476	-	-	-5,4300003000	0,0139848520
MAP_2487c	-	carbonic anhydrase	-3,8600001000	0,0213230270
MAP_2512	-	Diguanylate cyclase/phosphodiesterase with PAS/PAC sensor(s)	-6,0125003000	0,0004616673
MAP_2529	-	Carboxymuconolactone decarboxylase protein	-4,6549997000	0,0030821569
MAP_2541c	mdh	malate dehydrogenase	-5,8700000000	0,0076740193
MAP_2564c	glgC	glucose-1-phosphate adenylyltransferase	-5,9725000000	0,0034624457
MAP_2581c	-	Hydrolase, alpha/beta fold family protein	-5,1250000000	0,0226570950
MAP_2583c	-	Aldehyde dehydrogenase (acceptor)	-6,7350000000	0,0101973280
MAP_2604c	-	Modular polyketide synthase, type I	-2,8050000000	0,0013208896
MAP_2626	-	-	-4,1100000000	0,0209973360
MAP_2644	-	-	-3,5425000000	0,0420261660
MAP_2652c	-	-	-4,4950000000	0,0084791025
MAP_2680c	-	PilT domain-containing protein	-7,8900003000	0,0000010171
MAP_2700	coaA	pantothenate kinase	-5,7850000000	0,0075066580
MAP_2733c	-	Rieske domain-containing protein	-4,7950000000	0,0029045780
MAP_2745c	-	-	-3,9850001000	0,0006091013
MAP_2797c	-	Chlorite dismutase protein	-7,1725000000	0,0000296179
MAP_2805	arsA	Permease	-5,2775000000	0,0331816230
MAP_2813c	-	-	-5,9825000000	0,0066314830
MAP_2841c	miaA	TRNA delta(2)-isopentenylpyrophosphate transferase	-8,2625010000	0,0000108864
MAP_2843c	-	Integral membrane protein	-2,8400002000	0,0391509980
MAP_2852	-	limonene-1,2-epoxide hydrolase	-5,9500000000	0,0082194330
MAP_2862	-	O-methyltransferase protein	-6,7275000000	0,0100324680
MAP_2874c	fadD13	AMP-dependent synthetase and ligase	-4,7225000000	0,0280202300
MAP_2879c	-	-	-7,1450000000	0,0012499625
MAP_2904	echA16	enoyl-CoA hydratase	-3,4074998000	0,0379716940
MAP_2924	nicT	High affinity nickel transporter protein	-2,1000000000	0,0406648700
MAP_2927	-	PPE family protein	-5,8375000000	0,0027041014
MAP_2941c	-	-	-1,4024999000	0,0164977820
MAP_2947	-	TolA protein	-3,9125000000	0,0128236650
MAP_2957	-	-	-3,8899999000	0,0135646880
MAP_2964c	-	Phage-related integrase/recombinase	-4,4400000000	0,0156704690
MAP_3021	-	Protein of unknown function DUF121	-6,6349998000	0,0002471616
MAP_3029c	gltS	glutamyl-tRNA synthetase	-6,7075000000	0,0004861200
MAP_3052c	-	Transcriptional regulator, TetR family	-3,6800000000	0,0333244060
MAP_3072	-	Lycopene cyclase domain protein	-3,9925000000	0,0406580700
MAP_3074	crtT	CrtT	-6,5450000000	0,0017282781
MAP_3086c	-	Phosphatidylethanolamine N-methyltransferase	-4,6150000000	0,0260657820
MAP_3128	-	-	-3,9899998000	0,0150348400
MAP_3147	-	Camphor resistance CrcB protein	-5,7600000000	0,0284659060
MAP_3163	-	N-acetylmuramyl-L-alanine amidase, negative regulator of AmpC, AmpD	-1,8325000000	0,0072748507
MAP_3186c	-	-	-5,5375000000	0,0155189670
MAP_3187	-	Phosphatase, inositol monophosphatase	-5,8600000000	0,0016469596
MAP_3193	-	L-carnitine dehydratase/bile acid-inducible protein F	-4,3375000000	0,0080857830
MAP_3207	nuoG	NADH dehydrogenase subunit	-3,8324997000	0,0035975473

Gene ID	Gene Name	Gene Product	log2 [ratio (Exp/ctrl)]	P-value
MAP_3228	-	monoamine oxidase	-4,4800000000	0,0356993300
MAP_3232	-	CheB methylesterase	-4,3675000000	0,0302705540
MAP_3235c	-	two-component system, chemotaxis family, response regulator CheB	-4,2500000000	0,0266703520
MAP_3238	-	acyl-CoA dehydrogenase-related protein, Putative	-4,7550000000	0,0020181471
MAP_3245	-	Glycosyl transferase, group 1 protein	-3,0800000000	0,0222642530
MAP_3249	-	Carbamoyltransferase protein	-6,0100000000	0,0108119230
MAP_3250	-	-	-7,5525000000	0,0000943363
MAP_3260	-	Aldo-keto reductase protein	-7,0700000000	0,0208990070
MAP_3264c	-	Response regulator receiver/ANTAR domain-containing protein	-9,1325000000	0,0141389490
MAP_3268	hsp18	Heat shock protein Hsp20	-5,3925000000	0,0173243500
MAP_3277c	-	YiaAB two helix domain-containing protein	-2,2750000000	0,0041378820
MAP_3278c	-	-	-7,6600000000	0,0004046686
MAP_3280c	-	Sodium/hydrogen exchanger	-2,9175000000	0,0469799040
MAP_3283c	-	Metal-dependent hydrolase, putative	-5,4925003000	0,0082271420
MAP_3287	-	Oxidoreductase, short-chain dehydrogenase/reductase protein	-3,5849998000	0,0066033592
MAP_3298	-	-	-5,1825000000	0,0032094324
MAP_3313	-	-	-4,8800000000	0,0080792000
MAP_3317	-	GCN5-related N-acetyltransferase	-1,4600000000	0,0341825450
MAP_3318c	-	Integral membrane protein	-3,0974998000	0,0147018020
MAP_3319	-	Diacylglycerol kinase, catalytic region	-5,1549997000	0,0070747460
MAP_3320	whiB1	Transcription factor, WhiB	-4,6025000000	0,0265765260
MAP_3337	fadA6	acetyl-CoA acyltransferase	-5,6675000000	0,0012522715
MAP_3351c	-	S-isoprenylcysteine methyltransferase-like protein	-1,5225000000	0,0220044420
MAP_3368c	-	Bifunctional phosphoglucose/phosphomannose isomerase	-4,8525000000	0,0050306306
MAP_3376	-	DNA modification methyltransferase, putative Type	-5,9399996000	0,0008233804
MAP_3380c	rmlD	dTDP-4-dehydrorhamnose reductase rmlD	-3,4775000000	0,0012140108
MAP_3401	-	Maf-like protein	-2,8575000000	0,0469132900
MAP_3402	sseA	thiosulfate/3-mercaptopyruvate sulfurtransferase sseA	-2,3025000000	0,0013806093
MAP_3418	-	Lipoprotein LprJ	-3,7600000000	0,0182922870
MAP_3428c	-	Cutinase	-6,8125000000	0,0000953464
MAP_3445	-	-	-6,2750000000	0,0180777960
MAP_3446c	sigJ	RNA polymerase sigma factor SigJ	-4,2050000000	0,0027005647
MAP_3452c	-	Ribonuclease BN	-2,5125000000	0,0103110940
MAP_3457	metC	O-acetylhomoserine aminocarboxypropyltransferase	-6,1425004000	0,0234809440
MAP_3459	-	Methyltransferase type 11 protein	-5,9150000000	0,0005286576
MAP_3464	-	NADH:flavin oxidoreductase/NADH oxidase	-2,7550000000	0,0123612440
MAP_3474	spoU	TRNA/rRNA methyltransferase	-7,1200004000	0,0003947539
MAP_3476c	dnaE2	DNA polymerase III, alpha subunit	-9,6975000000	0,0007298608
MAP_3483	-	-	-12,4900000000	0,0000000036
MAP_3491	-	HAD-superfamily hydrolase family protein	-6,6775000000	0,0000184435
MAP_3550	ephF	Alpha/beta hydrolase fold protein	-4,0975000000	0,0136283080
MAP_3602	-	Putative ABC transporter, permease protein	-8,1825000000	0,0000030551
MAP_3619	-	dihydrodipicolinate reductase protein, Hypothetical protein	-5,4224997000	0,0167055350
MAP_3637c	mmpL11	MmpL11	-6,3525000000	0,0016443471
MAP_3655c	lipW	esterase / lipase	-4,0699997000	0,0285027250
MAP_3656	lipC	Esterase/lipase protein	-6,7225000000	0,0209526510
MAP_3666c	-	-	-6,1324997000	0,0001034104
MAP_3696	-	Flavin reductase domain protein FMN-binding	-1,4450000000	0,0386904000
MAP_3716c	fadE6	Acyl-CoA dehydrogenase domain protein	-4,9500003000	0,0090717840
MAP_3737	-	PPE family protein	-2,3475000000	0,0376274030
MAP_3743	-	-	-7,4925000000	0,0000678006
MAP_3761c	-	Integral membrane protein	-5,2525000000	0,0188577140
MAP_3772c	-	Cobalamin synthesis protein/P47K:cobalamin synthesis CobW	-1,9925001000	0,0403092240
MAP_3787	-	Peptidase S8 and S53, subtilisin, kexin, sedolisin	-9,0850000000	0,0195998900
MAP_3811	-	-	-5,4050000000	0,0166859310
MAP_3816	-	-	-2,7750000000	0,0179359760
MAP_3844	-	Serine/threonine protein kinase Signal transduction histidine kinase sensor	-4,8725000000	0,0054994000
MAP_3851c	-	Nitric oxide dioxygenase	-5,7174997000	0,0475360700
MAP_3856	-	Short-chain dehydrogenase/reductase SDR	-2,2100000000	0,0452045000
MAP_3857	umpA	orotate phosphoribosyltransferase	-4,3350000000	0,0029220153
MAP_3871	purT	phosphoribosylglycinamide formyltransferase 2	-6,3025002000	0,0005015883
MAP_3878c	fadE7	glutaryl-CoA dehydrogenase	-3,1950002000	0,0135126360
MAP_3880	-	integral membrane protein, Putative	-3,8350000000	0,0150579990
MAP_3884	-	Luciferase-like protein alkanesulfonate monooxygenase	-2,0400000000	0,0082288245
MAP_3920	-	-	-4,2500000000	0,0072341347
MAP_3926c	-	-	-8,2775000000	0,0000469652
MAP_3959c	-	Transcriptional regulator, XRE family	-5,8224998000	0,0000228331
MAP_3968	-	Hbha / Iron-regulated heparin binding hemagglutinin hbhA (adhesin)	-4,1525000000	0,0147471630
MAP_3977c	-	Short-chain dehydrogenase/reductase SDR	-3,9000000000	0,0079406660

Gene ID	Gene Name	Gene Product	log2 [ratio (Exp/ctrl)]	P-value
MAP_4021	-	Protein of unknown function DUF121	-5,0550000000	0,0162591880
MAP_4069c	-	Protein of unknown function DUF88	-1,0250000000	0,0165303830
MAP_4086	-	MCE-family protein MCE1C	-4,9550000000	0,0209933650
MAP_4093c	-	exodeoxyribonuclease V beta subunit	-7,8849998000	0,0004244963
MAP_4124	-	-	-5,0125003000	0,0475712700
MAP_4147	-	FAD-dependent pyridine nucleotide-disulphide oxidoreductase	-4,3925000000	0,0336022560
MAP_4177	rplN	50S ribosomal protein L14	-7,9875000000	0,0000509530
MAP_4196	-	DNA gyrase, A subunit	-6,9475000000	0,0034085987
MAP_4211	-	Histidinol-phosphate aminotransferase	-4,5850000000	0,0488178770
MAP_4214c	fadE9	Acyl-CoA dehydrogenase protein	-6,2400000000	0,0006389539
MAP_4230	rpsM	30S ribosomal protein S13	-5,2725000000	0,0033734275
MAP_4297c	-	Acetyl-CoA acetyltransferase-like protein	-7,9300003000	0,0275026500
MAP_4318c	-	Two-component sensor histidine kinase	-7,1524997000	0,0000984470
MAP_4336	-	virulence factor / Serine/threonine protein kinase	-5,0425000000	0,0001678101

Appendix 5

Primer sequences used in this study and Real-Time qPCR analysis of selected genes

Gene ID	Primer name	Primers sequence (5'-3')
rRNA 16s	MAP 16S FW	GCCGTAAACGGTGGGTACTA
	MAP 16S RV	TGCATGTCAAACCCAGGTAA
MAP 3738c	MAP 3738C FW	CCCACATTGGGATATGAAGC
	MAP 3738C RV	CTGAGGATCCTGGAGACGAG
MAP 3522	MAP 3522 FW	CTACCGGGAGCGTTATGTGT
	MAP 3522 RV	ACGATGGACGCCCAACTA
MAP 1317c	MAP 1317c FW	CAGGTGGTATTCGCCTTCTC
	MAP 1317c RV	ATGAACCCGATACCAATCCA
MAP 0654	MAP 0654 FW	GCAGGACTACACCATCGTCAT
	MAP 0654 RV	GTAGTCCTCCGTCGCCTTCT
MAP 1535	MAP 1535 FW	GTGTTCGTCTACGCGTTGCT
	MAP 1535 RV	ACCATGTAGAGGCGGTCCAC
MAP 2055	MAP 2055 FW	GAAATATCAATGGCCGCAAG
	MAP 2055 RV	AAGTTCAGTCGCAGGTGTCC

Transcriptome
***Map* acid-nitrosative stress**

Gene ID	Gene name	Gene Product	Microarray fold change	P-value	RT-qPCR fold change	SD
MAP 3738c	-	Methyltransferase type 12 / Cyclopropane-fatty-acyl-phospholipid synthas	-2,78465771	0,00216317	-2,89	0,17
MAP 3522	*oxyS*	Transcriptional regulator, oxyS	4,02084912	0,00065264	2,66	0,60
MAP 1317c	-	Acid-resistance membrane protein	2,34566990	0,00074380	1,36	0,88

Transcriptome
***Map* THP-1 infection**

Gene ID	Gene name	Gene Product	Microarray fold change	P-value	RT-qPCR fold change	SD
MAP 0654	*phoT*	phosphate transporter ATP-binding protein	-42,44433187	0,02392446	-16,81	0,91
MAP 1535	*pgsA2*	CDP-diacylglycerol--glycerol-3-phosphate 3-phosphatidyltransferase	6,40855813	0,00166329	-71,53	6,99
MAP 2055	-	cystathione beta-lyase	-9,04737958	0,00004972	-36,48	0,64

9. PERMISSIONS

This study has been published in part:

Andrea Cossu, Valentina Rosu, Daniela Paccagnini, Davide Cossu, Adolfo Pacifico, Leonardo Antonio Sechi, MAP3738c and MptD are specific tags of Mycobacterium avium subsp. paratuberculosis infection in type I diabetes mellitus, *Clinical Immunology* 141 (2011) 49-57.

Granted Permission:

--- Mar 12/7/11, Parker, Kerry (ELS-OXF) <*Kerry.Parker@elsevier.com*>
Da: Parker, Kerry (ELS-OXF) <Kerry.Parker@elsevier.com>
Oggetto: RE: Obtain Permission
A: andrea_corsican84@yahoo.it
Data: Martedì 12 luglio 2011, 11:12

We hereby grant you permission to reprint the material below at no charge in your thesis subject to the following conditions:

1. If any part of the material to be used (for example, figures) has appeared in our publication with credit or acknowledgement to another source, permission must also be sought from that source. If such permission is not obtained then that material may not be included in your publication/copies.
2. Suitable acknowledgment to the source must be made, either as a footnote or in a reference list at the end of your publication, as follows: "This article was published in Publication title, Vol number, Author(s), Title of article, Page Nos, Copyright Elsevier (or appropriate Society name) (Year)."
3. Your thesis may be submitted to your institution in either print or electronic form.
4. Reproduction of this material is confined to the purpose for which permission is hereby given.
5. This permission is granted for non-exclusive world English rights only. For other languages please reapply separately for each one required. Permission excludes use in an electronic form other than submission. Should you have a specific electronic project in mind please reapply for permission.
6. Should your thesis be published commercially, please reapply for permission.

Kerry Parker :: :: Rights Associate
Global Rights Dpt :: :: Elsevier Ltd

Requested permission details:

-----Original Message-----
From: andrea_corsican84@yahoo.it [mailto:andrea_corsican84@yahoo.it]
Sent: 11 July 2011 09:26
To: Health Permissions (ELS-PHI)
Subject: Obtain Permission

This Email was sent from the Elsevier Corporate Web Site and is related to Obtain Permission form:

Product: Customer Support Component: Obtain Permission

Web server: http://www.elsevier.com IP address: 193.204.206.252

Client: Mozilla/5.0 (Windows NT 6.0; rv:5.0) Gecko/20100101 Firefox/5.0

Invoked from: http://www.elsevier.com/wps/find/obtainpermissionform.cws_home?isSubmitted=yes&navigateXmlFileName=/store/p65idstarget/act/framework_support/obtainpermission.xml

Request From:

Andrea Cossu

University of Sassari

DEP. OF BIOMEDICAL SCIENCES - Viale S. Pietro 43/B

07100 Sassari Italy

Contact Details:

Telephone: Fax:

Email Address: andrea_corsican84@yahoo.it

To use the following material:

ISSN/ISBN: doi:10.1016/j.clim.2011.05.002

Title: Clinical Immunology

Author(s): Cossu, Rosu, Paccagnini, Cossu, Pacifico, Sechi

Volume: - Issue: - Year: - Pages: - - -

Article title: MAP3738c and MptD are specific tags of ...

How much of the requested material is to be used: Entire article

Are you the author: Yes

Author at institute: Yes

How/where will the requested material be used: In a thesis or dissertation

Details: Ph.D. Thesis

Additional Info:

As author of the article:

TITLE: MAP3738c and MptD are specific tags of Mycobacterium avium subsp. paratuberculosis infection in type I diabetes mellitus

AUTHORS: Andrea Cossu, Valentina Rosu, Daniela Paccagnini, Davide Cossu, Adolfo Pacifico, Leonardo Antonio Sechi

PUBLICATION: Clinical Immunology

PUBLISHER: Elsevier

DATE: 14 May 2011

doi:10.1016/j.clim.2011.05.002

I would like to reuse the full article both in print and electronic format without translating it in other language, as part of my doctoral dissertation.

The requested permission extends to any future revisions and editions of my dissertation, and to the prospective publication of my dissertation by University of Sassari (UnissResearch database). These rights will in no way restrict republication of the material in any other form by you or by others authorized by you.

At your request the content of the thesis may not be immediately available for editorial reasons after delivery of the thesis for a period of 6/12/18 months.

[acronym]

- end -

10. ACKNOWLEDGMENTS AND FUNDING

This work was supported by the POR Sardegna "Young Researchers, European Social Fund 2007- 2013, L.R.7/ 2007 “Promotion of Scientific Research and Technological Innovation in Sardinia".

Special thanks go to my colleague Dr. Valentina Rosu and Mr. Edmondo Manca for logistic assistance and Porto Conte Ricerche S.r.l – Alghero for array scanning instrumentation.